Aus dem Institut für Transfusionsmedizin und Immunologie
der Medizinischen Fakultät Mannheim
Direktor: Prof. Dr. med. Harald Klüter

Effects of hyperglycemia on adipose-derived mesenchymal stromal cells: a study on their proangiogenic and immunomodulatory potential

Inauguraldissertation
zur Erlangung des akademischen Grades
Doctor scientiarum humanarum (Dr. sc. Hum.)
Der Medizinischen Fakultät Mannheim
der Ruprecht-Karls-Universität
zu
Heidelberg

vorgelegt von
Agnese Fiori

aus
Sassuolo, Italien
2019

Dekan: Prof. Dr. med. Sergij Goerdt

Referentin: Prof. Dr. rer. nat. Karen Bieback

To myself.

To everything that this experience has provided

to my personal life and professional career.

Data reported in this dissertation are part of manuscripts submitted/to be submitted.

More detailed information reported in chapter 1 “Introduction” can be found in the published review “Fiori, A., et al., *Mesenchymal stromal/stem cells as potential therapy in diabetic retinopathy.* Immunobiology, 2018. **223**(12): p. 729-743”.

TABLE OF CONTENTS

Page

ABBREVIATIONS

2-NBDG	D-Glucose, 2-deoxy-2-((7-nitro-2,1,3-benzoxadiazol-4-yl)amino)
A	
α-SMA	Alpha smooth muscle actin
ADA	Adipogenic differentiation
AGE	Advanced-glycation end product
Ang	Angiopoietin
APC	Allophycocyanin
ASC	Adipose derived mesenchymal stromal cells
B	
BMA	Basal matrix angiogenesis assay
BM-MSC	Bone marrow derived mesenchymal stromal cells
C	
CAF	Cancer-associated fibroblasts
CBA	Cytometer bead array
CB-MSC	Cord Blood derived mesenchymal stromal cells
CCL	Chemokine ligand
CD	Cell doubling
CD4	Cluster of differentiation 4
CM	Conditioned media
D	
DAG	Diacylglycerol
DAMPs	Danger-associated molecular patterns
DME	Diabetic macular edema
DR	Diabetic retinopathy
DT	Doubling time
E	
EBM	Endothelial basal medium
EC	Endothelial cells
ECGM	endothelial cell growth medium
ELISA	Enzyme-linked immunosorbent assay
eNOS	Endothelial nitric oxide synthase
EV	Extracellular vesicles
F	
F-6-P	Fructose 6 phosphate
FGF	Fibroblast growth factor
FITC	Fluoresceinisothiocyanat
FoxP3	Forkhead box P3
FSC	Forward scatter
G	
GAPDH	Glyceraldehyde 3-phosphate dehydrogenase
GFAP	Glial fibrillary acidic protein
GFP	Green fluorescence protein
GlcNAc	N-acetylglucosamine
GSH	Glutathione

H	
HG	High glucose
HGF	Hepatocyte growth factor
HIF	Hypoxia inducible factor
HLA	Human leucocyte antigen
HRMVEC	Human retinal microvascular endothelial cells
HRMVPC	Human retinal microvascular pericytes
HUVEC	Human umbilical vein endothelial cells
I	
ICAM	Intercellular adhesion molecule
IDO	Indolamin-2,3-Dioxygenase
IFN	Interferon
IL	Iterleukin
iPSC-MSC	Induced pluripotent stem cells-MSC
ISCT	International society for cell therapy
iTreg	Induced Treg
J	
K	
L	
M	
MCP-1	Monocyte chemoattractant protein 1
MLR	Mixed lymphocyte reaction
MSC	Mesenchymal stromal cells
N	
NF-κB	Nuclear factor kappa-light-chain-enhancer of activated B cells
NG	Normal glucose
NG-2	Neural/glial antigen 2
nTreg	Natural Treg
NO	Nitric oxide
NOD	Non obese diabetic
NPDR	Non proliferative diabetic retinopathy
O	
OD	Optical density
ODA	Osteogenic differentiaiton
OIR	Oxygen induced retinopathy
P	
PBMC	Peripheal blood mononuclear cells
PD-1	Programmed cell death protein 1
PDGF	Platelet-derived growth factor
PDR	Proliferative diabetic retinopathy
PE	Phycoerythrin
PFA	Paraformaldehyd
PGE2	Prostaglandin E2
PHA	Phytohaemagglutinin
PKC	Protein kinase C
Q	
R	

RAGE	Receptor of advanced glycation end product
RGC	Retinal ganglion cell
ROP	Retinopathy of prematurity
ROS	Reactive oxygen species
S	
SSC	Side scatter
STZ	Streptozotocin
T	
T1D	Type 1 diabetes
TGF-β	Transforming growth factor beta
Th	T helper
Tie	Angiopoietin receptor
TNF	Tumor necrosis factor
Treg	Regulatory T cells
U	
V	
VCAM	Vascular cell adhesion molecule
VEGF	Vascular endothelial growth factor
VEGFR	Vascular endothelial growth factor receptor
VPD+/-	Violet proliferation dye +/-
W	
WJ-MSC	Warton Jelly deriveved mesenchymal stromal cells
X	
Y	
Z	

1 INTRODUCTION

1.1 Mesenchymal stromal cells

1.1.1 General overview

Mesenchymal stromal cells (MSC) were described for the first time in 1970 by Friedenstein and colleagues [1]. These cells, addressed as fibroblast colony-forming cells were isolated from the bone marrow and displayed an osteogenic differentiation potential. At that time, they were already defined by Friedenstein as an important component in bone-marrow transplantation, suggesting their fundamental role in the support of the hematopoietic stem cells niche [1]. Indeed, these “bone-marrow adherent cells” were later demonstrated to support hematopoiesis *in vitro* for weeks [2]. Moreover, evidence of their differentiation potential to osteoblasts as well as chondrocytes was rapidly provided [3]. From these first findings, the research on MSC and on their potential application in medicine has widely expanded [4]. As a result of these broad investigations MSC were found also to be isolated from several tissue sources such as adipose tissue (adipose tissue-derived stromal cells – ASC) [5, 6], umbilical cord/cord blood (CB-MSC) [7], dental pulp [8], Wharton´s jelly (WJ-MSC) [9] and many others [10]. However, the use of different protocols for MSC isolation and culture generated a huge amount of conflicting data dealing with MSC characterization and especially with their therapeutic potential [11]. In their review Phinney and Sensebe summarized misconceptions about MSC and listed the following points as general reminder: (1) MSC from different tissue sources are different in terms of phenotype and function, (2) lack of complete correspondence of MSC function *in vitro* and *in vivo*, (3) heterogeneity of MSC among different species and (4) the need for clinical data to assess their effective mode of action [11].

To create uniform and at least minimal criteria for the characterization and definition of MSC, the International Society of Cellular Therapy (ISCT) proposed some guidelines [12] where MSC are defined as a fibroblast-like multipotent progenitor cells with a solid proliferation capacity. They should retain a trilineage mesenchymal differentiation capacity to adipocytes, chondroblasts and osteoblasts as well as some characteristic cell surface markers. For instance, MSC have to be negative for hematopoietic and leukocyte markers (CD34, CD45) and at least positive for CD73, CD90 and CD105 [12, 13]. However, as studies on MSC characterization are still on going, these criteria

are continuously expanding, becoming more and more specific in the attempt to give a better understanding of MSC potential [14-16].

MSC multipotency, together with an increased understanding of their capacities, brought these cells on the spot, causing a tremendous increase of studies addressing their therapeutic potential on several contexts of disease. MSC have been investigated in tumors [17-19], wound healing [20, 21], graft vs host diseases [22-24], autoimmune diseases [25-27] and diabetes [28-30]. The great interest in using MSC as tool for cell-based therapy relies on multiple findings, which characterized the potential mode of action of MSC when interacting with other cell types in physiological/diseased microenvironments. Indeed, the “modes of action” of MSC can be allocated to three different main mechanisms: (1) the trophic potential, (2) the immunomodulatory function and (3) the differentiation potential (Figure1).

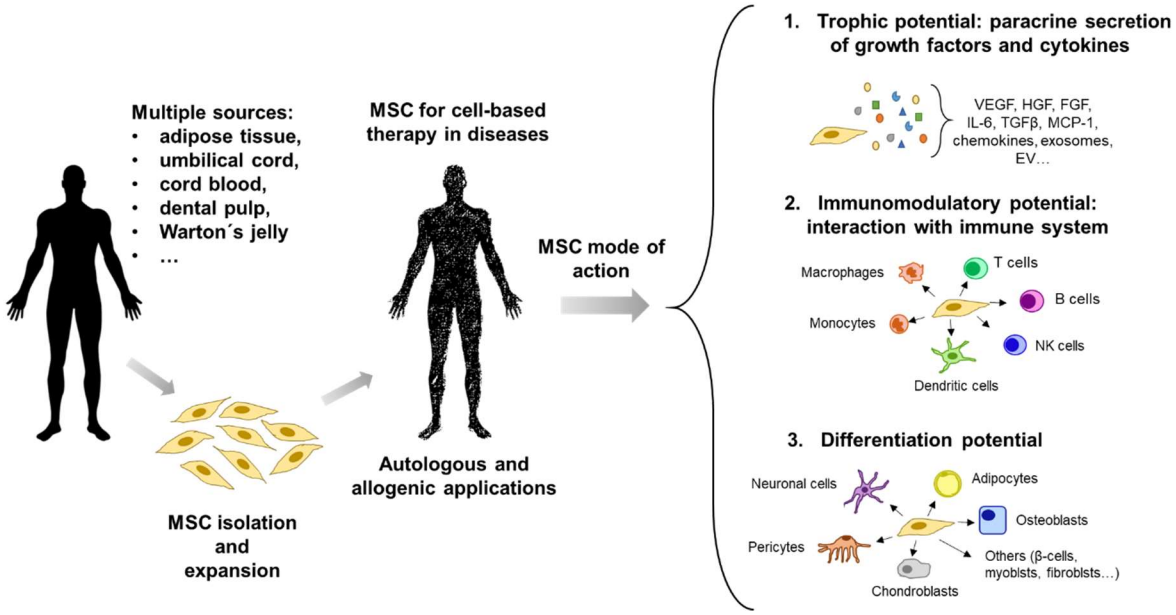

Figure 1 Concept of MSC application in cell-based therapy. MSC can be isolated from different sources, expanded and in line with the type of application, possibly modified (e.g. genetically). They can be applied in several disease contexts acting in accordance to their modes of action: trophic potential, immunomodulatory potential and differentiation potential. VEGF: vascular endothelial growth factor; HGF: hepatocyte growth factor; FGF: fibroblast growth factor, IL-6: interleukin 6, TGF-β: transforming growth factor beta, MCP-1: monocyte chemotactic protein-1, EV: extracellular vesicles.

(1) The trophic potential of MSC resides in their ability to secrete a wide range of paracrine factors such as cytokines and growth factors, which have been shown to modulate their surrounding microenvironment and mediate the interaction with other cell types [31, 32]. Recently MSC have been reported to produce extracellular vesicles

(EV) and exosomes, denoting a new possible paracrine mechanisms. This option has raised the new intriguingly paradigm of MSC-cell free based therapeutic potential aiming to replace MSC in favor of their secretome-derived products [33].
(2) The immunomodulatory function of MSC concerns not only their low immunogenicity, but it is also related to their interaction with cells of the immune system, generating an overall modulation of the immune response. Indeed, MSC were characterized for a low expression of human leucocyte antigen (HLA) class I molecules and the lack of costimulatory ones such as CD80 and CD86 [34]. This was interpreted as MSC being immune-privileged. In addition, the MSC-mediated inhibition of T cell proliferation, together with their ability of inducing regulatory T cells (Treg) are some of the most studied topics regarding MSC-mediated immunomodulation [34-36].
(3) The differentiation potential comes from their natural multipotency. Because of their differentiation ability to osteogenic and chondrogenic lineages, MSC have been thoroughly investigated in the context of bone and cartilage repair [37, 38] and even potential neuron-like differentiation has been proposed [39]. They have been also reported to differentiate into β-pancreatic cells to restore β-cell failure in diabetes [40]. Despite the great interest in this last topic, the underlying mechanisms related to MSC-migration, homing to injured site, effective differentiation and functional engraftment still require further elucidations.
All these aspects contribute to make MSC still a hot topic in terms of therapeutic cell-based approaches.

1.1.2 The proangiogenic potential

As already described previously, MSC are well-known for their trophic support, which is dependent on their ability of secreting a large number of cytokines and growth factors. In particular, studies in the cardiovascular field have largely demonstrated that MSC retain important proangiogenic features [41]. Media obtained from cultured MSC have been reported to be rich in proangiogenic factors such as vascular endothelial growth factor (VEGF), hepatocyte growth factor (HGF), fibroblast growth factor (FGF) and monocyte chemotactic protein-1 (MCP-1) [42, 43]. MSC conditioned media (CM) supported angiogenesis of human umbilical vein endothelial cells (HUVEC) *in vitro* and this effect was abrogated after pretreatment with neutralizing antibody against VEGF, MCP-1 and interleukin-6 (IL-6). In the same study, identical results were obtained when the CM was locally injected in a mice model of hind limb ischemia and promoted

angiogenesis as well as reduction of inflammation [44]. In another approach, the analysis of the secreted proteome in CM from MSC, revealed a notable overrepresentation of proteins related to the development and function of the cardiovascular system clustering in processes like angiogenesis, neovascularization and development of blood vessels [45]. Notably, intravenous injection of MSC-CM preserved cardiac function in a pig model of myocardial infarction increasing capillary density and reducing the infarct size [45]. These promising evidences introduced MSC into the cardiovascular research and many clinical trials investigating their safety and efficacy were initiated [46-48]. Besides these obvious implications in the cardiovascular field, many studies are still going on to characterize the crosstalk between MSC and endothelial cells (EC) [49]. In fact, other angiogenesis-related pathways are emerging as being regulated by MSC. For instance, the angiopoietin-1 (Ang-1)/angiopietin-1 receptor (Tie2) pathway and the VEGF/VEGF receptor-2 (VEGFR2) pathway resulted to be upregulated promoting angiogenesis and vascular stabilization *in vitro* and *in vivo* in a mouse model of cerebral artery occlusion [50]. In addition to that, proangiogenic growth factors and cytokines might act via exosomes or EV. Beneficial effects of MSC-derived exosomes have been provided in several studies of ischemic heart disease [51, 52] and wound healing [53]. However, the proangiogenic ability of MSC may have some side effects, especially in tumor diseases. Indeed, tumor angiogenesis is a critical aspect in cancer diseases, mediating tumor progression and metastasis [54]. Some evidences suggested that MSC could promote *in vitro* and *in vivo* tumor neo-angiogenesis via paracrine secretion of proangiogenic factors and inducing remodeling in endothelial cell organization [55-57]. Although mechanisms are still under investigation, these effects seemed to be mediated by a sort of “malignant transformation” of MSC or from the so called cancer-derived fibroblast (CAF), which might originate from recruited MSC. Once in the tumor stroma these cells might sense the altered microenvironment and, in the crosstalk with tumor cells, starting to co-evolve with the disease, contributing to the progression through physical and chemical remodeling of the tumor microenvironment [58, 59].

Overall, these data indicate that MSC retain strong proangiogenic capacities. Moreover, as demonstrated in the case of CAF, MSC are susceptible to their surrounding microenvironment, which may induce changes in their phenotype as well as functions and drive their beneficial potential to a dangerous one. Therefore, in the development of MSC-mediated or MSC-free therapeutic approaches, it is important to

define risks and benefits of a potential induction of angiogenesis. While this may be the goal of ischemia and non-perfusion-related diseases, the same should be avoided in diseases where pathological angiogenesis is the cause of the disease such as angiogenic tumors, chronic inflammation or retinopathies [60]. A comprehensive knowledge of the disease and MSC potential in that context represents a fundamental step in the elaboration of cell/cell-free therapy.

1.1.3 The immunomodulatory potential: focus on MSC and T cell interaction

As introduced previously, MSC can act also as potent immunomodulators regulating the immune response and generally skewing it towards a pro-regenerative/anti-inflammatory milieu rather than to a pro-inflammatory one [61, 62].

It is long established that MSC exert a strong inhibition on activated T cells. Indeed when T cells are triggered by mitogenic stimuli such as phytohaemagglutinin (PHA) or anti-CD3/CD28 monoclonal antibodies, MSC can firmly restrict their proliferation [63-65]. However, contrasting observations suggested that MSC could also induce the survival of quiescent/not-stimulated T cells [66]. Although this appeared to be related to culture condition i.e. MSC/mononuclear cell ratio [67], this aspect should be taken into account in the context of clinical application. Molecular mechanisms regulating MSC/T cell interplay rely on both cell-to-cell contact and secretion of soluble factors [34]. It has been demonstrated that CM from MSC containing IL-10 and indoleamine 2,3-dioxygenase (IDO) induced apoptosis in splenocytes, while the direct contact with MSC promoted splenocytes cell arrest in the G0/G1 phase [68]. Similarly, in direct and indirect cocultures of MSC and peripheral blood mononuclear cells (PBMC), it was observed that both IL-10 and transforming growth factor beta (TGF-β) were important mediators in the induction of programmed cell death 1 receptor (PD-1) on T cells. The latter was partially involved in MSC-mediated T cell apoptosis via the PD-1/B7-H1 axis [65]. In addition to that, MSC priming via interferon gamma (IFN-γ), resulted in IDO up-regulation which potentiated the suppressive potential of MSC on stimulated PBMC, suggesting that MSC activity can be modulated by surrounding stimuli [69, 70].

Another important immunoregulatory function of MSC concerns their ability to affect the balance of the CD4 T helper (Th) subsets both *in vitro* and *in vivo* [71]. CD4 Th cells are normally classified into:

(1) Th1, involved in the activation and recruitment of macrophages as well as in the IgG production by B cells, which secrete IFN-γ and tumor necrosis factor (TNF);

(2) Th2, which produce IL-4, IL-5, IL-9, IL-13 and IL-10 and mediated the switch of antibody secretion in B cells;
(3) Th17, which role in inflammation concerns the recruitment of neutrophils and the secretion of IL17a-f, IL-21 and IL-22 and
(4) Treg, a subset of CD4 cells commonly described as CD4+CD25+ forkhead box P3 positive (Foxp3+), which are essential in the regulation of the inflammatory process and to prevent autoimmunity [72].

In vitro cocultures of MSC and CD4 cells showed that MSC could exert a potent inhibition of undifferentiated CD4 T cells, however, once the differentiation to Th1 and Th17 was already initiated, MSC were able to suppress only Th1 cells, while the pro-inflammatory Th17 were promoted [73]. In another study, MSC decreased IFN-γ secretion from Th1 while increasing IL-4 produced by Th2, suggesting a shift from pro-inflammatory to an anti-inflammatory background [74]. These effects were detected also in different disease model *in vivo*. For instance, an improvement of the Th1/Th2 balance, consistent with a reduction in Th17 and increase in Treg, has been documented in several models of type 1 diabetes (T1D) [75-77]. In a rat model of inflammatory bowel disease, treatment with ASC promoted an overall amelioration of the disease through impairment of Th1 expansion and Th1 cytokine secretion in association with Treg induction, which were highly immunosuppressive *in vivo* and *in vitro* [62]. Many of these studies, together with the inhibition of Th1/Th17 subsets, often reported a concomitant induction of Treg cells. As introduced before, Treg exert a fundamental role in the regulation of the immune response modulating the activation of Th subsets. They are usually distinguished into natural or naïve Treg (nTreg) originating in the thymus and induced Treg (iTreg), which come from the differentiation of peripheral CD4 T cells [78]. Treg characterization has a long story started more than 20 years ago when CD4+CD25+ cells were found to be fundamental in mediating self-tolerance [79]. To date, many markers have been tested and introduced in their characterization. The positivity for transcription factor FoxP3 as well as the lack of CD127 expression are commonly accepted as Treg markers [80]. Importantly, CD4+CD25+CD127- were found to better reproduce the inhibitory activity of CD4+CD25+FoxP3+ cells suggesting that the combination of these four markers was highly representative of functional Treg [81]. Cocultures of MSC and CD4 cells reported an induction of CD4+CD25+FoxP3+ Treg cells mediated by the production of prostaglandin E_2 (PGE2) and transforming growth factor β (TGF-β) [82]. The induction

of IL-10 producing Treg by ASC in coculture with PBMC corroborated these findings [61]. In another study Melief and colleagues demonstrated that TGF-β, produced by MSC, was a key factor in mediating Treg induction, which was also supported by monocytes. Notably, MSC and their CM supported monocyte survival while promoting their switch to a M2 (anti-inflammatory) phenotype enabling them to secrete chemokine ligand 18 (CCL-18), which was found to be essential in inducing Treg [83]. Also IL-2 has been demonstrated to be instrumental for Treg induction [84]. Many of these findings were recapitulated *in vivo* in several settings, highlighting the protective effect of MSC via Treg induction [85-87].

The evaluation of MSC-mediated effects on the immune response following their transplantation/application in diabetic settings has a long history with promising outcomes [88]. For instance, MSC injections in STZ rats lowered blood glucose levels, ameliorated insulin secretion and promoted pancreatic islets renewal [89, 90]. Likewise, in pre-diabetic non obese diabetic (NOD) mice, intravenous injection of human MSC delayed the onset of diabetes and reduced high levels of pro-inflammatory cytokines [91]. These evidences, in addition to the growing interest in developing MSC-mediated therapies, promoted many clinical studies, which gave successful and promising results [92-94]. However, investigations on specific MSC immuno-mediated effects on diabetic complication are still under evaluation. Especially in diabetic retinopathy (DR), where the MSC therapeutic potential is mainly investigated in terms of provision of trophic factors and structural support (pericyte-like function), the role of MSC as immunomodulators is almost not considered.

Taken together these studies constitute a solid base for further pre-clinical and clinical studies in many disease settings from autoimmune diseases to transplantation. A continued investigation on the complex interactions between MSC and cells of the immune system will be required to gain further insights on the MSC-mediated immunomodulation.

1.2 Mesenchymal stromal cells in diabetic retinopathy

1.2.1 Diabetic retinopathy

Diabetes mellitus is a pathological condition, which comprehends a large group of metabolic disorders characterized by two distinctive traits: high levels of glucose in the blood stream and impaired glycemic control. Diabetic patients may often develop eye-related complications and the most common is known as DR [95]. While its onset is asymptomatic, the appearance of first clinical signs described as “at least one microaneurysm” denotes already the stage of a mild non-proliferative DR (NPDR). The disease can then progress to moderate NPDR where microaneurysms appear together with hemorrhages. The severe NDPR is internationally classified as followed [96, 97]: (1) more than 20 intraretinal hemorrhages in each of four quadrants and (2) venous beading and prominent intraretinal microvascular abnormalities in two/one or more quadrants. The last stage of the disease is the proliferative DR (PDR) characterized by retinal neovascularization, vitreous/preretinal hemorrhages and even traction retinal detachments [96, 97]. Another important classification in DR is that of the diabetic macular edema (DME), which can occur across all stages of DR. This represents the main cause of vision loss through fluids accumulation in the neural retina as well as cystoid edema of the macula [98].

DR is a progressive neurovascular disease, which involves the microvascular and neuronal compartments of the eye [99]. Following the hypothesis of the neurovascular unit, microvascular and neuronal changes might be interconnected, contributing together to the progression of the disease [99]. Although the temporal connection between vascular and neuronal changes is unclear and physio-pathological mechanisms still need elucidation, many papers reported early degeneration in the neuronal district. For instance, apoptosis of retinal ganglion cells (RGC), reduction in photoreceptors and alteration in the inner neuronal retina were documented prior to vascular changes [100-102]. The glial fibrillary acidic protein (GFAP) has also been proposed as marker to target activation/alteration in Müller glial cells in early phases of diabetes [103]. Starting from these findings, the concept of inflammation as one of the leading processes in the early pathogenesis of the disease arose [104]. Indeed, many “classical” inflammatory markers such as tumor necrosis factor α (TNF-α), IL-1β, IL-6 and intercellular adhesion molecule 1 (ICAM-1) were identified at high concentration in eyes of diabetic patients [105-107]. In addition, “traditional

inflammatory processes" such as increased vascular permeability, tissue edema, microglia activation and macrophage infiltration have been described in many animal models [108-110].

The retinal microvascular compartment can be simultaneously considered as the source and the consequence of retinal inflammation. Pro-inflammatory cytokines were found to be produced directly by endothelial cells as well as by infiltrating leukocytes. Several studies demonstrated that increased leakage in retinal vessels and consequent infiltration of immune cells (monocytes) were related to a rising expression of adhesion molecules such as ICAM-1 and vascular cell adhesion molecule 1 (VCAM-1) [111]. Similarly, in a streptozotocin (STZ) mouse model, it was observed that inhibition of ICAM-1 prevented the adhesion of leukocytes to the retinal capillaries, which started to take place immediately after induction of diabetes [112]. Damaged endothelial cells can also act as principal mediators of the inflammation supporting the angiogenic response typical of the PDR. Indeed, it has been demonstrated that the expression of VEGF can be sustained and promoted by pro-inflammatory cytokines such as TNF-α and IL-6 [113]. Similarly, VEGF could act as pro-inflammatory cytokine itself favoring other pro-inflammatory mediators [114, 115]. Overall this self-propagating mechanism contributes to retinal degeneration, supporting vascular alterations not only at early stages of DR but also in later ones guiding and promoting the angiogenic response.

Focusing only on the microvascular retina, is it possible to define two cell type, which are mainly involved in the vascular degeneration, pericytes and endothelial cells.

Pericytes are cells of mesodermal origin with a perivascular location, wrapping around micro and macro-vessels, establishing a very tight contact with endothelial cells [116]. Studies on these cells revealed a large heterogeneity of this cell population, mainly related to their location and function [117]. Regarding their function, pericytes are generally involved in the regulation and preservation of vascular homeostasis participating in processes like angiogenesis and vascular permeability [118]. PDGF-β/PDGFR-β, Ang1-2/Tie2 and Notch signaling are the signals which mediate the interaction with endothelial cells in the developing and resting retina, promoting homeostasis or angiogenesis [119]. Moreover, the 1:1 ratio between pericytes and endothelial cells is fundamental to maintain the tightness of the blood retinal barrier (BRB) [120]. In DR, because of the hyperglycemia-mediated insults, the normal

communication and interaction between EC and pericytes is interrupted. Indeed, pericyte loss is one of the earliest changes in the diabetic retina [121]. Even if the temporal relation between loss of pericytes and duration of diabetes in humans is still unclear, the loss of pericytes contributes to the vascular remodeling, which leads first to acellular capillaries, microaneurysms and non-perfused area, ending up with vessel hyper proliferation to counteract the retinal ischemia [121].

These changes in pericyte-endothelial cell interactions, together with hyperglycemia-mediated cell damage in the retinal endothelium and the spreading inflammation, contribute to the pathogenesis of DR (Figure 2).

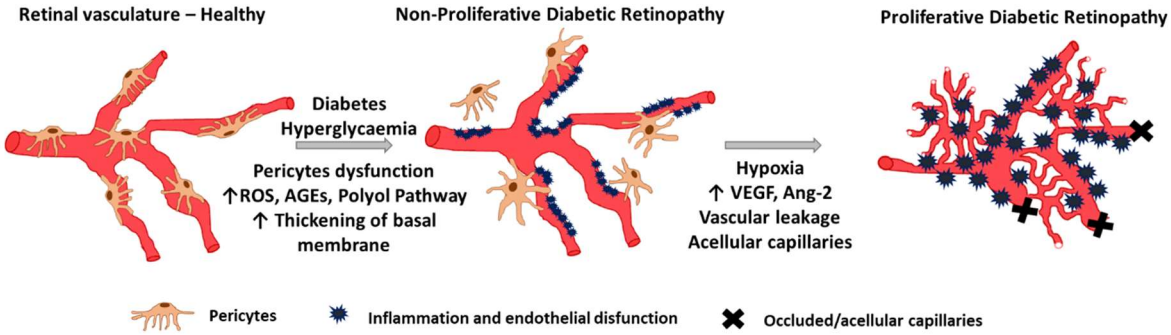

Figure 2 Progression of DR and factors involved in the pathogenesis. ROS: reactive oxygen species, AGEs: advanced glycation end products, VEGF: vascular endothelial growth factor.

To date, the majority of therapeutic strategies in the cure of DR, target mainly late stage of the disease. Together with tight glycemic control, laser photocoagulation, injection of anti-VEGF antibodies, corticosteroids, non-steroidal anti-inflammatories as well as inhibitors of the renin-angiotensin system are some of the most used therapeutic approaches [122]. However, it is now clear that specifically targeting the early phases of DR would lead to a notable improvement in preventing or delaying the progression of the disease. In this sense, cell-based therapy may represent a good option because of their potential ability to replace/promote tissue repair in the damaged retina [123].

1.2.2 MSC-based therapeutic approach in DR

The role of MSC as cell-therapy approach to DR has been intensively studied in several animal models, producing interesting and promising results. For instance, beneficial effects of ASC were demonstrated *in vitro* and *in vivo* in a study from Rajashekhar and

colleagues [124]. Cocultures of ASC and retinal endothelial cells (REC) revealed that ASC supported REC angiogenic network formation and intravitreal injection of ASC in a STZ mice reduced vascular leakage and inflammation in the retina. Notably, ASC were localized in proximity of retinal vessel, suggesting a potential pericyte-like function [124]. Similarly, ASC were found to induce a cytoprotective microenvironment in the retina of STZ mice, preventing pathological neovascularization through reduction of oxidative stress and prevention of retinal ganglion cell loss [75]. An important evaluation on timing of MSC injection has been provided by Mendel and colleagues in a mice model of oxygen-induced retinopathy (OIR) [125]. They found that injection of ASC before OIR vessel destabilization prevented capillary dropout in addition to a perivascular/pericyte-like localization around retinal vessels. The ASC even expressed pericyte markers such as neural/glia antigen 2 (NG-2) and α smooth muscle actin (α-SMA). Similar findings were recapitulated also in a DR Akimba mouse model [125]. The pericyte-like behavior of ASC was also confirmed in a mouse model of retinopathy of prematurity (ROP) [126]. Here, changes in inflammatory and angiogenesis-related cytokines were found in comparing ASC-treated/non-treated mice, suggesting an active modulation of retinal microenvironment by ASC. Similarly, beneficial effects of ASC were demonstrated also *in vitro*, where ASC CM abrogated HG-induced oxidative stress and NF-κB activation in endothelial cells exposed to hyperglycemia [126]. Finally, the interaction between ASC and REC has been shown to be dependent on NOTCH signaling [127]. In summary, all these studies characterized at least two main roles of MSC in DR. The first one is related to the ability of MSC to tightly interact with endothelial cells in the retinal microvasculature, acquiring a pericytes-like phenotype suggesting a potential role as modulator of vascular homeostasis. Secondly, thanks to their trophic potential, MSC can secrete numbers of cytokines and growth factors, which can modulate the local microenvironment resulting in a modulation of retinal inflammation.

As mentioned before, among MSC capacities, the immunomodulatory potential is one of the most studied in several disease contexts. These capacities are until now almost not considered in DR and beside findings confirming the reduction of pro-inflammatory cytokines upon MSC application, no real evidences about an interaction with microglia or T cells were reported. Although, these cells could play a relevant role in DR, as suggested by a recent paper [128]. Indeed, Deliyanti and colleagues investigated

whether Treg were detectable in the retina at different time points after the generation of OIR in mice. They found that while in controls Treg were residing within the vasculature, the acute phase (switch from hyperoxia to hypoxia) caused an extravasation of Treg cells in the retinal tissue. At the same time point, Treg were also expanding in spleen and lymph nodes. Besides this, they also showed that these cells were of therapeutic relevance: increasing the Treg numbers via IL-2/anti-IL-2 mouse antibody or via adoptive transfer, not only reduced retinal neovascularization but also favored an anti-inflammatory switch of the microglia, both *in vivo* and *in vitro* [128]. These data demonstrated that acute retinal ischemia represented a stimulus to induce transient Treg expansion, which migrated to retina. Once there, however, quantities were not enough to modulate the microenvironment and restrict pathological neovascularization. Notably, increasing the number of circulating Treg, caused a delay in the progression of the disease and prevented neovascularization. These promising evidences introduced the hypothesis of Treg manipulation as potential treatment of retinopathies. Because of this, the potential use of MSC in cell-based therapeutic approach of DR, might start to consider MSC-mediated Treg induction as a possible therapeutic mechanism beside pericytes-like function and trophic support.

Despite the promising results obtained in animal models, further studies are still required to clarify safety and efficacy of MSC-mediated cell therapy. Moreover, important aspects such as timing and route of administration, allogenic versus autologous MSC and the fine characterization of the MSC potential in retinal microenvironment have to be taken in consideration [123].

1.3 Molecular mechanisms of hyperglycemia-mediated cell damage

Hyperglycemia and poor glycemic control are two main features of diabetes mellitus. People affected by this disease are prone in developing serious secondary complications, which actually affect their life resulting in impaired life quality and even increased mortality [129]. Some of those secondary complications are microvascular pathologies, which can affect the retina (DR), kidney (diabetic nephropathy) and peripheral nerves (diabetic neuropathy) [130]. The pathophysiological features of these complications are very similar in the three different districts and concern a progressive microvascular degeneration, which impairs the normal microvascular functions and

vascular permeability. With time, these alterations lead to cell loss, overproduction of extracellular matrix and capillary occlusion, which are the preamble for ischemia, hypoxia-induced neovascularization, edema and matrix deposition [131, 132].

Hyperglycemia is considered one of the leading factors driving diabetic complications, especially because of glucose-mediated cell damage, which is particularly evident in endothelial cells. Four mechanisms have been proposed to explain how hyperglycemia-induced damage takes place and were gathered together by Brownlee in the “unifying hypothesis” [133, 134]. The mechanisms are the following: (1) increased flux in the polyol pathway as well as (2) through the hexosamine pathway; (3) abnormal activation of protein kinase C (PKC) and (4) increased formation of advanced glycation-end products (AGE) [134]. The upstream factor initiating this cascade of events is indeed glucose, which uptake in endothelial cells is insulin-independent. Therefore, too high glucose concentrations in the blood stream corresponds with high glucose concentrations in the cells [135]. Increased glucose influx in the cells may be directed to the (1) polyol pathway and metabolized by aldose reductase through NADPH consumption. Similarly, exceeding fructose-6-phosphate (F-6-P) obtained by metabolized glucose in the first step of glycolysis, may be directed to (2) the hexosamine pathway. Here, F-6-P may act as substrate for enzymes driving protein glycosylation by addiction of N-acetylglucosamine (GlcNAc), which has been demonstrated to modulate the activity of transcription factors. Also (3) PKC activation is mediated by high intracellular glucose levels, since this may cause increased production of diacylglycerol (DAG). DAG mediates PKC activation, which may act as second messenger to the modulation/activation of several enzymes/pathways such as endothelial nitric oxide synthase (eNOS), VEGF production, NF-κB (nuclear factor kappa-light-chain-enhancer of activated B cells) and NADP(H) oxidase activation. Lastly, glucose may contribute to (4) AGE formation through the generation of glucose-derived precursors (like glyoxal or methylglyoxal). Increased production of AGE may: (1) affect normal cell function via AGE-modification of proteins, (2) impair cell adhesion, via generation of AGE-modified extracellular matrix and (3) activate the NF-κB pathway through AGE-receptor of AGE (RAGE) stimulation [134].
The “unifying hypothesis” proposed by Bronwlee, suggested that all these pathogenic mechanisms, induced by hyperglycemia, may contribute to a single, unique process: superoxide production by the mitochondrial electron transport chain. Superoxide

production by mitochondria has been demonstrated to be strictly related to the cell metabolic status and glucose consumption. Moreover, superoxide can reduce glyceraldehyde-3-phospathe dehydrogenase (GAPDH) activity resulting in accumulation of glucose metabolites, which will be directed to the polyol and hexosamine pathways. Similarly, GAPDH inhibition may promote PKC activation and formation of AGE caused by triose phosphate accumulation [134].
As microvascular complications arise mainly from endothelial dysfunction, the reported molecular pathways were largely investigated in endothelial cells [135]. However, many cell type resulted impaired by hyperglycemia. For instance, retinal pericytes [121], neuronal cells [136] and even cells of the immune system [137].

1.3.1 Are MSC affected by hyperglycemia/diabetes?

The large interest in the therapeutic use of MSC comes not only from their multipotency but also from their relatively easy isolation and expansion *in vitro*. For instance, large quantities of ASC can be isolated with non-invasive procedures, rendering them a very promising candidate for autologous treatment [138, 139].
However, as introduced previously, diabetes is a particular metabolic condition where normal cell metabolism and functions are altered. Moreover, dysfunction in the homeostasis of adipose tissue has been strongly related to obesity and related disorders [140]. Considering these aspects, we asked: whether, how and how much hyperglycemia/diabetes can impair MSC?
To date, despite several studies investigated the effect of diabetes (both T1D and type 2), conflicting results did not help in finding a clear answer. While some papers reported similarities in potency and functions of MSC/ASC isolated from healthy or diabetic patients [141, 142], others denoted important differences [143, 144]. This, of course may impair their therapeutic function, opening questions on whether the use of autologous or rather allogeneic MSC is favored in potential cell-based interventions. Comparing ASC isolated from fat pads of diabetic and healthy mice, Cianfarani and colleagues observed a differential expression of surface markers, suggesting a depletion of certain cell subpopulations, which might affect their therapeutic potential. Indeed, the efficacy of wound healing support of ASC isolated from diabetic mice was reduced compared to the one from healthy ones [145]. In similar studies, the angiogenic potential of ASC isolated from diabetic mice was impaired *in vivo* and *in vitro* and this was related to a depletion in certain ASC subpopulations. Rennert and

colleagues identified a depletion in CD45-CD31-CD34+ ASC from stromal vascular fractions (SVF) of diabetic patients, while Inoue et al. observed that reduced CD271+ subpopulation in CD34+CD31−CD271+ ASC was critical for the impairment of diabetic ASC. [146, 147]. In a model of DR, diabetic ASC did not improve retinal vascularization, despite no metabolic differences in terms of ATP-dependent, uncoupled and non-mitochondrial respiration [148].
Taking into account these studies, autologous MSC from diabetic patients should not be then considered totally safe. Indeed, it has been demonstrated that genetically modified diabetic ASC, expressing the enzyme glyoxalase-1 (GLO-1), had improved viability, migration and proangiogenic capacity and were equal to healthy ASC in restoring blood perfusion [149]. Similarly, pretreatment of diabetic MSC with deferoxamine resulted to be significant in increasing VEGF, hypoxia inducible factor-1 (HIF-1) and FGF-2 restoring their angiogenic potential [150].

Asking on whether, how and how much hyperglycemia affects MSC functions, Hajmousa and colleagues recently reported a specific hyperglycemia-mediated effect on ASC [151]. ASC cultured in media with high glucose concentration (HG; 30 mM) were characterized by changes in the bioenergetics of metabolism, denoting increased reactive oxygen species (ROS) production and mitochondrial reorganization. Despite this, ASC in presence of HG, reduced glucose uptake, denoting their great plasticity in adapting to the surrounding microenvironment [151]. Another study demonstrated the involvement of ROS as consequence of hyperglycemia in MSC [152]. Indeed, HG exposure altered mRNA expression of adipokines and transcriptional factors in adipocytes differentiated from BM-MSC. These changes did not interfere with the differentiation process, but were all associated to increased intra- and extracellular ROS production [152]. In contrast to previous studies, hyperglycemia was found to induce BM-MSC apoptosis in a time dependent manner, while increased production of ROS was also confirmed [153].

These discrepancies highlight that more studies are still needed to fully elucidate whether MSC transplantation can be considered as a therapeutic alternative in diabetic disorders. At the same time, investigations on diabetic/hyperglycemia-mediated effects that may occur once healthy MSC are in a diabetic/hyperglycemic environment can

give important insights on how MSC-mediated cell therapy can be improved in this particular pathological setting.

2 AIM OF THE STUDY

The study of MSC as tools for cell-based therapy in several diseased contexts represents one of the most investigated fields of the last twenty years. However, in some situations, the lack of homogenous results still limits the translation to the clinical research. This is the case in the field of diabetes. Indeed, while transplantation/application/infusion of allogenic MSC is widely investigated as previously reported, the research on the application of autologous MSC is still lagging behind. It has been proven that in diabetes and hyperglycemia-related syndromes, high glucose concentrations in the blood flow, together with poor glycemic control, represent one of the first causes of cell damage. Hyperglycemia-mediated cell damage has been largely documented especially in endothelial cells uncovering mechanisms of the pathogenesis of some diabetes-related microvascular diseases, such as DR and diabetic nephropathy. However, effects of hyperglycemia on MSC are poorly studied and to date some contrasting evidences have proposed that MSC isolated from diabetic patients may be impaired in their therapeutic potential.

Hypothesizing that ASC may serve as future cell-based therapy to prevent or ameliorate pathological consequences of DR by exerting pericyte-like/proangiogenic functions, we asked whether ASC are affected by hyperglycemia and if so, which of the proposed therapeutic mechanisms is changed: the angiogenic function, the pericyte-like, and/or the immunomodulatory capacity. Therefore, we developed our research strategy around four main aims here presented (Figure 3).

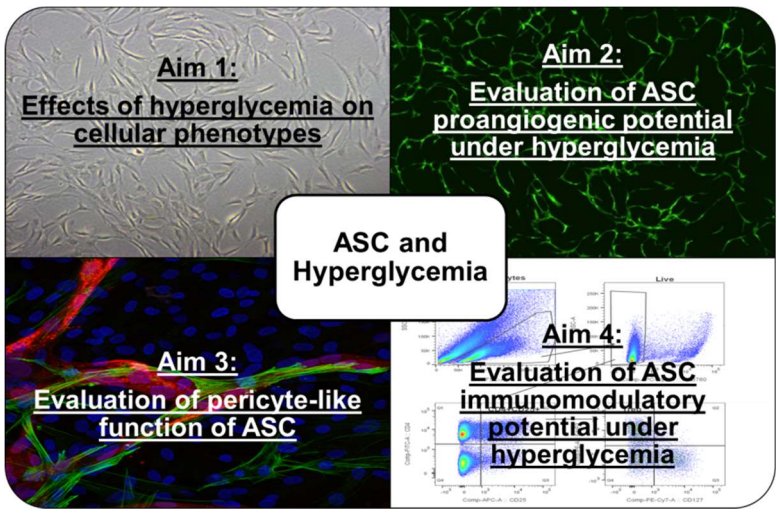

Figure 3 Aims of the study.

(1) Aim 1: Evaluating effects of hyperglycemia on cellular phenotypes.

Postulating that hyperglycemia-mediated effects on ASC would have been detectable on their phenotype, ASC were isolated from lipoaspirate of multiple donors and directly after isolation, cells from the same donor were cultured in normal glucose (ASC_{NG}; 1g/L) and high glucose (ASC_{HG}; 4.5 g/L) cell culture medium. These two counterparts were compared in terms of phenotype, cell growth, differentiation potential and cell surface markers. Oxidative stress (total intracellular ROS content) and glucose uptake were also measured.

Similarly, hyperglycemia-mediated effects were also assessed on microvascular retinal endothelial cells (HRMVEC). Growth rate of NG and HG cultured HRMVEC was monitored as well as oxidative stress and glucose uptake. Angiogenic potential of NG/HG HRMVEC was tested trough basement matrix angiogenesis (BMA) assays on gel membranes.

(2) Aim 2: Evaluation of ASC proangiogenic potential under hyperglycemia.

Hypothesizing that the proangiogenic potential of ASC would not be affected by HG, we established cocultures with EC, analyzing their supernatants for angiogenic growth factors.

First, ASC_{NG-HG} were cocultured with GFP-transfected human umbilical vein endothelial cells ($HUVEC_{GFP}$). Coculture supernatants were assessed comparing ASC_{NG} cocultures in NG and HG culture media.

Second, cocultures between ASC_{NG-HG} and GFP-transfected HRMVEC ($HRMVEC_{GFP}$) were set and coculture supernatants were analyzed comparing ASC_{NG-HG} monoculture with cocultures (in NG culture media).

Third, supernatants of cocultures and ASC monocultures were used as conditioned media (CM) for culturing HG HRMVEC in BMA assays.

(3) Aim 3: Evaluation of pericyte-like function of ASC.

We hypothesized that ASC could serve as functional pericytes interacting and stabilizing endothelial cells independently of HG. Immunofluorescence was used to investigate ASC for pericyte-like markers when cocultured with dTomato transfected HRMVEC. Anti-α-SMA and anti-NG-2 antibodies were tested. Moreover, the proangiogenic capacity of retinal pericytes as well as pericyte markers were tested in coculture angiogenesis assays of pericytes and

$HUVEC_{GFP}$/$HRMVEC_{GFP}$ in NG/HG culture media hypothesizing that pericyte functions might be impaired by HG.

(4) Aim 4: Evaluation of ASC immunomodulatory potential under hyperglycemia.

To verify whether ASC immunomodulatory potential is affected by HG, interactions between ASC_{NG-HG} and CD4 T cells were characterized through ASC_{NG-HG}:PBMC direct and indirect (transwell) cocultures. Two distinct conditions were evaluated: (a) stimulated coculture, where PBMC were stimulated with CD3/CD28 beads and (b) not-stimulated cocultures. For both (a) and (b) CD4 T cell proliferation, quantification of CD4+CD25+ and Treg fractions and analysis of coculture supernatants were performed.

3 MATERIAL AND METHODS

3.1 Material

3.1.1 Cells

Product	Company	Catalog No.
Adipose derived mesenchymal stromal cells (ASC)	Self-isolated; Mannheim Ethics Commission II (vote numbers 2006-192 N-MA).	
Human umbilical vein endothelial cells (HUVEC)	Self-isolated; Mannheim Ethics Commission II (vote numbers 2010-262 N-MA)	
Human retinal microvascular endothelial cells (HRMVEC)	PeloBiotech	PBCH-1608511
Human retinal microvascular pericytes (HRMVPC)	PeloBiotech	PBCH-0612211
293FT cells	Kindly provided by Prof. Patrick Maier, Department of Radiation Oncology, University Medical Centre Mannheim, Germany.	
Peripheral blood mononuclear cell (PBMC)	Self-isolated from Buffy coat provided by the German Red Cross Blood Donor Service in Mannheim.	

3.1.2 Cell culture/cell isolation products

Product	Company	Catalog No.
NB6 GMP grade collagenase	SERVA Electrophoresis	17458
Collagenase	Gibco	17100017
EDTA	Applichem	A3145,0500
DMEM (normal glucose 1g/L)	PAN Biotech	P04-01500
DMEM (no glucose)	PAN Biotech	P04-01549
Pooled human allogeneic serum from AB donors (AB serum)	German Red Cross Blood Donor Service, Institute Mannheim	
Penicillin/Streptomycin	PAN Biotech	P06-07100
L-glutamine	PAN Biotech	P04-80100

D-glucose	Sigma-Aldrich	G7021
Endothelial cell basal medium (EBM)	PromoCell	C-22011
Supplement Mix endothelial cell growth medium 2	PromoCell	C-39216
Pericytes Growth Medium	PeloBiotech	PB-MH-0314000
Speed Coating Solution	PeloBiotech	PB-LU-000-0002-00
Trypsin/EDTA	PAN Biotech	P10-024100
Fetal Bovine Serum	Sigma	F7524
Dymethylsulphoxide (DMSO)	Wak-chemie Medical GmbH	WAK-DMSO-10
Ficoll-Paque™ Premium	GE Healthcare Bio-science AB	17-5442-03
DPBS (1X)	Gibco	14190-094
Albumin fraction V (bovine serum albumin)	Carl Roth	8076.2
RPMI 1640	Lonza	12-918F
RPMI 1640 (no glucose)	Gibco	11879020
IL-2 human recombinant	PromoCell	C-61240
Casy-Ton	OMNI Life Science	5651808
Mesenchymal Stem Cell Adipogenic Differentiation Medium	Promocell	C-28016
Supplement mix Adipogenic Differentiation Medium	Promocell	C-39816
Mesenchymal Stem Cell Osteogenic Differentiation Medium	Promocell	C-28013
Supplement mix Osteogenic Differentiation Medium	Promocell	C-39813
Hoechst 33342	Invitrogen	H3570 917368
Geltrex™ LDEV-Free Reduced Growth Factor Basement Membrane Matrix	Gibco	A14132-01
N-Acetylcysteine (NAC)	Sigma	A9165
WZB-117 (3-hydroxy-benzoic acid, 3-fluoro-1,2-phenylene)ester	Cayman Chemicals	19900
Speed Coating Solution	PeloBiotech	PB-LU-000-0002-00

3.1.3 Cell culture media

Name	Composition
DMEM AB or DMEM AB NG (normal glucose 1 g/L)	500 ml DMEM normal glucose
	10% AB serum
	1% Penicillin/Streptomycin
	2% L-glutamine
DMEM AB HG (high glucose 4.5 g/L)	500 ml DMEM normal glucose
	10% AB serum
	1% Penicillin/Streptomycin
	2% L-glutamine
	4.5 g/L D-glucose
Complete ECGM-2 NG (normal glucose 1 g/L)	500 ml EBM (Endothelial basal medium)
	12.5 ml ECGM-2 supplement mix endothelial cell growth medium 2
Complete ECGM-2 HG (high glucose 4.5 g/L)	500 ml EBM
	12.5 ml ECGM-2 supplement mix endothelial cell growth medium 2
	4.5 g/L D-glucose
¼ ECGM-2 NG (normal glucose 1 g/L)	7.5 ml EBM
	2.5 ml ECGM-2 supplement mix endothelial cell growth medium 2
¼ ECGM-2 HG (high glucose 4.5 g/L)	7.5 ml EBM
	2.5 ml ECGM-2 supplement mix endothelial cell growth medium 2
	4.5 g/L D-glucose
Reduced RPMI 1640	500 ml RPMI 1640
	2.5% FBS
	1% Penicillin/Streptomycin
	2% L-glutamine
Glucose starvation medium	500 ml RPMI1640 (no glucose)
	1% Penicillin/Streptomycin
	2% L-glutamine
Full RPMI 1640	500 ml RPMI 1640
	10% FBS
	1% Penicillin/Streptomycin

3.1.4 Solutions

Name	Composition
Erythrocyte lysis buffer	1 mM EDTA
	1.55 mM NH_4Cl
	0.1 M NH_4HCO_3
Stopping Medium	50 ml DPBS
	10% FBS
PBS/EDTA	500 ml DPBS
	2mM EDTA
Freezing Medium	FBS
	10% DMSO

3.1.5 Cell transfection

3.1.5.1 Plasmids

Name	Reference
dTomato pHR′SIN-cPPT-SEW	Kindly provided by Prof. Patrick Maier, Department of Radiation Oncology, University Medical Centre Mannheim, Germany. See Appendix 8.1, Figure 40 for maps.
GFP pHR′SIN-cPPT-SEW	
pCMVDR8.91	
pMD.G	

3.1.5.2 Reagents

Product	Company	Catalog No.
LB Broth	Sigma	L3022
LB Broth with Agar	Sigma	L2897
E. Coli DH5alpha	Bioline	BIO-85025
SOC medium	Sigma Aldrich	S1797
Ampicillin	Calbiochem	2776677

EndoFree Palsmid Maxi Kit	Quiagen	12362
Metafectene	Biontex	T020-2.0
Na-butyrat	Sigma	B5887
PolyDLysine Hydrobromide	Sigma	27964-99-4
Polybrene	Sigma	107689
EcoRI	Thermo Science	ERO271
XBal	Thermo Science	ERO685
Tango Buffer	Fermentas	BY5
EcoRI Buffer	Thermo Science	B12
Agarose	Bioron	HS-LF45140050
Loading Dye	Invitrogen	R0611
Tris Base	Serva	37180
Acetic acid	J.T. Baker	6052
EDTA	Applichem	A3145,0500
TAE Buffer	40 mM Tris Base, 20 mM Acetic acid, 1mM EDTA	
Broth Culture medium	20g LB Broth in 1L of distilled water	
Culture plate Agar	35g LB Broth with Agar in 1L of distilled water	

3.1.6 Flow Cytometry

3.1.6.1 Flow cytometry solutions

Name	Composition
FACS Buffer	1L DPBS
	0.4% BSA
	0.02% NaN_3
MACS Buffer	1L DPBS
	2mM EDTA
	0.5% BSA
Cell wash	BD Catalog No. 349524

3.1.6.2 Fixation/Permeabilization Buffers

Product	Company	Catalog No.
Transcription Factor Buffer Set	BD Pharmingen	562574
IC Fixation Buffer	eBioscience	00-8222-49
Permeabilization Buffer 10x	Invitrogen	00-8333-56

3.1.6.3 Conjugated Antibodies

Antibody	Fluorochrome	Clone	Catalog No.	Brand
Anti-IDO	PE	eyedio	12-9477-42	eBioscience
Treg characterization				
Anti-CD4	FITC	RPAT4	555346	BD
AntiI-CD25	APC	M-A251	555434	BD
Anti-CD127	PE-Cy7	REA614	130-099-719	Miltenyi Biotec
Anti-FoxP3	PE	259D/C7	560046	BD
ASC characterization				
Anti-CD29	Alexa Fluor 488	TS2/16	303016	BioLegend
Anti-CD73	PE	AD2	550257	BD

Anti-CD90	APC	5E10	559869	BD
Anti-CD44	APC	IM7	103012	BioLegend
Anti-CD106	FITC	51-10C9	551146	BD
Anti-CD146	PE	TEA1/34	A07483	Beckman Coulter
Anti-CD3	FITC	UCHT1	300406	BioLegend
Anti-CD14	FITC	M5E2	555397	BD
Anti-235a	FITC	GA-R2	559943	BD
Anti-CD19	FITC	HIB19	555412	BD
Anti-CD45	FITC	HI30	555482	BD
Anti-CD34	PE	8G12	345802	BD
CD105	APC	SN6	17-1057-42	eBioscioence
Anti-CD15	FITC	HI98	555401	BD
Anti-CD31	APC	WM59	17-0319-73	EBioscience
Anti-CD133_1	APC	AC133	Miltenyi	BD
Anti-CD144	PE	TEA1/31	A07481	Beckman Coulter
Anti-HLA-DR	FITC	L234	307618	BioLegend
Anti-HLA-ABC	APC	G46-2.6	555555	BD
HUVEC characterization				
Anti-CD34	FITC	581	555821	BD
Anti-VEGF-R2	PE	89106	FAB357P	RnD
Anti-CD31	FITC	WM59	555445	BD
Anti-CD133/1	APC	AC133	130-090-826	Miltenyi
Anti-CD144	PE	TEA1/31	A07481	Beckman Coulter
Anti-CD105	APC	SN6-4	17-1057-42	eBioscience

Anti-CD45	FITC	HI30	555482	BD
Anti-CD146	PE	TEA1/34	A07483	Beckman Coulter
Anti-CD62P	APC	AK-4	550888	BD
Anti-CD14	FITC	M5E2	555397	BD
Anti-CD117	PE	104D2	332785	BD
Anti-CD62E	APC	68-5H11	551144	BD

3.1.6.4 Viability dyes and other reagents

Product	Company	Catalog No.
FcR blocking reagent (human)	Miltenyi Biotec	130-059-901
Fixable Viability dye eFluor780 (eF780)	eBioscience	65-0865-14
BD Horizon™ Violet Proliferation Dye 450 (VPD450)	BD	562158
Sytox Blue	Invitrogen	S34857
Sytox Red	Invitrogen	S34859
Carboxy-H_2DFFDA	Thermo Fisher Fisher	C13293
2-NBD Glucose (2-NBDG)	Cayman Chemicals	11046
Precision Count beads	BioLegend	424902

3.1.7 Immunofluorescence

3.1.7.1 Reagents

Product	Company	Catalog No.
DPBS (1X)	Gibco	14190-094
Paraformaldehyde (PFA)	Roth	0335.3
Triton x100	Sigma Aldrich	23,472-9

Albumin fraction V (bovine serum albumin)	Carl Roth	8076.2
DAPI	Sigma	1.24653
Mounting medium	ibidi	50001

3.1.7.2 Solutions

Name	Composition
2% PFA	50 ml DPBS
	1 ml PFA
0.1% Triton	50 ml DPBS
	50 µl Triton x100
2% BSA	50 ml DPBS
	1 ml Bovin serum albumin
0.1% BSA	50 ml DPBS
	50 µl Bovin serum albumin

3.1.7.3 Primary Antibodies

Product	Clone	Species	Type	Company	Catalog No.
Anti human-alpha smooth muscle actin	ASM-1	Mouse	Monoclonal IgG_{2a}	PROGEN	65001
Anti-human NG-2	9.2.27	Mouse	Monoclonal IgG_{2a}	Santa Cruz	sc-80003

3.1.7.4 Secondary Antibody

Product	Clone	Species	Type	Company	Catalog No.
Anti mouse-alexa Fluor 488 $F(ab')_2$	Polyclonal	Goat	IgG, IgM (H+L)	Invitrogen	A10684

3.1.8 Protein/Cytokine detection

3.1.8.1 Reagents

Product	Company	Catalog No.
L-Kynurenine	Santa Cruz	Sc-202688
Trichloroacetic acid	Roth	8789.2
para-Dimethylaminobenzaldehyde	Santa Cruz	Sc202888
Acetic acid	J.T.Baker	6052
DPBS	Gibco	14190-094
Tween-20	Serva	37470.01
Albumin Fraction V (bovine serum albumin)	Roth	8076.2
Color Reagent A (H_2O_2)	R&D Systems	DY999
Color Reagent B (Tetramethylbenzidine)	R&D Systems	DY999
2N H_2SO_4 (ELISA Stop soultion)	Sigma	1.60313
ELISA Wash Buffer	0.05% Tween-20 in DPBS	
ELISA Dilution Reagent	1% BSA in DPBS, 0.22 µm filtered	

3.1.8.2 Kits

Product	Company	Catalog No.
BD Cytometric Bead Array (CBA) Human Th1/Th2/Th17 Cytokine kit	BD	560484
LEGENDplex Human Angiogenesis Panel 1 (10-plex)	BioLegend	740698
LEGENDplex Human Th Cytokine Panel (13-plex)	BioLegend	740722
Human TGF-β1 DuoSet ELISA	R&D Systems	DY240-05
Human TNF-α DuoSet ELISA	R&D Systems	DY210-05
Human CCL-18/PARC DuoSet ELISA	R&D Systems	DY394-05
Human Angiogenesis Array C1000	RayBiotech	AAH-ANG-1000-4

3.1.9 Consumables

Product	Company	Catalog No.
96-well cell culture plate	Eppendorf	0030 790.119
24-well cell culture plate	Thermo Fisher	142475
12-well cell culture plate	Thermo Fisher	150628
6-well cell culture plate	Thermo Fisher	140675
Transwell inserts (pore size 0.4 µm transparent ThinCerts-TC inserts)	Greiner bio-one	657641
175 cm^2 cell culture flasks	Thermo Fisher	159910
25 cm^2 cell culture flasks	Thermo Fisher	156367
96-well black cell culture plate	Perkin Elmer	6005550
8-well µ-slide	ibidi	80826
Petri dish	Corning	353803
50 ml Cell star tubes	Greiner bio-one	188271
15 ml Cell star tubes	Greiner bio-one	227261
1000 µl sterile filter tips	SurPhob	VT0263X
200 µl sterile filter tips	SurPhob	VT0243X
10/20 µl sterile filter tips	Star Lab	S1120-3710
10 ml PD sterile tips	brand	631060
5 ml PD sterile tips	brand	702390
2.5 ml PD sterile tips	brand	702388
1.25 ml PD sterile tips	brand	702386
25 ml serological sterile pipettes	Star Lab	190105-071
10 ml serological sterile pipettes	Star Lab	180720-070
5 ml serological sterile pipettes	Star Lab	180806-069

100 µm EASY strainer	Greiner	542000
Rotilabo syringe filters 0.22 µm	Roth	SE2M035I07
0.2 ml Thin tubes with flat caps	Thermo Fisher	AB0622
5 ml Polystyrene round FACS bottom tubes	Corning	352052
CASY cup	OMNI Life Science	5651794
CASY Ton	OMNI Life Science	5651808
50 ml syringes	Dispomed	21050
Vivaspin 20, 100.000 MWCO PES	Sartorius	VS2041

3.1.10 Laboratory equipment

Device	Name	Provider
Centrifuge	ROTINA 450	Hettich Zentrifugen
Centrifuge	ROTINA 450R	Hettich Zentrifugen
Cell counter	CASY	OMNI Life Science
Cell counter	Nucleo Counter	Chemometec
Plate washer	Well wash 4MK2	Thermo Fisher
Small Centrifuge	Minispin	Eppendorf
Microscope	Axiovert 100	ZEISS
Microscope Camera	AxioCam M Rc	ZEISS
Live imaging microscope	IncuCyte Zoom live imaging device	Essen BioScience, Ltd.
Laminar flow hood	Hera safe	Thermo Fisher
Chemical flow hood	Airflow-Control EN14175	Caspar and Co. Labora
Cell culture incubator		Binder
Microplate reader	TECAN infinite M200PRO	Tecan

Flow cytometer	BD FACS Canto II	BD
Flow cytometer	FACS Aria IIu	BD
Confocal microscope	SP5 MP	Leica
Thermal cycler	DNA Engine Peltier thermal cycler	BIO-RAD
Chemiluminescent detector	UVP Epi Chemi II Darkroom	UVP Inc.

3.1.11 Software for data analysis

Software	Version	Company
FlowJo	10	FlowJo, LLC, Ashland, OR, USA
FlowJo	7	FlowJo, LLC, Ashland, OR, USA
GraphPad Prism	7	GraphPad Software Inc. San Diego, USA
ImageJ	1.51j8	NIH
i-Control	1.10	TECAN
LEGENDplex™ Data Analysis Software	8.0	BioLegend
FCAP Array Software	3.0	BD
IncuCyte S3 software	S3	Essen BioScience, Ltd.
DoubleDigest Calculator Free Software		Thermo scientific

3.2 Methods

Methods are here gathered following the four different aims presented in section 2:

(1) Aim 1: Evaluating effects of hyperglycemia on cellular phenotype;

(2) Aim 2: Evaluation of ASC proangiogenic potential under hyperglycemia;

(3) Aim 3: Evaluation of pericyte-like function of ASC;

(4) Aim 4: Evaluation of ASC immunomodulatory potential under hyperglycemia.

3.2.1 Methods Aim 1: Evaluating effects of hyperglycemia on cellular phenotype

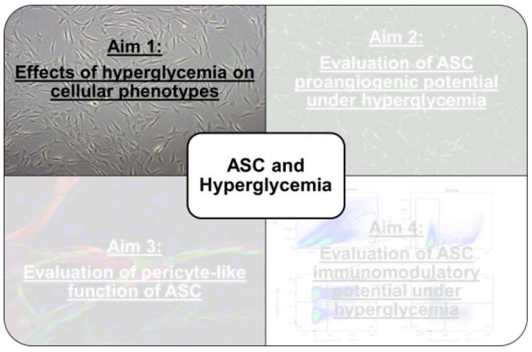

To investigate the impact of glucose on ASC and HRMVEC, cultures and experiments in NG/HG culture media were established. ASC were, immediately after their isolation, continuously cultured in either NG or HG media; they were fully characterized following ISCT guidelines and compared in regard of their cell growth, differentiation potential and cell surface marker expression.
Hyperglycemia-mediated effects were also evaluated on HRMVEC cell growth and angiogenic potential. For both ASC and HRMVEC intracellular oxidative state and glucose uptake were assessed upon HG exposure.

3.2.1.1 Adipose derived mesenchymal stromal cells

Adipose derived mesenchymal stromal cells were isolated from multiple donors after having obtained informed consent (Mannheim Ethics Commission II; vote numbers 2006-192 N-MA).
Briefly, raw lipoaspirate was washed with DPBS to remove cellular debris and red blood cells and centrifuged at 420g for 10 minutes. Washed lipoaspirate was treated with NB6 collagenase (final concentration 0.15 PZU/ml) in 1:1 dilution with pure DMEM and left for 50 minutes at 37°C under gentle agitation. After incubation, collagenase was inactivated with an equal volume of DMEM 10% FBS and the solution was centrifuged at 1200g for 10 minutes, to obtain the high-density stromal vascular fraction (SVF). Supernatant was aspirated and incubated for 10 minutes at room temperature (RT) with erythrocytes lysis buffer, to eliminate the excess of red blood cells. Another centrifugation step followed and afterwards, the SVF-pellet was resuspended in pure DMEM. The SVF-pellet was filtered through a 100 µm nylon mesh filter and again centrifuged. The remaining SVF was resuspended in DMEM AB NG or HG and plated in a T25 or T175 (in accordance to pellet size), incubated at 37°C with 5% CO_2. The day after, flasks were extensively washed with DPBS prior to media change.
After isolation, ASC were routinely cultured in T175 flasks at 200 cells/cm^2 in DMEM AB NG and HG and therefore named as ASC_{NG} and ASC_{HG}, respectively.

Upon 70-80% confluence, ASC were passaged with Trypsin/EDTA, counted using a CASY cell counter and seeded according to the experimental conditions. Cell morphology was constantly monitored by microscope observation.
ASC growth rate was monitored recording cell number at every passage. Cell Doublings (CD) and Doubling Time (DT) were calculated as follow:

$$\text{Cell Doublings (CD)} = \frac{Log10\ (Fcn) - Log10\ (\text{Icn})}{Log10\ (2)} \qquad \text{Doubling Time (DT)} = \frac{Culture\ duration}{CD}$$

Where: Fcn is final cell number and Icn initial cell number.
All cells were cryopreserved in FBS with 10% DMSO in liquid nitrogen, thawed and cultivated for at least one passage before use.
Before use, each newly generated batch of $ASC_{NG\text{-}HG}$ was thoroughly characterized based on growth potential, differentiation potential and expression/non-expression of MSC-specific surface markers, mycoplasma testing, microbial and viral sterility testing (the latter at German Red Cross Blood Donor Services Baden-Württemberg – Hessen, Institute Mannheim).

3.2.1.1.1 ASC characterization

3.2.1.1.1.1 Adipogenic differentiation

To assure ASC differentiation capacity, ASC were cultured in adipogenic differentiation medium (Mesenchymal Stem Cell Adipogenic Differentiation Medium) and in DMEM AB NG or HG media as control. On day 14th, $ASC_{NG\text{-}HG}$ were fixed in 10% PFA for 30 minutes, washed and incubated with Hoechst-33342 (1:100 final concentration, 10 mg/ml stock) for other 30 minutes. Hoechst fluorescence (excitation/emission (nm): 354/442) was measured on a plate reader and considered as baseline for normalization. Adipogenic differentiation was measured with AdipoRed Assay following the manufacturer's instructions. Briefly, after washing with DPBS, Adipored (5 µl/well in a 96 well plate) diluted in 200 µl of DPBS was added and incubated in the dark for 15 minutes. After incubation, AdipoRed fluorescence was measured on a plate reader at 485/572 nm. AdipoRed OD (optical density) were normalized on Hoechst OD and presented as Normalized Ratio.

3.2.1.1.1.2 Osteogenic differentiation

ASC were cultured in osteogenic differentiation medium (Mesenchymal Stem Cell Osteogenic Differentiation Medium) and in DMEM AB NG or HG media as control. On day 14th, ASC_{NG-HG} were fixed in 10% PFA for 30 minutes, washed and incubated with Hoechst-33342 (1:100 final concentration, 10 mg/ml stock) for other 30 minutes. Hoechst fluorescence (excitation/emission (nm): 354/442) was measured on a plate reader and considered as baseline for normalization. Osteogenic differentiation was measured with Osteoimage Mineralization Assay following the manufacturer's instructions. Briefly, after washing with Wash Buffer, Osteoimage staining reagent (1:100 final dilution in Staining Reagent Dilution Buffer) was added to the cells and left in incubation for 30 minutes at RT. After incubation, staining reagent was removed and Wash Buffer was used to perform three washing steps. Fluorescence was measured on a plate reader at 492/520 nm. Osteoimage OD were normalized on Hoechst OD and presented as Normalized Ratio.

3.2.1.1.1.3 Immunophenotype

ASC from multiple donors were analyzed at passage 2 for their immunophenotype. $1x10^5$ ASC were collected in FACS tubes and resuspended in FACS buffer. 10 µl of FcR blocking reagent were added to each tube and incubated at 4°C for 5 minutes. Next, staining with the following anti-human antibodies was performed: Anti-CD29 Alexa Fluor 488, Anti-CD73-PE, Anti-CD90-APC, Anti-CD44-APC, Anti-CD106-FITC, Anti-CD146-PE, Anti-CD3-FITC, Anti-CD14-FITC, Anti-235a-FITC, Anti-CD19-FITC, Anti-CD45-FITC, Anti-CD34-PE, Anti-CD105-APC, Anti-CD15-FITC, Anti-CD31-APC, Anti-CD133_1-PE, Anti-CD144-PE, Anti-HLA-DR-FITC and Anti-HLA-ABC-APC. All antibodies were used in optimal concentrations after proper titration. After staining, cells were incubated 20 minutes in the dark at 4°C. Prior to be analyzed, cells were washed in Cell wash twice and finally resuspended in SYTOX blue dead cell stain (final dilution 1:2000 in FACS buffer). 10,000 viable cells were acquired with BD FACS Canto and .fcs files analyzed with FlowJo 10 software.

3.2.1.2 Human retinal microvascular endothelial cells (HRMVEC)

Human retinal microvascular endothelial cells (HRMVEC) were purchased from PeloBiotech. Cells were cultured following the provider's instructions. Briefly, a frozen vial of HRMVEC was thawed in a 37°C water bath. The cell suspension was transferred

in a 15 ml tube containing 9 ml of complete ECGM-2 and centrifuged at 200g for 5 minutes. Supernatant was discarded, cell were resuspended in complete ECGM-2 and placed into one T25 previously coated with Speed Coating Solution. Cells were maintained at 37°C, 5% CO_2. Cell morphology was constantly monitored by microscope observation. Upon confluence, HRMVEC were first washed with DPBS and then treated with trypsin/EDTA for 5 minutes. Trypsin was stopped with stopping medium, cells collected and counted with the CASY cell counter. Cells were cultured in complete ECGM-2 at $4x10^4$ cells/cm^2 for normal maintenance or seeded according to the experiment.

All cells were cryopreserved in FBS with 10% DMSO thawed and cultivated for at least one passage before use.

To test hyperglycemia-mediated effects on cell growth, HRMVEC were cultured in HG ECGM-2 medium. Hypothesizing that the high content of growth factors in the complete medium might hide HG detrimental effects, cells were also cultured in growth factor-reduced medium (¼ ECGM-2) and cell growth was assessed.

3.2.1.2.1 HRMVEC angiogenic potential: basement matrix angiogenesis assay (BMA assay)

17,000 HRMVEC/well were seeded in a 96 well plate on top of 50 µl/well layer of Geltrex™ LDEV-Free Reduced Growth Factor Basement Membrane Matrix, in ¼ ECGM-2 NG and HG. Phase contrast pictures were taken every 30 minutes with the IncuCyte Zoom live cell imaging system. Tube length and number of junctions were measured after 4 hours, analyzing pictures with the Angiogenesis tool plug-in on ImageJ software (Figure 4).

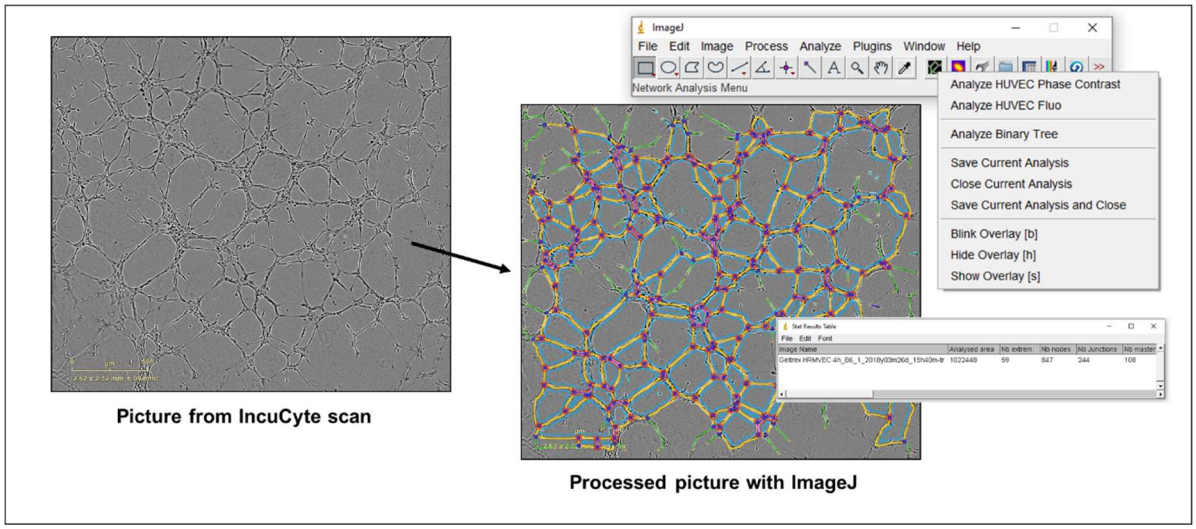

Figure 4 Representative picture of analysis of BMA assay. Pictures collected at 4 hours from IncuCyte are analyzed with the Angiogenesis tool plug-in on ImageJ software. The tool processes the image and quantifies tube formation giving multiple parameters. For our analysis "total length" and "number of junctions" were used.

3.2.1.3 Measurement of intracellular oxidative stress (total reactive oxygen species measurements)

20,000 ASC_{NG} and ASC_{HG} per well or $1x10^5$ HRMVEC/well were seeded in 12-well plate in reduced RPMI 1640 with/without HG. After overnight incubation, cells were treated/untreated for 1 hour with the antioxidant N-Acetylcysteine (NAC, 1mM final concentration). Carboxy-H_2DFFDA (10µM final concentration) was then added for 45 minutes. Afterwards, cells were harvested with trypsin/EDTA, collected in FACS tubes and resuspended in FACS Buffer supplemented with SytoxRed (1:2000 final dilution). Cell suspensions were immediately analyzed at BD FACS Canto II. Fluorescence of Carboxy-H_2DFFDA was measured in linear scale and .fcs files analyzed with FlowJo 10 software. Carboxy-H_2DFFDA MFI on viable cells was analyzed and reported as ratio normalized on ASC_{NG} and NG HRMVEC.

In regard of ROS measurement with carboxy-H_2DFFDA or DCF, DCFDA-derived products it is important to give some specifications. Indeed, as carboxy-H_2DFFDA penetrates in cells, it is subjected to oxidation by several cytoplasmic ROS species such as hydrogen peroxide, organic hydroperoxides, nitric oxide and peroxynitrite, which turn it into being fluorescent. Moreover, its oxidation has been found to be influenced by glutathione (GSH) [154]. Thus, carboxy-H_2DFFDA oxidation results to be dependent on several intracellular oxidative stressors as well as anti-oxidant mechanisms. Therefore, as suggested by Jakubowski and Bartosz "…increased H_2DCF oxidation should be referred to as an index of oxidative stress rather than of

increased ROS formation unless a more precise statement can be fully justified." [154]. In line with this, in our work, decreases/increases in total ROS measurement are interpreted as decreases/increases in the overall intracellular oxidative stress level.

3.2.1.4 Measurement of glucose uptake

To monitor glucose uptake in NG and HG cultivated cells, 2-NBD glucose (2-NBDG) was applied following the manufacturer´s instructions. Briefly, 10,000 ASC_{NG-HG}/well and 20,000 HRMVEC/well were seeded in a 96 black well plate and left overnight in NG or HG culture conditions. The next day, ASC and HRMVEC were put 2 hours in glucose starvation medium and incubated at 37°C. To inhibit glucose uptake, samples were treated during starvation with the GLUT-1 inhibitor WZB-117 at 100 µM and 10 µM final concentration for ASC and HRMVEC, respectively. After 2 hours, 2-NBDG was added for 10 minutes at a final concentration of 150 µg/ml for ASC and 25 µg/ml for HRMVEC. 2-NBDG fluorescence was detected with a plate reader using 485 nm excitation and 535 nm emission wavelengths. At last, Hoechst staining (1:2000 final concentration in DPBS) was performed and used to normalize 2-NBDG signals. Data are reported as ratio calculated on ASC_{NG} and NG HRMVEC.

3.2.2 Methods Aim 2: Evaluation of ASC proangiogenic potential under hyperglycemia

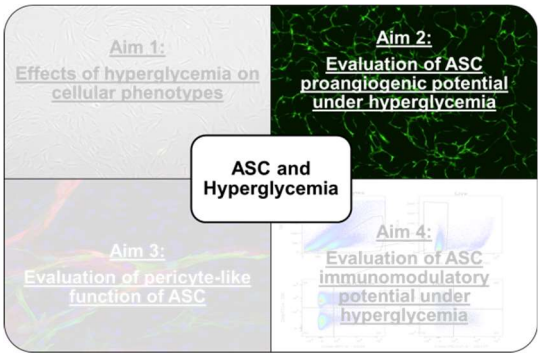

The proangiogenic potential of ASC_{NG-HG} was evaluated establishing cocultures with HUVEC and HRMVEC in NG/HG culture media. To monitor tube formation, both HUVEC and HRMVEC were transfected with lentivirus expressing either green fluorescent protein (GFP) or dTomato fluorescent protein. Supernatants collected from ASC:HUVEC and ASC:HRMVEC were screened for proangiogenic factors comparing them in respect of the culture medium (NG vs HG) and ASC (ASC_{NG} vs ASC_{HG}).

3.2.2.1 Human Umbilical Vein Endothelial Cells (HUVEC)

Human umbilical vein endothelial cells (HUVEC) were isolated from multiple donors after having obtained informed consent (Mannheim Ethics Commission II; vote numbers 2010-262 N-MA).

Cord blood was first washed out using DPBS and the cord placed in a glass petri dish. Then 1 cm from each end was cut. A buttoned cannula was inserted in the vein, fixed with a clip and the whole cord blood fixed to a vertical support. The cannula was used to flush solutions inside the vein. A 50 ml syringe filled with DPBS was used to flush the vein and 100 U/ml of collagenase (final concentration) diluted in EBM were prepared in a 10 ml syringe. As this solution was pushed through the cord vein, the opposite end of the cord was clipped, and the whole collagenase solution pushed through. The buttoned cannula was then closed and the whole cord put into a glass backer with warm DPBS. This was incubated at 37°C for 1 hour. After incubation, the cord was cut at the lower end and the fluid poured into a 50 ml tube. The vein was flushed with 10 ml of EBM and the solution collected. The tube was then centrifuged 10 minutes at 420g and the supernatant aspirated. The pellet was resuspended in complete ECGM-2 and seeded in a T25 cell culture flask. Cells were incubated at 37°C with 5% CO_2.

After isolation, HUVEC were routinely cultured in T75 flaks at $8x10^3$ cells/cm^2 in complete ECGM-2. Cell characterization including morphological and growth assessment as well as immunophenotypic characterization were performed as previously reported [155].

Upon confluence, HUVEC were passaged with Trypsin/EDTA, counted and seeded according to the experimental conditions. Cell morphology was constantly monitored by microscope observation.

All cells were cryopreserved in FBS with 10% DMSO in liquid nitrogen, thawed and cultivated for at least one passage before use.

HUVEC were also transfected with GFP and dTomato lentiviruses (used for immunofluorescence) to obtain green/red fluorescent cells (see section 3.2.2.2).

3.2.2.1.1 HUVEC characterization

HUVEC from multiple donors were analyzed for their surface cell markers. $1x10^5$ HUVEC were collected in FACS tubes and resuspended in FACS buffer. 10 µl of FcR blocking reagent were added to each tube and incubated at 4°C for 5 minutes. Next,

staining with the following anti-human antibodies was performed: Anti-CD34-FITC, Anti-VEGF-R2-PE, Anti-CD133/1-APC, Anti-CD31-FITC, Anti-CD144-PE, Anti-CD105-APC, Anti-CD45-FITC, Anti-CD146-PE, Anti-CD62P-APC, Anti-CD14-FITC, Anti-CD117-PE and Anti-CD62E-APC. All antibodies were used in optimal concentrations after proper titration. After staining, cells were incubated 20 minutes in the dark at 4°C. Prior to be analyzed, cells were washed in Cell wash twice and finally resuspended in SYTOX blue dead cell stain (final dilution 1:2000 in FACS buffer). 10,000 viable cells were acquired with BD FACS Canto and .fcs files analyzed with FlowJo 10 software.

3.2.2.2 Production of fluorescent cells

To monitor tube formation in the angiogenesis coculture assays, HUVEC and HRMVEC were stably transfected with a lentiviral vector expressing GFP. In addition, HUVEC and HRMVEC were also transfected to express dTomato fluorescent protein. These cells were used in angiogenesis cocultures established for Aim 3 to determine pericyte-like markers on ASC.

3.2.2.2.1 Plasmid amplification

To perform plasmid amplification, LB medium as broth culture medium and LB-medium with agar were prepared. Both solutions were autoclaved at 121°C for 15 minutes and after cooling, ampicillin was added (final concentration 100µg/ml). LB-medium with agar was poured in petri dishes to create selective bacterial growth plates.

Competent E. coli, were gently thawed on ice and 50µl were moved into four pre-chilled Eppendorf tubes. 400 ng of each plasmid (dTomato or GFP, pMD.G and pCMVDR8.91; Appendix 8.1.1) were added to the 50µl of bacterial suspension and thoroughly mixed. These mixtures were incubated 15 minutes in ice. Afterwards, a heat shock at 42°C for 42 seconds was provided, followed by 5 minutes of incubation in ice. 300µl of SOC medium were added to each tube, which was incubated on a thermomixer for 1 hour at 37°C with 300 rpm shaking. After incubation, 50µl of transfected bacterial suspension were plated on LB-agar plates with ampicillin and left overnight upside down at 37°C.

The following day, one bacterial colony was picked up from each of four selective plates and transferred into Erlenmeyer flasks with 200 ml of LB-medium supplemented

with ampicillin (final concentration 100µg/ml) to expand the bacterial culture. Flasks were incubated overnight at 37°C under 200 rpm shaking.

The day after, plasmid DNA was isolated with the EndoFree Plasmid Maxi Kit (Qiagen), following the manufacturer's instructions. Briefly, 100ml of bacterial cultures from each plasmid were centrifuged in 50ml tubes at 6,000g for 15 minutes at 4°C. Pellets from the same bacterial culture were combined and thoroughly resuspended in 10 ml of P1 buffer. Next, 10 ml of P2 buffer were added, the tube inverted for 5 times and incubated at room temperature (RT) for 5 minutes. To enhance genomic DNA precipitation, 10 ml of P3 buffer were added to the lysate solution and mixed vigorously. The lysate was then transferred to the QIAfilter Cartridge and incubated 10 minutes at RT. After inserting the plunger, the lysates were filtered into a 50 ml tube. 2.5 ml of ER Buffer were added to the filtrate lysates, mixed and incubated on ice for 30 minutes. Filtered lysates were applied to the QIAGEN-tip and the flow through discarded. After washing step with QC Buffer, plasmid DNA was eluted with the application of 15 ml of QN Buffer and collected into 50 ml tubes. DNA was precipitated with 0.7 volumes of isopropanol and the solution mixed and centrifuged at 15,000g for 30 minutes at 30°C. Subsequently, pellets were washed with 70% ethanol and centrifuged at 15,000g for 10 minutes. Pellets were air dried and dissolved in 100µl of distilled water and stored at -30°C.

To determine the yield of plasmid DNA extraction, DNA concentration was determined by spectrophotometry with 260/280 nm readings.

3.2.2.2.2 Plasmid validation

To validate plasmid amplification and extraction, all four plasmids (dTomato, GFP, pMD.G and pCMVDR8.91) were crosschecked with enzymatic restriction on agarose gel to check if the number of fragments after restriction was as expected, according to the plasmid maps. Restriction enzymes and related buffer are reported in the following table.

	dTomato	**GFP**	**pMD.G**		**pCMVDR8.91**	
			Mix 1	Mix 2	Mix 1	Mix 2
Plasmid DNA	1 µg	1 µg	1 µg	1 µg	1 µg	1 µg

Buffer	Tango 2X	Tango 1X	EcoRI buffer	Tango 2X	Tango 2X	EcoRI buffer
Enzyme 1	EcoRI	-	EcoRI	EcoRI	EcoRI	EcoRI
Enzyme 2	XBal	XBal	-	XBal	XBal	-
H_2O	Up to 20µl total volume	Up to 20µl total volume	Up to 20µl total volume	Up to 20µl total volume	Up to 20µl total volume	Up to 20µl total volume

These mixtures were incubated for 1 hour at 37°C. After incubation, 10µl of each mixture sample were mixed with 2 µl of Loading Dye. 10 µl of this mixture were loaded on 1% agarose gel and run for 45 minutes at 150 V.
Once checked that the enzymatic restriction gave the number of expected fragments, plasmids were used to produce viral particles (Appendix 8.1.2., Figure 41).

3.2.2.2.3 Lentivirus production

293FT cells were kindly provided by Prof. Patrick Maier (Department of Radiation Oncology, University Medical Centre Mannheim, Germany) and used as packaging cell line to produce viral particles. Cells were maintained in DMEM 10% FBS without antibiotics at 37°C, 5% CO2. Upon confluence, cells were washed with DPBS and treated with trypsin/EDTA. Trypsin was blocked after 5 minutes with stopping media and detached cells collected in a 15 ml tube. Cells were counted, and seeded $2x10^4$ cells/cm^2 for normal maintenance or according to the experimental condition. All cells were cryopreserved in FBS with 10% DMSO, thawed and cultivated for at least three passages before use.
Prior to use, Petri dishes were coated with poly-D-Lysine (final concentration 0.1 mg/ml in DPBS) and washed. $5x10^6$ 293FT/petri dish were seeded in 14 ml of DMEM 10% FBS and left overnight at 37°C. The next day, cells were transfected with the following procedure. 4.4 µg of lentiviral plasmid (GFP or dTomato), 3.4 µg of pCMVDR8.91 and 2.2 µg of pMD.G (overall 10 µg of plasmid/petri dish) were mixed in pure DMEM without additives. Separately, a solution of pure DMEM without additives and metafectene (3.2% final concentration) was prepared. The two solutions were mixed 1:1 and added dropwise on top of the cell monolayer. Treated cells were incubated overnight at 37°C. The next day, cell medium was changed twice: in the morning, with DMEM 10% FBS supplemented with Na-butyrate (10 mM final concentration) and in the evening with DMEM without additives. The day after, supernatants were collected form each petri dish and filtered through a 0.44 µm filter. Viral supernatants were concentrated using

Vivaspin-tubes under 3000 rpm centrifugation at 4°C, until a volume of 1 ml was obtained. Viruses were stored in 50 µl aliquots at -80°C.

3.2.2.2.4 HUVEC/HRMVEC transfection and selection

Lentiviruses containing dTomato or GFP inserts were used to transfect HUVEC and HRMVEC with the following procedure. $1x10^4$ HUVEC or HRMVEC/well were seeded in a 24 well plate in six replicates in ECGM-2 media and left overnight at 37°C. The day after, transfection medium was prepared as follow. Solutions of pure GFP or dTomato lentivirus were diluted 1:100 in ECGM-2 media supplemented with polybrene (8 µg/ml final concentration). This transfection medium was added to the cells and left for an overnight incubation. The next day, transfection medium was replaced with fresh ECGM-2 in which cells were left for two days. Cells were later harvested with trypsin/EDTA and prepared for sorting. They were first stained with Sytox Red and Blue for viability discrimination and GFP/dTomato positive cells were sorted with FACS Aria IIu. A representative sorting scheme for GFP HUVEC is reported in Appendix 8.1.3, Figure 42. After sorting, GFP/dTomato HUVEC or HRMVEC were cultured following normal culture conditions.

3.2.2.3 Coculture angiogenesis assay

30,000 ASC_{NG-HG}/well were seeded in a 96 well plate in ECGM ¼ Medium NG or HG for 1 hour. Then, 5,000 $HUVEC_{GFP}$ or $HRMVEC_{GFP}$ were seeded on top of the ASC monolayer. Cocultures were incubated for 72 hours. Phase contrast and fluorescent pictures were taken every 4 hours with IncuCyte Zoom live imaging device. Tube formation was measured with the IncuCyte S3 software, through quantitative kinetic processing metrics derived from time-lapse image acquisition and presented as total tube length per square centimeter (mm/mm²) over time (Figure 5). After 72 hours of coculture, CM of ASC_{NG-HG} coculture was collected and frozen at -80°C.

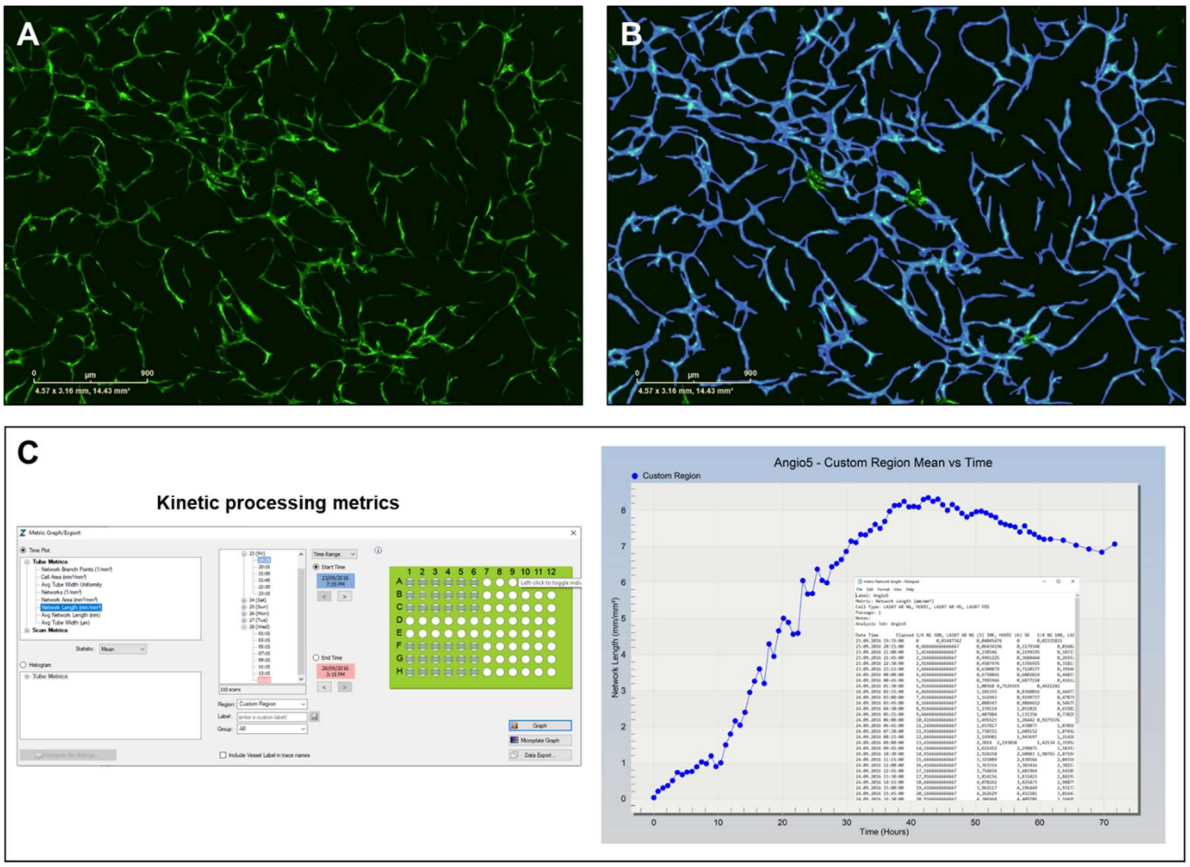

Figure 5 Representative image of IncuCyte S3 software quantification of total tube length in a coculture angiogenesis assay. A) Fluorescent images are taken from each well at the desired time point. B) Analysis of angiogenesis: the software provides a metric for network length analysis. Parameters are defined by a customable processing definition, which is visualized as a blue mask. C) All pictures are analyzed over time and kinetic representation of the assay is provided as a graph and related raw data.

To specifically test CM from these cocultures under similar conditions as used for assessing ROS (paragraph 3.2.1.3) $4x10^5$ $ASC_{NG\text{-}HG}$ /well were seeded in a 24 well plate in RPMI 1640 with 2.5% FBS in HG for 1 hour. Afterwards, $2.4x10^4$ $HRMVEC_{GFP}$ were added on top of the ASC monolayer. After 72 hours of coculture, supernatants were collected, centrifuged at 420g for 10 min and freshly used in a BMA assay (paragraph 3.2.2.5). Phase contrast pictures were taken every 30 minutes with the IncuCyte Zoom system. Tube length was measured after 4 hours, analyzing pictures with the Angiogenesis tool plug-in on ImageJ software.

3.2.2.4 Detection of proangiogenic growth factor in angiogenesis coculture supernatants

Supernatants from angiogenesis cocultures were analyzed with two flow-cytometry based kits for detection and quantification of proteins involved in angiogenesis: the

Human Angiogenesis Array C1000 and the LEGENDplex Human Angiogenesis Panel 1.

3.2.2.4.1 Human Angiogenesis Array C1000

CM collected from ASC:HUVEC coculture angiogenesis assays were analyzed with the human angiogenesis antibody array kit (RayBiotech, AAH-ANG-1000-4), following the manufacturer´s instructions. Briefly, each membrane was incubated with blocking buffer for 30 minutes at RT. After blocking, 1 ml of undiluted conditioned media pooled from four different experiments was added and incubated overnight at 4°C. Membranes were washed 5 times with wash buffer and subsequently incubated for 2 hours with the biotinylated antibody cocktail. As the last step before chemiluminescence detection, two hours incubation with HRP-Streptavidin was performed. Chemiluminescence was measured with a chemiluminiscent detector (UVP Epi Chemi II Darkroom). Signal intensities on membranes were analyzed with the Protein Array Analyzer plug-in on ImageJ software. A representative picture of membranes analysis with ImageJ is reported below (Figure 6).

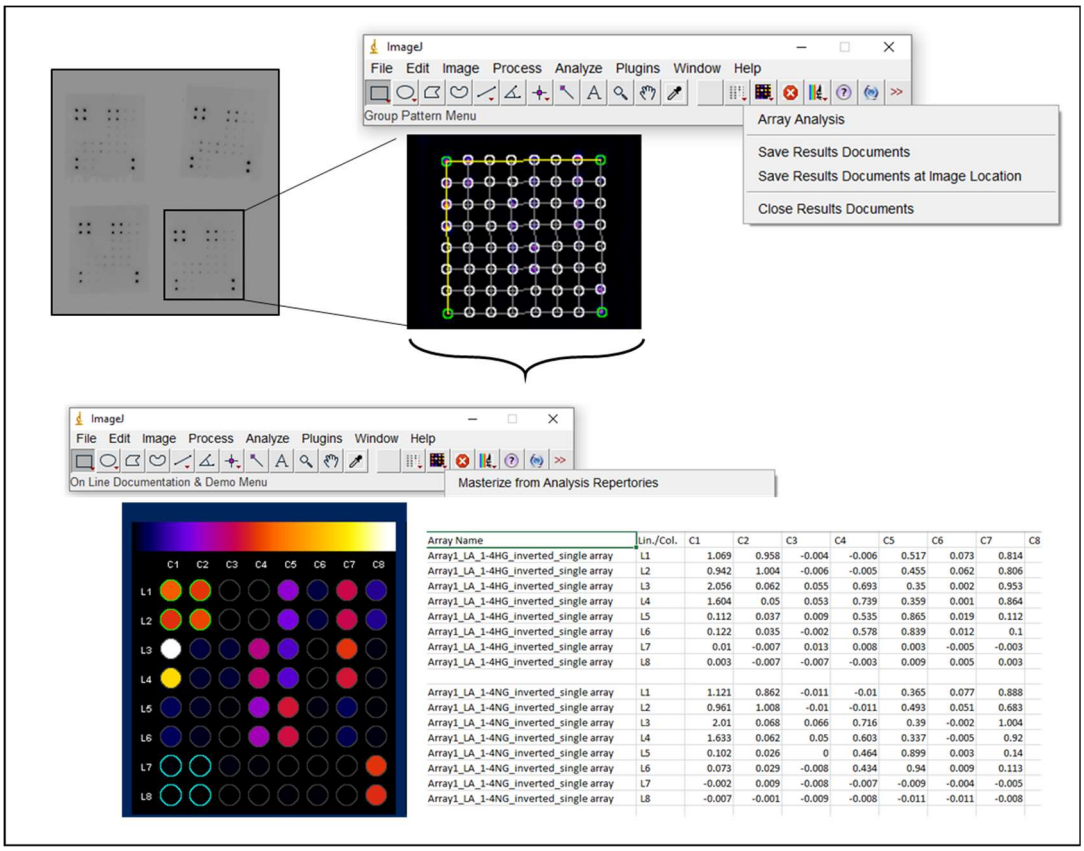

Figure 6 Analysis of membranes of the Human Angiogenesis antibody array kit (RayBiotech, AAH-ANG-1000-4). Images of membranes were taken with a chemiluminiscent detector and each single membrane was analyzed as follow. Positions of spots are first defined in the matrix as well as blank, positive and negative controls. Next with

the function “Masterize” matrixes are normalized and analyzed. Numerical values of spots´ intensities are given as results.

3.2.2.4.2 LEGENDplex Human Angiogenesis Panel 1

CM collected from angiogenesis assays were analyzed with the LEGENDplex Human Angiogenesis Panel 1 (10-plex; Cat. No. 740698).

Briefly, standards were reconstituted in Assay buffer and 1:4 serial dilutions were prepared to obtain an 8-points standard curve. A V-bottom plate was loaded first with 15 µl/well of samples and standards in a 1:1 dilution with Assay Buffer and then 15 µl of Premixed Beads were added to each well. The plate was sealed and incubated for 2 hours at RT under 800 rpm agitation. After incubation, each well was washed with 150 µl of Wash Buffer, followed by 5 minutes centrifugation at 250g. The plate was again decanted, washed and centrifuged prior to the addiction of Detection Antibody (15 µl/well). 1 hour of RT incubation under 800 rpm shaking followed. Afterwards, SA-PE was added in each well and incubated 30 minutes at RT with 800 rpm agitation. Finally, the plate was washed twice and the content of each well resuspended in 150 µl of Wash Buffer. Each probe was transferred in FACS tube prior to BD FACS Canto II analysis. Data were acquired limiting the acquisition rate on 300 beads/analyte.

Data analysis was performed with the LEGENDplex™ Data Analysis Software according to the manufacturer’s instructions.

3.2.2.5 Assessing the proangiogenic potential of coculture conditioned medium

17,000 HRMVEC/well were seeded in a 96 well plate on top of 50 µl/well layer of Geltrex™ LDEV-Free Reduced Growth Factor Basement Membrane Matrix. To maintain the same culture condition of ROS measurement (paragraph 3.2.1.3), BMA assay was set also in reduced RPMI medium (supplemented with 2.5% FBS). The following conditions were tested: (1) NG, (2) HG, (3) NG+NAC (final concentration 1mM), (4) HG+NAC (5) CM from coculture angiogenesis assay, (6) CM from ASC monoculture. CM were always used freshly after harvesting. Phase contrast pictures were taken every 30 minutes with the IncuCyte Zoom live imaging device. Tube length was measured after 4 hours, analyzing pictures with the Angiogenesis tool plug-in on ImageJ software.

3.2.3 Methods Aim 3: Evaluation of pericyte-like function of ASC

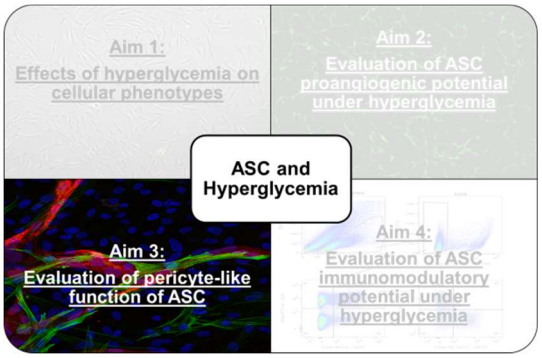

Immunofluorescent staining was used to evaluate the expression of pericyte markers in ASC cocultured with HUVEC and HRMVEC. To compare pericytes to ASC in regard of their proangiogenic potential, coculture angiogenesis assays with HUVEC/HRMVEC and pericytes were established in NG/HG culture medium.

3.2.3.1 Coculture immunofluorence

To perform immunofluorescence, coculture angiogenesis assays were set on 8-well µ-slides as follow. $1x10^5$ ASC/well were seeded in ECGM ¼ Medium NG or HG for 1 hour. Then, $5.5x10^4$ $HRMVEC_{GFP}$ were added on top of the ASC monolayer in a total volume of 300 µl of medium/well. Tube formation was monitored over 72h. On day 3, µ-slides were prepared for immunofluorescence staining (see below).

After culture medium aspiration, each well was washed with 300 µl of DPBS and subsequently fixed in 2% PFA for 30 minutes at RT. After fixation, wells were washed and permeabilized with 0.5% TritonX100 solution for 3 minutes at RT. Then blocking with 2% BSA for 15 minutes was performed after washing. Before the addition of the primary antibody, each well was thoroughly washed with DPBS. Then, 50µl/well of anti-human α-SMA were added and incubated for 1 hour in the dark at RT. After washing with 0.1% BSA solution, the secondary antibody Anti mouse-Alexa Fluor 488 $F(ab´)_2$ (1:1000 final dilution) was added and incubated for 1 hour in the dark at RT. The washing step with 0.1% BSA was followed by DAPI staining (1:1000 final dilution of 1mg/ml stock) for 3 minutes. Finally, wells were washed and embedded in Ibidi mounting medium.
Slides were analyzed at confocal microscope (Leica SP5 MP, Lima Core Facility, Center for Biomedicine and Medical Technology Mannheim (CBTM)) with 40x/1.3 NA oil objective.

3.2.3.2 Pericytes: endothelial cells coculture

Human retinal microvascular pericytes (HRMVPC) were purchased from PeloBiotech and cultured following the manufacturer's instructions. A frozen vial of HRMVPC was thawed in a 37°C water bath for 1 minute. Cell suspension was transferred in a 15 ml tube containing 10 ml of Pericytes Growth Medium (PGM) and centrifuged at 200g for 5 minutes. Supernatant was discarded, cell were resuspended in 10 ml of PGM and placed into one T25 previously coated with Speed Coating Solution. Cells were maintained at 37°C, 5% CO_2. Cell morphology was constantly monitored by microscope observation.

Upon confluence, HRMVPC were first washed with DPBS and then treated with trypsin/EDTA. Cell detachment was monitored under microscope observation for 1 minute. Detached cells were resuspended in PGM. Cell were counted with NucleoCounter cell counter and seeded in two T25 cell culture flask (1:2 passaging ratio) for normal maintenance or seeded according to the experimental conditions.

All cells were cryopreserved in FBS with 10% DMSO in liquid nitrogen, thawed and cultivated for at least one passage before use.

HRMVPC were used in angiogenesis coculture assays as followed. 30,000 pericytes/well were seeded in a 96 well plate in ECGM ¼ Medium NG or HG for 1 hour. Then, 5,000 $HUVEC_{GFP}$ or $HRMVEC_{GFP}$ were seeded on top of the HRMVPC monolayer. Cocultures were incubated for 72 hours. Phase contrast and fluorescent pictures were taken every 4 hours with IncuCyte Zoom system. Tube formation was measured with the IncuCyte S3 software, through quantitative kinetic processing metrics derived from time-lapse image acquisition and presented as total tube length per square centimeter (mm/mm²) over time. As performed with ASC, HRMVPC were also used in cocultures for immunofluorescent staining (paragraph 3.2.3.1).

3.2.4 Methods Aim 4: Evaluation of ASC immunomodulatory potential under hyperglycemia

Cocultures between ASC_{NG-HG} and stimulated/resting PBMC were set to investigate the immunomodulatory potential of ASC dissecting the interaction with CD4 T cells. Coculture supernatants were analyzed with ELISA and FACS-based protein detection assay.

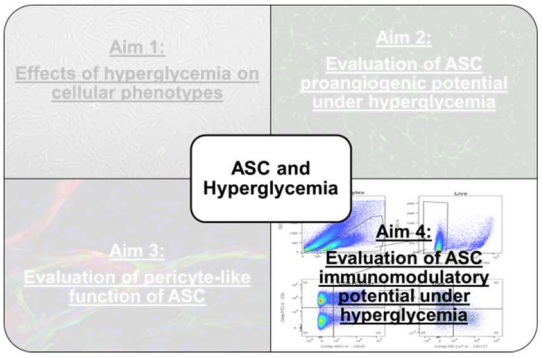

3.2.4.1 Peripheral blood mononuclear cell (PBMC) isolation

Human PBMC were isolated from buffy coat from healthy donors, provided by the German Red Cross Blood Donor Service Institute Mannheim. Buffy Coats were collected into 50 ml tubes and diluted 1:1 with DPBS/EDTA. 25 ml of diluted Buffy coat were gently poured on top of 10 ml of Ficoll-Paque in a 50 ml tube and centrifuged 30 minutes at 420g (with lowest deceleration factor). After centrifugation, supernatants containing plasma were aspirated and the interphase collected with a glass Pasteur pipette. Interphases from same donors were collected together in 50 ml tubes and washed with DPBS/EDTA. Tubes were centrifuged for 10 minutes at 420g. To eliminate contaminating red blood cells, pellets were washed with erythrocyte lysis buffer and left 10 minutes in incubation at RT. After a centrifugation step, pellets were resuspended in DPBS/EDTA and counted with the CASY cell counter.

3.2.4.2 ASC: PBMC coculture

For assessment of T cell proliferation, $3x10^7$ PBMC were resuspended in DPBS and stained with violet proliferation dye (VPD450 final concentration 1µM in DPBS). After 15 minutes incubation at 37°C, cells were washed, centrifuged and resuspended in RPMI 1640 10% FBS. Depending on the experimental conditions, PBMC were treated with/without CD3+CD28+ loaded Anti-Biotin MACSiBead particles (T cell Activation/Expansion kit human) using one loaded Anti-Biotin MACSiBead particle per two PBMC (bead to cell ratio 1:2) following the manufacturer´s instructions. In short, Anti-Biotin MACSiBead particles were thoroughly mixed with CD3-Biotin, CD28-Biotin and MACS buffer. This mixture was then incubated for 2 hours at 4°C under gentle

rotation. Prior to addiction to PBMC, loaded Anti-Biotin MACSiBead particles were washed with RPMI 1640 10% FBS. The treatment defined stimulated (with beads) and not stimulated (without beads) PBMC, which were then directly used to set cocultures with ASC.

$2x10^5$ $ASC_{NG\text{-}HG}$ were seeded in full RPMI 1640 on the bottom of a 6-well plate. Directly after isolation, $1x10^6$ VPD450 stained stimulated/not stimulated PBMC were added either *(a)* directly on top of the ASC monolayer (direct coculture) or *(b)* in a transwell insert placed in suspension in the same well of ASC (transwell coculture). As control, VPD450 stained stimulated/not stimulated PBMC were seeded in full RPMI 1640 either in a 6-well plate alone (direct coculture setting) or in a transwell insert placed in suspension in a well containing only media (transwell coculture setting). Direct and transwell cocultures each with stimulated/ not stimulated PBMC and their respective controls (PBMC alone) were set in parallel for each experiment. Controls and cocultures were treated with IL-2 (1:500 final dilution, 500 µg/ml stock). After 7 days cocultures were harvested and CM collected and stored at -80°C for further analysis. Harvested PBMC and ASC were processed following procedures reported in paragraphs 3.2.4.2.1 and 3.2.4.3.

To investigate the long-term effect of ASC on PBMC, not stimulated PBMC from transwell cocultures were further cultured without ASC for the following 7 days (total days of culture 14). In details, PBMC were harvested after 7 days of coculture and counted. The same number of PBMC was then seeded in 6-well plate in fresh full RPMI 1640 with IL-2 (1:500 final dilution, 500 µg/ml stock). The following conditions were defined: *(a)* PBMC (control condition of PBMC pre-cultured without ASC in the previous 7 days) and *(b)* ex-Coculture (PBMC cultured with ASC in the previous 7 days). After 7 days (total 14 days), PBMC were processed following procedures reported in paragraphs 3.2.4.2.1.1. The CM of these cultures was harvested, collected and stored at -80°C for further analysis. A representative picture of the whole work flow is reported below (Figure 7).

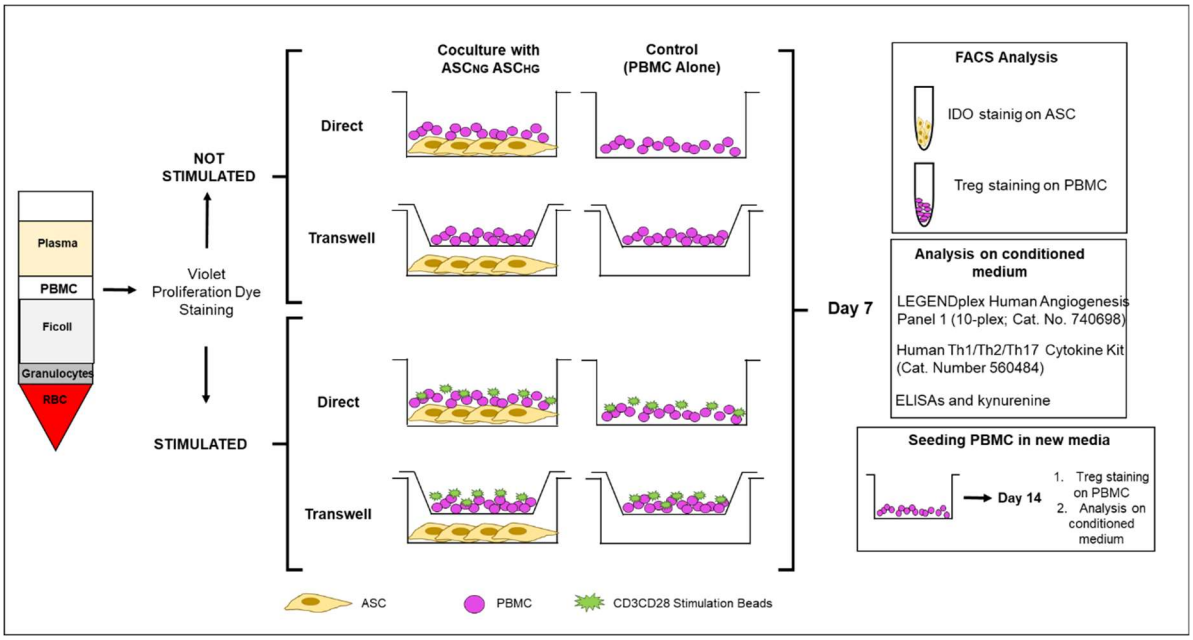

Figure 7 General work flow for ASC:PBMC cocultures. For each experiment fresh PBMC were isolated from buffy coat with Ficoll gradient and stained with violet proliferation dye. Stimulated and not stimulated cocultures were established with CD3/CD28 treated/not treated PBMC in direct and transwell settings with their respective controls. After 7 days PBMC and ASC were harvested and processed as reported in paragraph 3.2.4.2.1. CM was also harvested and frozen for further analysis. PBMC from transwells were also re-seeded and further cultured for 14 days.

3.2.4.2.1 Treg staining and detection

After 7 days of culture, VPD450 stained stimulated/not stimulated PBMC were harvested from cocultures and controls. Mouse anti-human antibodies were used to specifically stain activated CD4 cells and Treg.

3.2.4.2.1.1 Treg panel

After harvesting, PBMC were collected in FACS tubes, washed with PBS and resuspended in FACS Buffer. After 5 minutes incubation with 10 µl of FcR blocking reagent, antibodies for surface cell staining were added: Anti-CD4, Anti-CD25 and Anti-CD127 and incubated 20 minutes in dark at 4°C. After washing, PBMC were resuspended in PBS, stained with Fixable Viability dye eF780 (1:2000 final dilution) and incubated for 30 minutes at 4°C. To perform the intracellular staining, the BD Pharmingen Transcription Factor Buffer was used, following the manufacturer's instructions. Briefly, cells were resuspended by vortexing in 1 ml of 1X Fix/Perm Buffer and incubated for 50 minutes at 4°C. After incubation, two times washing step with 1X Perm/Wash Buffer were performed. Cells were then resuspended in 100 µl of 1X Perm/Wash buffer and stained with Anti-FoxP3. After 50 minutes of incubation at 4°C

cells were washed twice with 1X Perm/Wash buffer and finally resuspended in FACS buffer. 100 µl of cell suspension together with 25 µl of Precision count beads were analyzed immediately at BD FACS Canto II. Precision count beads were used during data analysis to calculate percentages of cell subpopulations. The .fcs files were analyzed with FlowJo 10 software. The gating strategy applied to calculate percentages of CD4+CD25+ and Treg cells in Live population is reported in Figure 8.

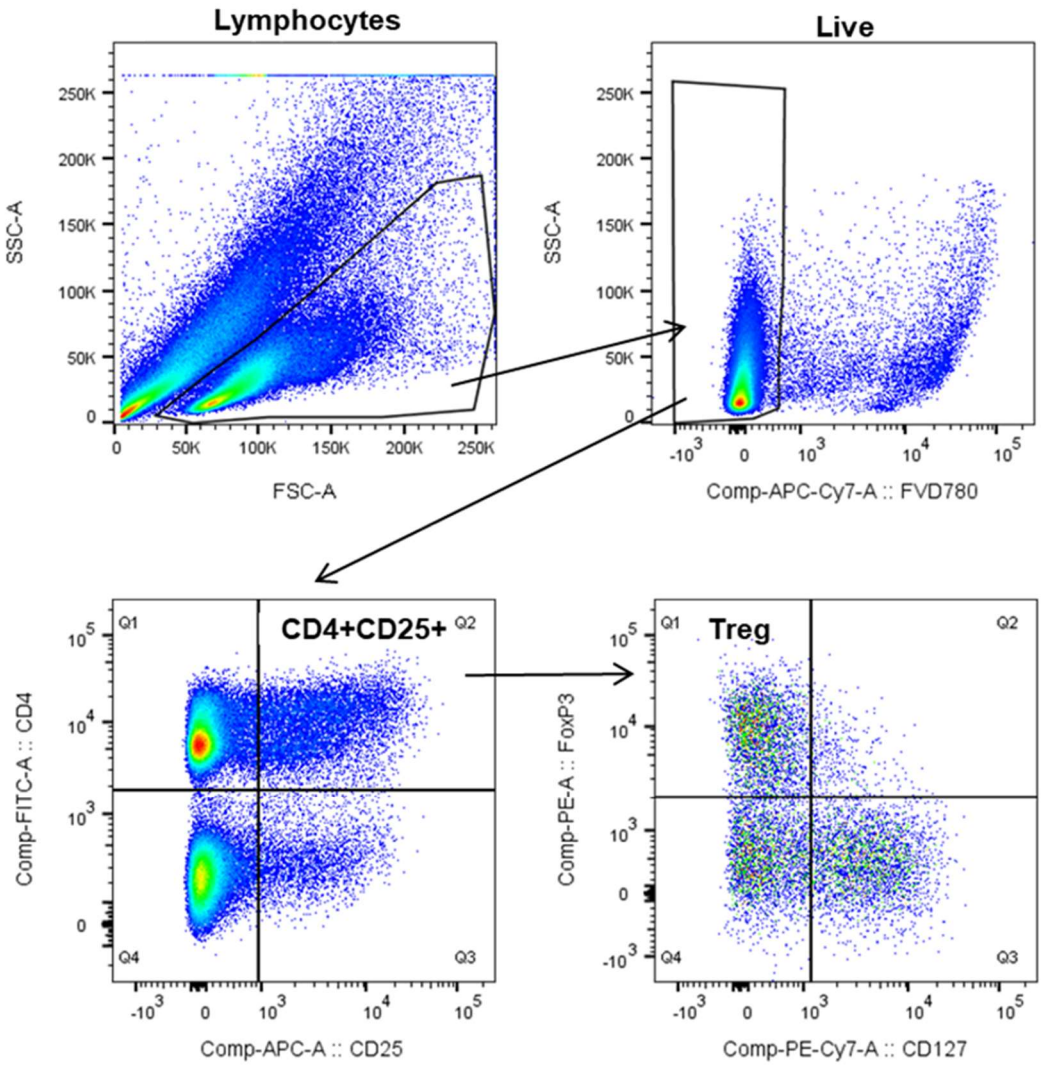

Figure 8 Representative gating strategy on Live population for CD4+CD25+ cells and Treg. Lymphocytes are gated on SSC and FSC, followed by a dead/live gating with FVD780, to define the Live population. The Live population is then inspected for CD4 and CD25 expression. Subsequently, CD127 and FoxP3 are assessed in the CD4+CD25+ population. CD4+CD25+CD127-FoxP3+ cells are defined as Treg.

3.2.4.2.1.2 Analysis of Proliferating/non proliferating subpopulations

To evaluate the extent of proliferation of CD4+ cells in cultures, living VPD450 stained stimulated/not stimulated PBMC were gated and analyzed as follow. As VPD450 dye is distributed uniformly between daughter cells, it is possible to monitor cell division over time. VPD+ cells, which retain the dye, are not proliferating cells, while VPD- are actively proliferating cells, progressively losing the dye. Therefore, starting from unstimulated and stimulated PBMC controls, it was possible to set gating for proliferating (VPD-) and non-proliferating (VPD+) cells. A representative picture of this gating strategy is reported in Figure 9.

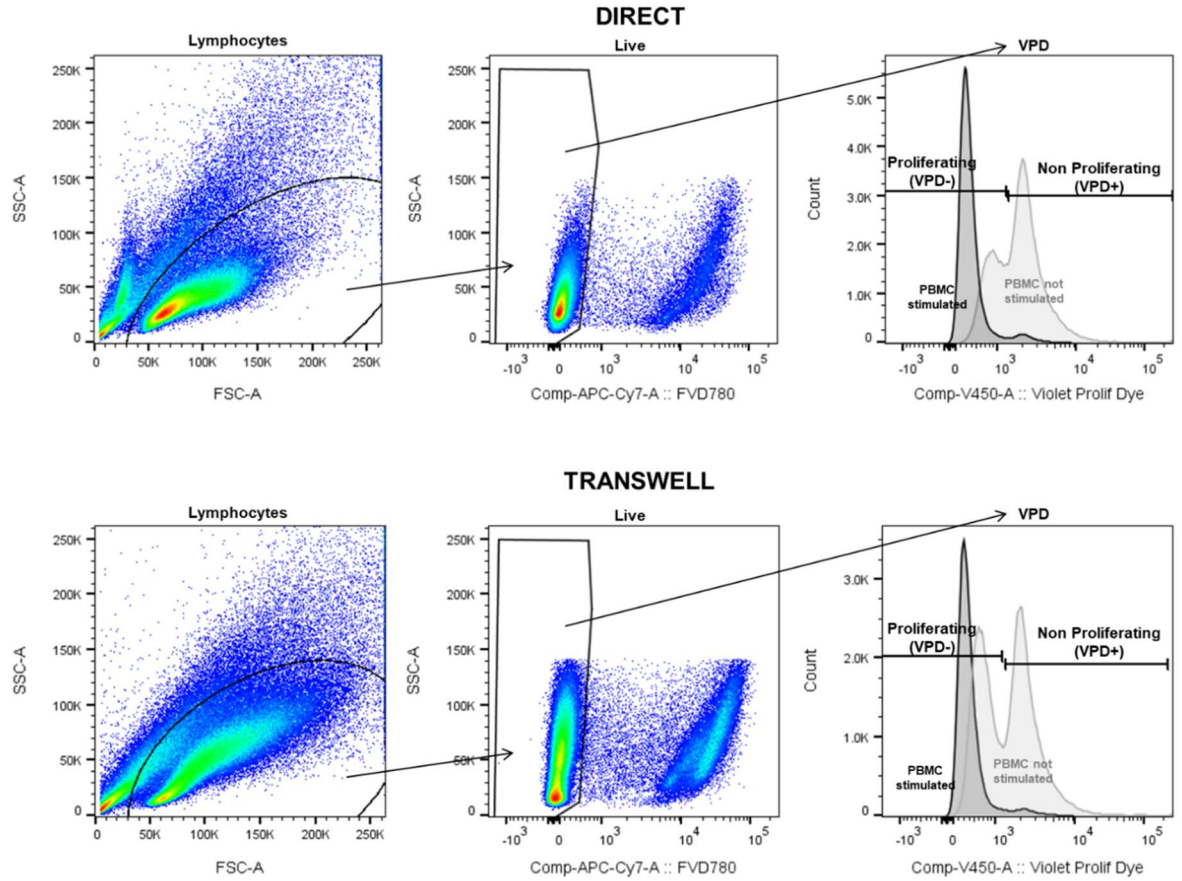

Figure 9 Proliferating (VPD-) and non proliferating (VPD+) gating are defined on stimulated/not-stimulated PBMC in direct and transwell. A representative gating strategy is reported. Lymphocytes are gated on SSC and FSC, followed by a dead/live gating with FVD780, to define the Live population. The Live population is inspected for the Violet Proliferation Dye (VPD). Stimulated PBMC (dark gray) and not stimulated PBMC (light gray) are compared and the gating for Proliferating cells (VPD-) and non proliferating cells (VPD+) set. The slight auto-stimulation in not-stimulated PBMC is useful in defining the gate.

Moreover, VPD-/+ fractions were further discriminated/gated for CD4+CD25+ cells and Treg. A representative picture of this gating strategy for CD4+CD25+ and Treg is reported in Figure 10.

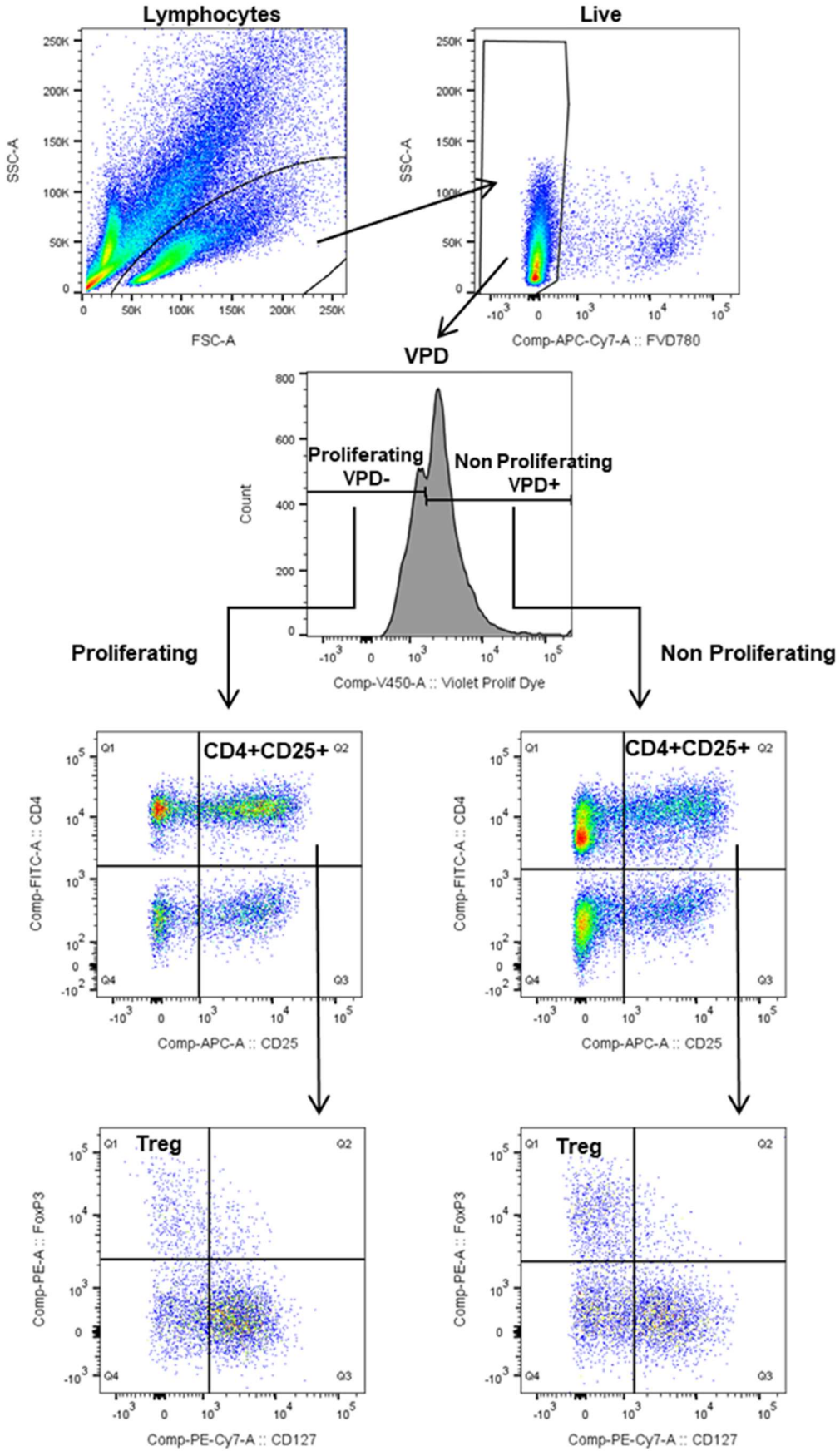

Figure 10 Representative gating strategy on VPD-/+ population to define VPD+ and VPD– fractions of CD4+CD25+ cells and Treg. Lymphocytes are gated on SSC and FSC, followed by a dead/live gating with FVD780, to define the

Live population. The Live population is inspected for the Violet Proliferation Dye (VPD). The gating defined in Figure 9, identify the VPD- and VPD+ fractions. The VPD- and VDP+ populations are then analyzed as reported in Figure 8.

CD4 cells proliferation was also analyzed with the Proliferation Tool of FlowJo 7 software. The Proliferation Tool in fact, applies mathematical models to the proliferation data and develops statistics to describe it. Particularly, we focused on the “division index”, which is described as followed: “The Division Index is the average number of divisions for all of the cells in the original starting population” (FlowJo 7 manual tutorial). A representative picture of how the Proliferation tool works is reported in Figure 11.

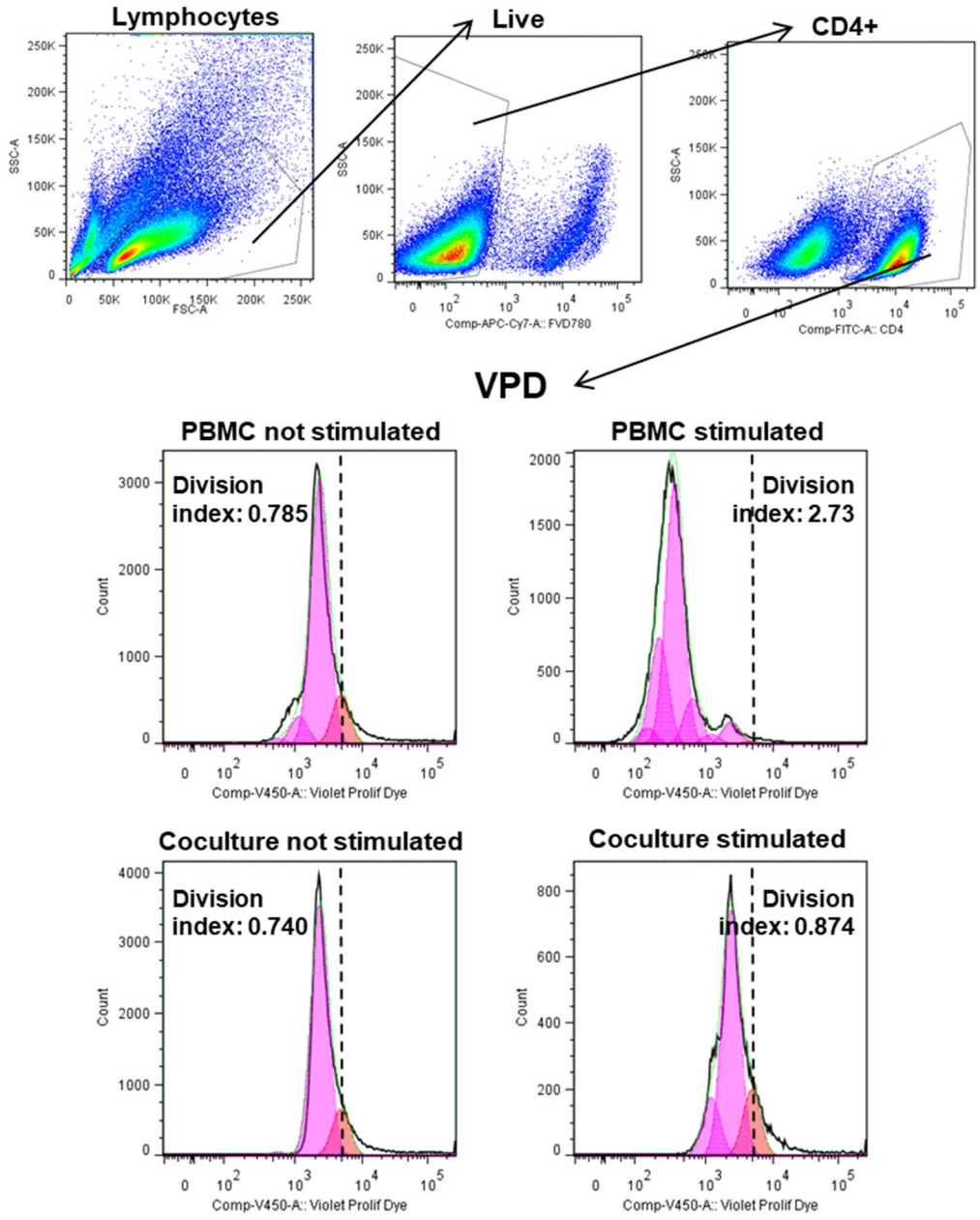

Figure 11 Representative picture of proliferation tool in FlowJo v.7 software. Lymphocytes are gated on SSC and FSC, followed by a dead/live gating with FVD780 to define the Live population. The Live population is then characterized for CD4 expression. CD4+ cells are subsequently evaluated for Violet Proliferation Dye (VPD) staining. The proliferation tool allows the custom to set a Peak zero, to define the original population. Peak zero (dashed line, orange peak) is here defined taking into account the VPD distribution in PBMC stimulated and not stimulated. After peak zero definition, the proliferation tool adjusts its algorithm on the curve and calculates the following proliferating generation (pink peaks) as well as the division index.

3.2.4.3 Cytokines and protein detection

To investigate the cytokine profile of CM collected from ASC:PBMC cocultures, two types of flow-cytometer based kits were used: the BD Cytometric Bead Array

(3.2.4.3.1) and the LegendPlex Human Th Cytokine Panel (3.2.4.3.2). In addition: (1) kynurenine in coculture supernatants was measured; (2) TGF-beta, TNF-alpha and CCL-18 were assessed with ELISA and (3) intracellular IDO was detected in ASC from cocultures.

3.2.4.3.1 BD Cytometric Bead Array (CBA)

The BD Cytometric Bead Array (CBA) Human Th1/Th2/Th17 Cytokine Kit (Cat. Number 560484) was used to analyze CM from 7 day stimulated/not stimulated transwell cocultures and PBMC as well as CM from PBMC after 14 total days of culture, following the manufacturer's instructions. Briefly, standards and samples were placed into FACS tubes followed by addiction of mixture of Capture beads. After the addiction of the Human Th1/Th2/Th17 PE Detection Reagent, CM was left 3 hours in incubation at RT. Then, a washing step with wash Buffer was performed and after aspiration of supernatants, tubes were ready for acquisition at the BD FACS Canto II. Data analysis on .fcs files was performed with the FCAP Array Software.

3.2.4.3.2 LegendPlex Human Th Cytokine Panel

CM collected from ASC:PBMC cocultures were analyzed with the LEGENDplex Human Th Cytokine Panel (13-plex; Cat No. 740722).

Briefly, standards were reconstituted in Assay Buffer and 1:4 serial dilutions were prepared to obtain an 8-points standard curve. A V-bottom plate was loaded first with 15 µl/well of samples and standards in a 1:1 dilution with Assay Buffer and then 15 µl of Premixed Beads were added to each well. The plate was sealed and incubated for 2 hours at RT under 800 rpm agitation. After incubation, each well was washed with 150 µl of Wash Buffer, followed by 5 minutes centrifugation at 250g. The plate was again decanted, washed and centrifuged prior to the addiction of Detection Antibody (15 µl/well). 1 hour at RT incubation under 800 rpm shaking followed. Afterwards, SA-PE was added in each well and incubated 30 minutes at RT with 800 rpm agitation. Finally, the plate was washed twice and the content of each well resuspended in 150 µl of Wash Buffer. Each probe was transferred in FACS tube prior to BD FACS Canto II analysis. Data were acquired limiting the acquisition rate on 300 beads/analyte.

Data analysis was performed with the LEGENDplex™ Data Analysis Software according to the manufacturer's instructions.

3.2.4.3.3 Kynurenine assay

Kynurenine was measured in CM of 7 days stimulated and not stimulated ASC:PBMC cocultures and controls as follow. 100 µl of probes and standards were distributed on a 96-well plate (LightCycler® 480 Multiwell Plates 96) and mixed with 50µl of 30% Trichloroacetic acid (TCA). The plate was incubated 30 minutes at 50°C. After the incubation, the plate was centrifuged at 4004g for 10 minutes at RT. Without touching the pellets, 75 µl of supernatants were collected from each condition and transferred in a 96-well plate. 75 µl of 2% para-Dimethylaminobenzaldehyde were added to each well and incubated for 15 minutes at RT. The OD of each well was determined using a microplate reader set to 492 nm. Standard, best fitting ($0.90 \leq R \leq 1$) curves were elaborated with GraphPad Prism 7 software. No kynurenine was found in ASC cultured alone used as control.

3.2.4.3.4 ELISAs

TGF-beta, TNF-alpha and CCL-18 (Duo Set, R&D systems) were analyzed in CM of 7 days and 14 days stimulated and not stimulated ASC:PBMC cocultures and controls following the manufacturer's instructions. Capture antibody diluted in DPBS was used to coat a 96-well plate, which was incubated overnight at RT. The following day, after three aspiration/wash steps with Wash Buffer, the plate was blocked with Reagent Diluent and incubated for 1 hour at RT. At the end of incubation, three aspiration/wash steps were performed and standards and samples added. The plate was left 2 hours in incubation at RT. Three aspiration/wash steps were repeated and afterwards the detection antibody was added, followed by 2 hours incubation at RT. As last steps after washing, Streptavidin-HRP was added for 20 minutes, followed by other 20 minutes of incubation with substrate solution (1:1 solution of Color reagent A and B). The plate was finally treated with stop solution (2N H_2SO_4). The OD of each well was determined using a microplate reader set to 450 nm with wavelength correction at 570 nm. Best fitting standard curves ($0.90 \leq R \leq 1$) were elaborated with GraphPad Prism 7.

3.2.4.3.5 Detection of indoleamine 2,3-dioxygenase (IDO)

Indoleamine 2,3-dioxygenase (IDO) detection in $ASC_{NG\text{-}HG}$ cocultured with stimulated/non stimulated PBMC, was measured as follow. After harvesting ASC from coculture, cells were collected in FACS tubes and washed with DPBS. IC Fixation Buffer was added to the cell suspension and left in incubation for 30 minutes at RT. After two washing/centrifuge steps with 1X Permeabilization Buffer, cells were stained

in 1X Permeabilization Buffer with IDO-PE and incubated for 30 minutes. After incubations, cells were washed and analyzed immediately at BD FACS Canto II. ASC in monoculture were used as control. The .fcs files were analyzed with FlowJo 10 software. Data are presented as Median Fluorescence Intensity (MFI) of IDO-PE in living cells corrected for the MFI´s of the control tube (ASC in monoculture).

4 RESULTS

The main focus of our study was to evaluate whether hyperglycemia might affect ASC in their phenotype and functions. Therefore, four aims were defined: (1) to evaluate glucose-mediated effects on ASC basic characteristic; (2) to assess whether hyperglycemia might affect the proangiogenic potential of ASC; (3) to investigate whether ASC might retain a pericytes-like phenotype and (4) to verify if HG might affect the immunomodulatory potential of ASC. Results of our research are presented below, following the distinctions between the four aims.

4.1 Effects of hyperglycemia on cellular phenotypes

The first aim of our study was to address glucose-mediated effects on basic characteristics of ASC such as cell growth, differentiation and cell surface phenotype. Intracellular redox balance and glucose uptake were also monitored. Similarly, HRMVEC were also characterized in regard of their glucose sensitivity.

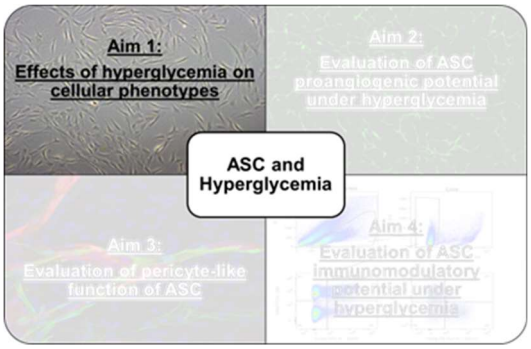

4.1.1 ASC basic characteristics are unaffected by HG

To test effects of HG, ASC were cultured in NG (ASC_{NG}) and HG (ASC_{HG}) medium directly after isolation from lipoaspirates. At passage 1 to passage 2 after isolation, HG caused a weak but significant reduction in cell doublings (ASC_{NG} vs ASC_{HG} , $p<0.01$; Figure 12 A, upper left panel) and correspondingly, an increased doubling time (ASC_{NG} vs ASC_{HG}, $p<0.05$; Figure 12 A, lower left panel). However, these differences were not detectable at following passages (Figure 12 A, right).

Adipogenic and osteogenic differentiation profile of ASC_{HG} was not different from ASC_{NG} (Figure 12 B).

Likewise, ASC_{NG} and ASC_{HG} had a similar immunophenotype (Figure 12 C).

Despite some early transient reduction in proliferation rate, HG exerted no long-term effects on ASC.

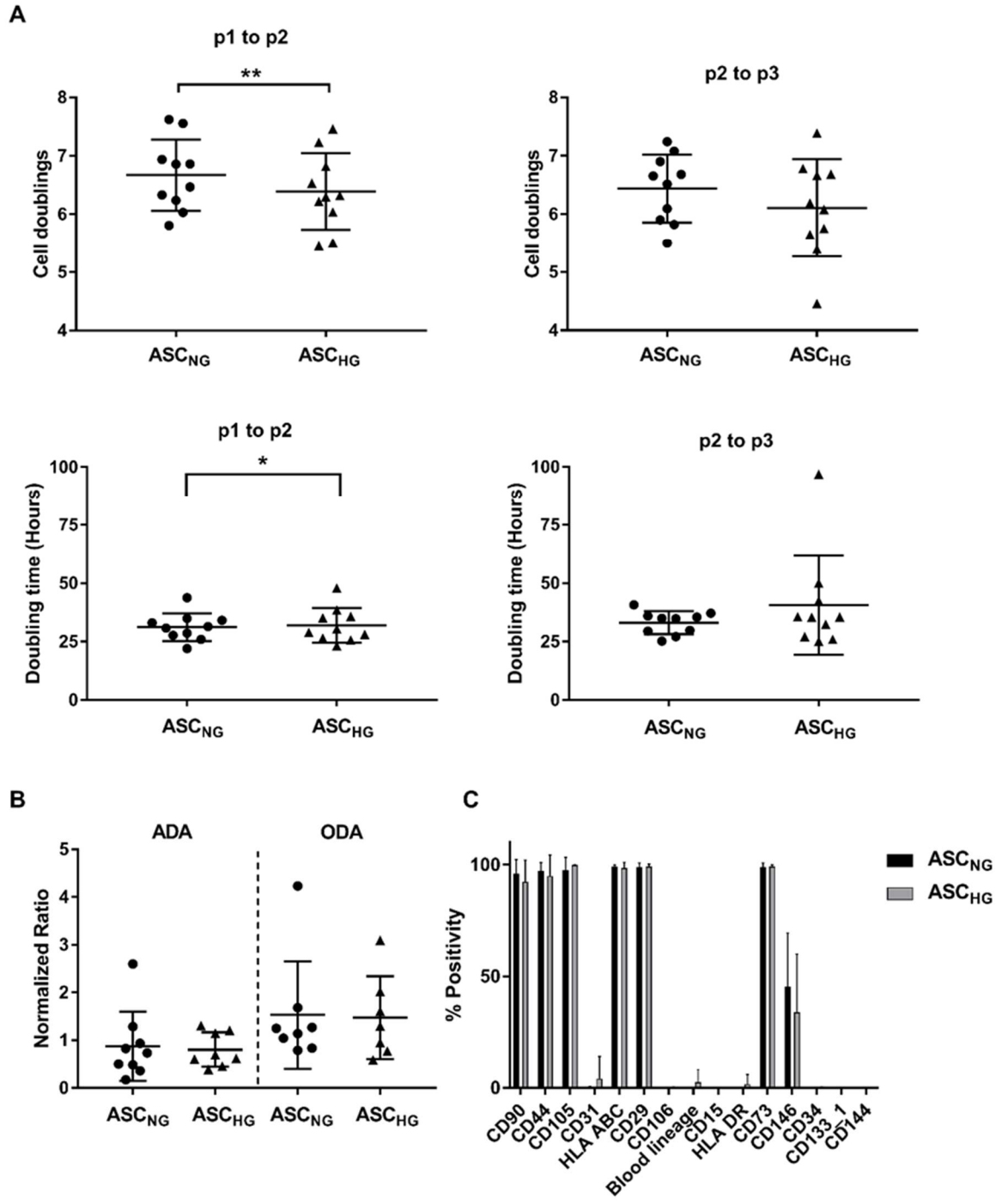

Figure 12 ASC characteristics are largely unaltered by HG. (A) HG reduces ASC growth rate only at early passage (cell number calculated at split p1 to p2). Cell doublings (upper left panel) are significantly reduced in ASC_{HG} (ASC_{NG} 6.67 ± 0.6 vs ASC_{HG} 6.39 ± 0.65, $p<0.01$, n=10, paired T-test). Doubling time (lower left panel) is significantly increased (ASC_{NG} 31.24 ± 5.9 hours vs ASC_{HG} 32 ± 7.4 hours, $p<0.05$, n= 10, paired T-test). From passage 2 to 3 on, cell doublings and doubling time (right panels) do not differ (n=10). (B) ASC_{NG} and ASC_{HG} do not differ in adipogenic and osteogenic differentiation potential (ADA and ODA respectively, AdipoRed and OsteoImage signal normalized to Hoechst signal, n=7; not significant, Paired t-test). (C) The immunophenotype of ASC_{NG} and ASC_{HG} addressed by flow cytometry is similar (n=8, not significant, 2-way ANOVA).

4.1.2 Oxidative stress in ASC is increased upon HG exposure and it is not concomitant to glucose uptake

Oxidative stress levels (total ROS measurement) were similar in ASC_{NG} and ASC_{HG} (Figure 13 A). The ROS inhibitor NAC had only a negligible effect on both, indicating a low basal oxidative stress level in ASC. However, a temporary switch of ASC to HG (ASC_{NG} in HG) increased oxidative stress up to 1.5-fold (ASC_{NG} in HG vs ASC_{NG} and ASC_{NG}: $p<0.01$ and $p<0.05$, respectively). This was significantly lowered by NAC treatment (ASC_{NG} in HG: +NAC vs –NAC: $p<0.01$). This suggested that ASC might adapt to prolonged HG conditions to maintain a low oxidative stress.

We next investigated the glucose uptake (Figure 13 B). In ASC_{NG}, glucose uptake was significantly inhibited by the GLUT-1 inhibitor WZB (ASC_{NG} –WZB vs +WZB: $p<0.0001$). Interestingly, glucose uptake of ASC_{NG} in HG and ASC_{HG} compared to ASC_{NG} was very low at levels comparable to ASC_{NG} cells treated with WZB (ASC_{NG} vs ASC_{HG} and ASC_{NG} in HG: $p<0.0001$). Even, the switch to HG revealed low glucose uptake with values comparable to levels obtained using the GLUT1 inhibitor WZB-117. This suggested that ASC might adapt rapidly to HG in the medium by reducing glucose influx.

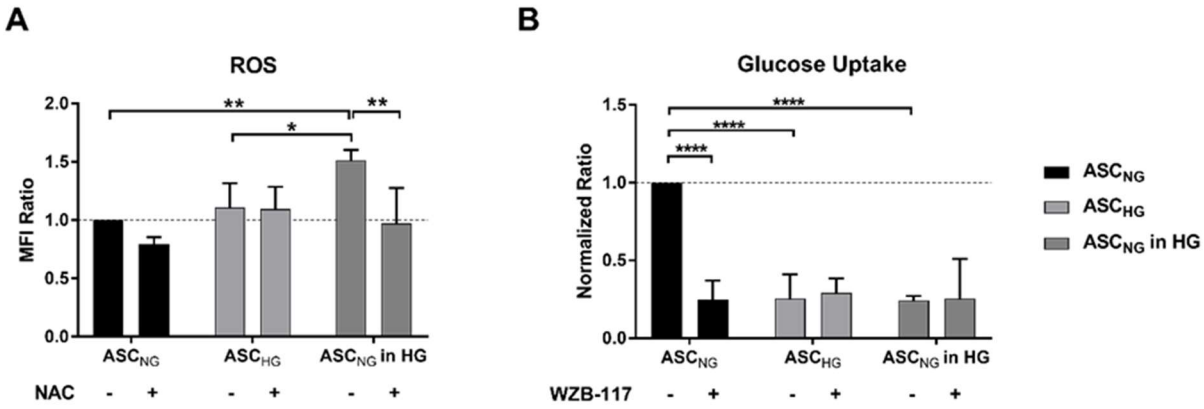

Figure 13 HG-dependent oxidative stress induction is not related to increased glucose uptake. ROS were measured in ASC via Carboxy-H2DFFDA staining. The antioxidant NAC was tested as inhibitor of ROS. In addition, glucose uptake was monitored trough 2-NBDG detection after a period of glucose starvation. WZB-117 a GLUT-1 inhibitor, was added to block glucose uptake. (A) Oxidative stress levels are comparable in ASC_{NG-HG} and only inhibited to a low extent by the antioxidant NAC (mean fluorescence intensity (MFI) values of ASC_{NG} set to 1). Switch of ASC_{NG} to HG (ASC_{NG} in HG) significantly increased ROS levels compared to ASC_{NG} and ASC_{HG} ($p<0.01$ and $p<0.05$). The same are inhibited by NAC treatment ($p<0.01$); n=3, 2-way ANOVA multiple comparison. (B) After glucose starvation, ASC_{NG} take up glucose (levels set to 1). This is significantly inhibited by the GLUT-1 inhibitor WZB-117 (ASC_{NG} –WZB vs +WZB: $p<0.0001$; n=3, 2-way ANOVA multiple comparison). Glucose uptake is significantly

reduced in ASC_{HG} and ASC_{NG} in HG to levels obtained with the WZB-117 inhibitor (ASC_{NG} vs ASC_{HG} and ASC_{NG} in HG: $p<0.0001$; 2-way ANOVA multiple comparison).

4.1.3 HG affects HRMVEC cell growth and angiogenic potential

In complete medium (ECGM-2), no effect of HG on HRMVEC proliferation was apparent (Figure 14 grey and black ■ lines). Hypothesizing that growth factors and especially VEGF, as suggested by different authors [156, 157], in ECGM-2 medium might protect ECs from hyperglycemia, cells were grown in growth factor-reduced medium (¼ ECGM-2). The growth rate significantly decreased comparing ECGM-2 with ¼ ECGM-2 (in NG media $p<0.01$ and HG media $p<0.001$, Figure 14, grey and black lines). Nevertheless, in both media HG did not reduce HRMVEC proliferation to a significant extent.

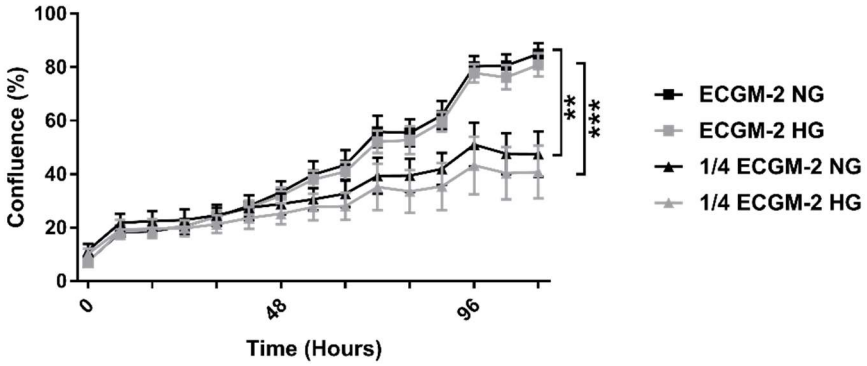

Figure 14 HG slightly impairs HRMVEC cell growth. Growth curves of HRMVEC reveal diminished proliferation in growth factor reduced medium, ¼ ECGM-2 (∆) compared to ECGM-2 (□) (NG-treated black lines: ¼ vs ECGM-2 $p<0.01$; HG-treated grey line:s ¼ vs ECGM-2; $p<0.001$, n=3; 2-way ANOVA multiple comparisons). HG had no significant effect.

The angiogenic potential of HG HRMVEC, tested in the BMA assay, however, revealed a significant reduction in total tube length ($p<0.001$, Figure 15 left panel) and in number of junctions ($p<0.001$, Figure 15 right panel). These differences were not seen in ECGM-2, supporting our notion that growth factors in the medium might overrule detrimental HG effects in endothelial cells (not shown).

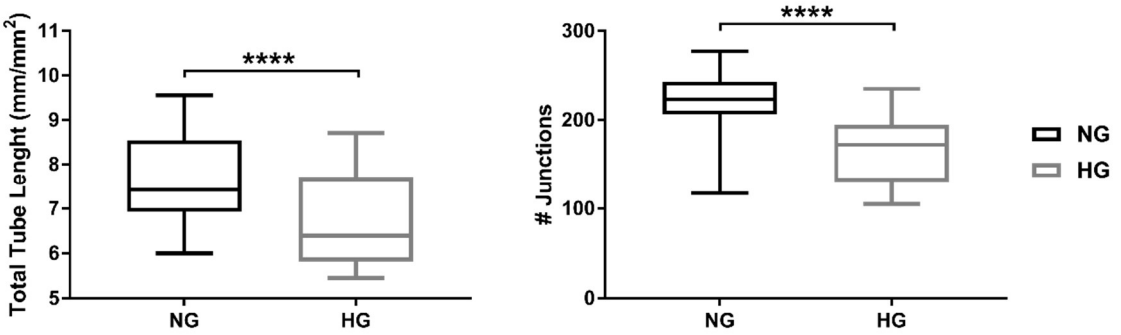

Figure 15 HG impairs the angiogenic potential of HRMVEC. HG let to reduced tube formation in BMA assay in ¼ ECGM-2. Left: total tube length HRMVEC NG-treated 7.52 ± 0.97 mm/mm^2 vs HG-treated 6.69 ± 1.02 mm/mm^2 p<0.0001 (n=4, Paired T-test). Right: number of junctions: NG-treated 217.3±35.57 vs HG-treated 165.8±38.7 p<0.0001 (n=4, Paired T-test).

4.1.4 Oxidative stress increases in HRMVEC upon HG treatment in absence of simultaneous rise in glucose uptake

As performed for ASC, we measured total ROS and glucose uptake in HRMVEC.
HRMVEC similarly to ASC displayed a low oxidative stress basal level (NG HRMVEC: –NAC vs +NAC, not significant; Figure 16 A). This was significantly increased in HG conditions (NG HRMVEC vs HG p<0.01) and efficiently inhibited by NAC (HG HRMVEC –NAC vs + NAC, p<0.01).
Glucose uptake (Figure 16 B) was reduced in HG condition compared to NG (NG HRMVEC vs HG: p<0.001). In contrast to ASC, where the GLUT-1 inhibitor greatly reduced glucose uptake almost to zero in all conditions, in HRMVEC glucose uptake levels were halved in NG HRMVEC (–WZB vs +WZB: p<0.001) and similarly reduced in HG conditions (HG –WZB vs +WZB: p<0.05). These findings suggested that while HG HRMVEC reduced glucose uptake compared to NG HRMVEC, the WZB-117 GLUT-1 inhibitor only halved this uptake, proposing that other GLUT channels might be involved. The oxidative stress appeared to be not directly linked to increased glucose influx.

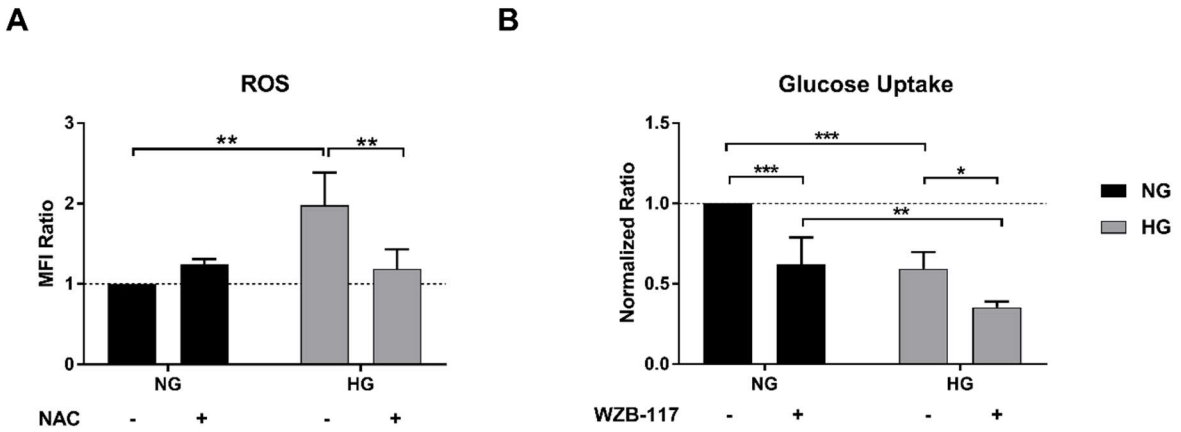

Figure 16 Total ROS were measured in HRMVEC via Carboxy-H2DFFDA staining. The antioxidant NAC was tested as inhibitor of ROS. In addition, glucose uptake was monitored trough 2-NBDG detection after a period of glucose starvation. WZB-117, a GLUT-1 inhibitor, was added to block glucose uptake. (A) In HRMEC, oxidative stress is significantly increased upon HG treatment ($p<0.01$; n=3, 2-way ANOVA multiple comparison) and significantly reduced by NAC treatment ($p<0.01$; n=3, 2-way ANOVA multiple comparison). (B) HG HRMVEC show reduced glucose uptake compared to NG ($p<0.001$; n=4, 2-way ANOVA multiple comparison). WZB-117 half-reduced glucose uptake in both conditions (NG: –WZB vs +WZB: $p<0.001$ and in HG: –WZB vs +WZB: $p<0.02$ and NG HRMVEC +WZB-117 vs HG HRMVEC +WZB-117 $p<0.01$; n=4, 2-way ANOVA multiple comparison).

4.2 Evaluation of ASC proangiogenic potential under hyperglycemia

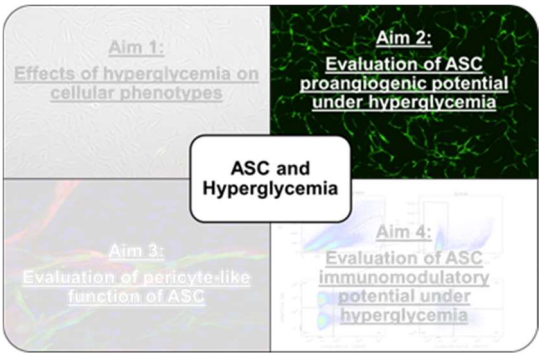

Having established that HG did not affect ASC and had only negligible effects on cell growth of HRMVEC while reducing their proangiogenic potential, we investigated ASC interaction with endothelial cells. As our second aim was to prove the proangiogenic potential of ASC and to verify whether this was affected by hyperglycemia, cocultures between ASC and both HUVEC and HRMVEC where established. Coculture supernatant was collected and assessed for proangiogenic factors.

4.2.1 ASC support HUVEC angiogenic potential independently of glucose and secrete proangiogenic factors

To investigate whether HG affected the proangiogenic potential of ASC, coculture angiogenesis assays in NG and HG culture media were run comparing $ASC_{NG\text{-}HG}$ and

NG/HG medium. ASC supported tube formation of $HUVEC_{GFP}$ in any condition (Figure 17 A and B).

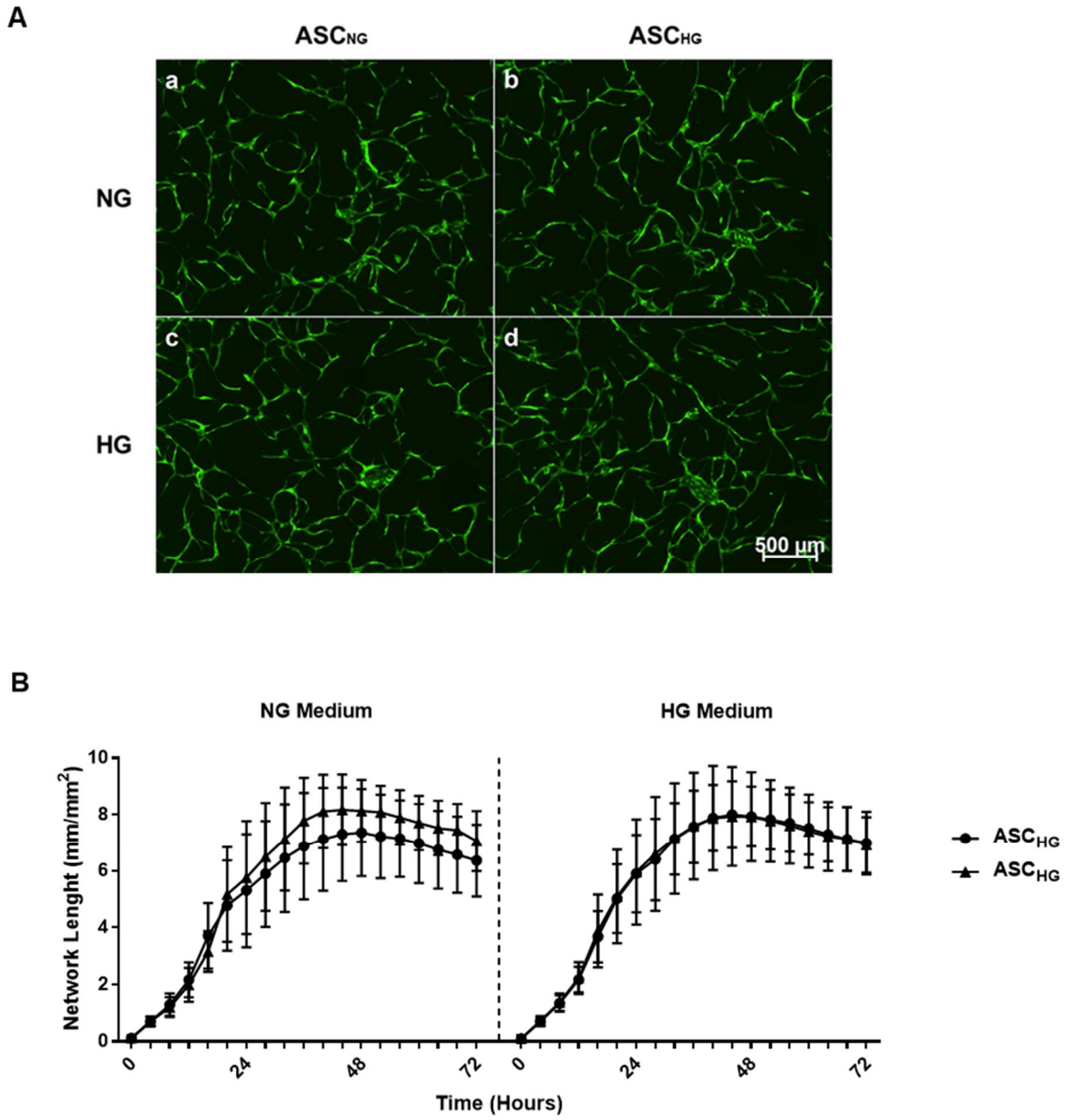

Figure 17 ASC_{NG} and ASC_{HG} similarly support HUVEC tube formation in an angiogenesis coculture assay. (A) Representative pictures of tube formation of $HUVEC_{GFP}$ in the coculture angiogenesis assay (a, b) ASC_{NG} + $HUVEC_{GFP}$ and ASC_{HG} + $HUVEC_{GFP}$ respectively, in NG media; (c,d) ASC_{NG} + $HUVEC_{GFP}$ and ASC_{HG} + $HUVEC_{GFP}$ respectively, in HG media. (B) Quantitative evaluation of tube network length (mm/mm^2) reveals no differences between ASC_{NG} (●) and ASC_{HG} (▲) in NG/HG medium (n=6, not significant, 2-way ANOVA).

To screen whether HG modified growth factor secretion within the supernatants, pooled CM from ASC_{NG}/HUVEC cocultures in NG and HG medium was analyzed using an angiogenesis protein array (Figure 18). Over all 43 cytokines analyzed, no significant difference was detectable. Despite the lack of significant changes (NG vs

HG, not significant), some factors in HG cocultures were found to be increased/decreased to a certain extent compared to NG cocultures. Among the increased factors, CCL-7 and PECAM-1 displayed a 2.8-fold and 1.9-fold respectively, while CCL-13 and MMP-1 had a 1.4-fold increase. On the other side, GM-CSF together with TNF-alpha was highly decreased in HG coculture (0.04-fold and 0.1-fold respectively). Similarly, CCL-1 (0.4-fold), PDGFB-BB (0.4-fold) and IL-4 (0.5-fold) were reduced in HG. All the other factors had a fold between 0.8 and 1.2.
These data indicated that HG did not affect the angiogenic supportive capacity of ASC on HUVEC whilst exerting some minor changes on the cytokine profile of the coculture.

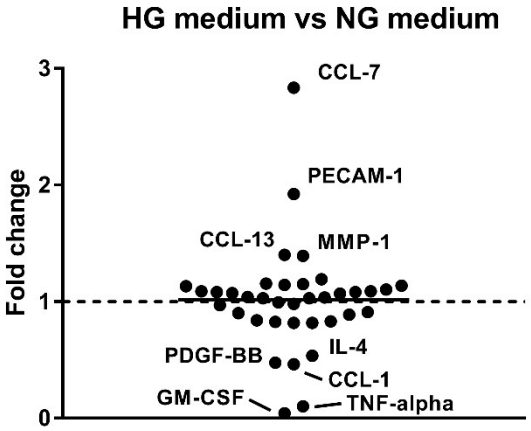

Figure 18 HG affects only few angiogenic factors in CM of ASC_{NG} + $HUVEC_{GFP}$ coculture angiogenesis assay. CM was collected and pooled from four different coculture experiments and analyzed using an angiogenesis protein array (43 factors). Fold change of HG compared to NG (set as 1), is calculated. Over all 43 factors, no significant difference was found comparing NG and HG medium (not significant, paired T-test). Proteins with 0.5≤ fold ≥1.4 are labeled. Proteins with fold change between 0.8 and 1.2 are bFGF, GRO, IFN gamma, IGF, IL-6, IL-8, MCP-1, PLGF, CCL5, TIMP-1, TIMP-2, VEGF-A, ANGPT1, ANGPT2, Angiostatin, Endostatin, CCL1, IL-1 alpha, IL-1 beta, IL-2, CXCL11, MMP-9, Tie2, uPAR, VEGFR2, VEGFR3.

4.2.2 HG HRMVEC angiogenic potential is rescued in coculture via secretion of proangiogenic factors by ASC

It was apparent that HRMVEC showed markedly lower angiogenic potential when compared to HUVEC, network length in ASC_{NG}:$HRMVEC_{GFP}$ vs ASC_{NG}:$HUVEC_{GFP}$ $p<0.0001$ (not shown). Although tube formation capacity of HG HRMVEC was found to be significantly reduced in the BMA assay (Figure 15, paragraph 4.1.3), in the coculture assay no differences were seen when using $ASC_{NG\text{-}HG}$ under NG/HG culture medium (Figure 19 A, B). These findings not only confirmed the supportive role of ASC

to the tube forming potential of endothelial cells, but also suggested that ASC may protect HRMVEC from detrimental effects of HG.

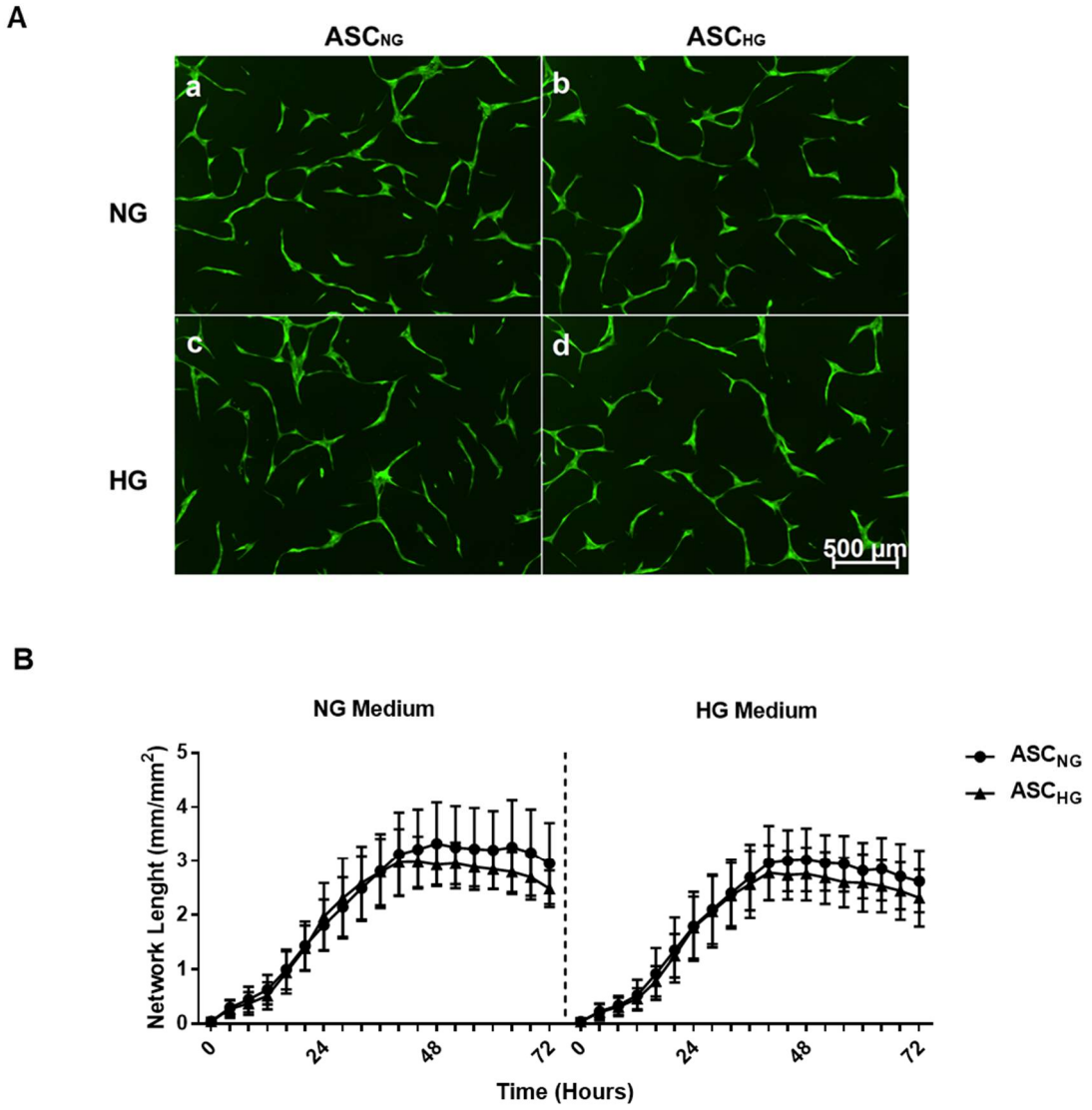

Figure 19 A) Representative pictures of coculture angiogenesis assay with $HRMVEC_{GFP}$; (a, b) ASC_{NG} + $HRMVEC_{GFP}$ and $ASCH_{G}$ + $HRMVEC_{GFP}$ respectively, in NG media; (c,d) ASC_{NG} + $HRMVEC_{GFP}$ and $ASCH_{G}$ + $HRMVEC_{GFP}$ respectively, in HG media. (B) ASC_{NG} (●) and ASC_{HG} (▲) equally support $HRMVEC_{GFP}$ tube formation independently of culture conditions (n=8).

We speculated that factors secreted from ASC might support endothelial angiogenic potential rescuing HRMVEC from HG detrimental effects. To test this, we analyzed the CM from $ASC_{NG\text{-}HG}$:HRMVEC coculture angiogenesis assays using a multiplex cytokine assay (Figure 20 A). Again, glucose in the media caused no differences in the growth factor content of $ASC_{NG\text{-}HG}$ (not shown). In the CM of cocultures, the majority of analyzed factors were higher than in the monocultures of ASC. Some factors were

significantly changed under HG, such as FGF significantly higher in ASC_{NG} cocultures than in ASC_{HG} cocultures ($p<0.05$) and higher in ASC_{NG} cocultures than in ASC_{NG} monocultures ($p<0.05$). VEGF, highly concentrated in ASC_{NG-HG} monocultures, was significantly decreased in CM of cocultures ($p<0.05$, VEGF panel in Figure 18 A). Despite the lack of significant differences, we also found that ASC_{NG-HG} monoculture produced considerably high amounts of Ang-2 (mean value ASC_{NG} monoculture 665±405 pg/ml), which were even increased in ASC_{NG-HG} cocultures (mean value ASC_{NG} coculture 2247±1130 pg/ml). Similarly, Ang-1 levels were reduced in ASC_{NG-HG} monoculture (ASC_{NG} mean value 110±134 pg/ml) and increased in coculture (ASC_{NG} mean value 319±360 pg/ml).

Importantly, we observed a correlation between the concentration of secreted factors and the proangiogenic supportive capacity of ASC by comparing individual ASC isolates (Figure 20 B). These data indicated that ASC secreted a variety of proangiogenic factors, largely unaffected by HG.

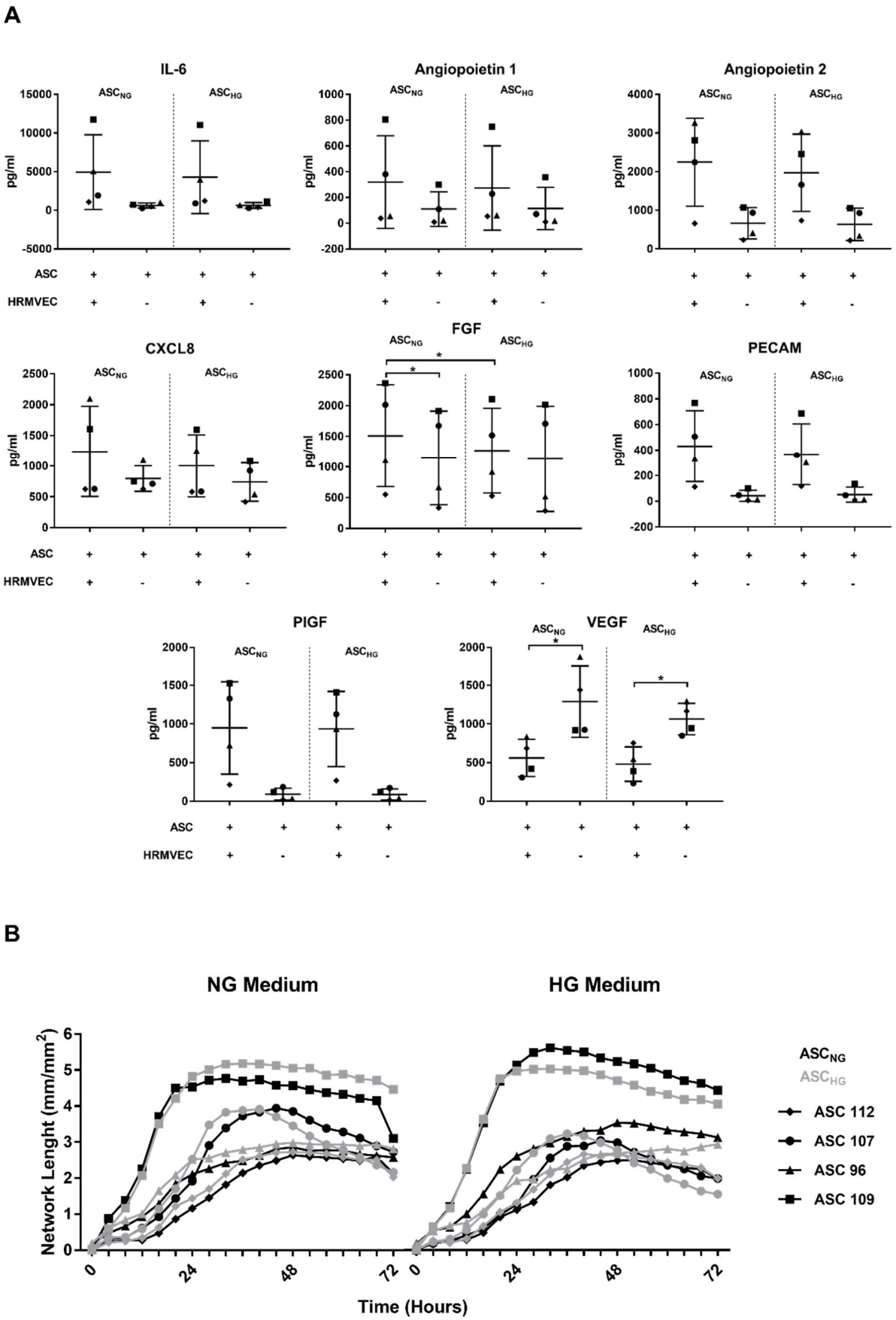

Figure 20 A) Angiogenic growth factor content in CM of NG $ASC_{NG\text{-}HG}$:HRMVEC cocultures and $ASC_{NG\text{-}HG}$ monocultures. FGF is significantly reduced in ASC_{HG} coculture compared to ASC_{NG} coculture ($p<0.05$). Moreover,

FGF is more concentrated in ASC_{NG} coculture than in ASC_{HG} monocultures ($p<0.05$). VEGF is higher in ASC_{NG-HG} monocultures than cocultures (both $p<0.05$). All n=4, One-way ANOVA. B) In angiogenic coculture assays, high angiogenic growth factor concentrations are linked to a better angiogenic support, dependent on ASC sample specificity (ASC_{NG}, ASC_{HG}; ♦, ●, ■, ▲ different ASC samples). Symbols to identify ASC samples are reported also in A.

4.2.3 Indirect proangiogenic supportive potential of ASC

So far we observed that hyperglycemia impaired the angiogenic potential of HRMVEC and that this was rescued in direct cocultures with ASC, independently of glucose in the culture media. Therefore, we tested whether the proangiogenic factors produced by ASC and detected in their CM, were sufficient to rescue HG HRMVEC impaired angiogenic potential. Having previously found that hyperglycemia exposure caused an increase in oxidative stress level of HG HRMVEC, to verify a possible link with the reduced angiogenesis, we further tested the effect of the antioxidant NAC on their tube forming potential. Hypothesizing that ASC secreted factors and an antioxidant stimulus might protect HRMVEC from HG-mediated insults, we checked HRMVEC in a BMA assay. The following conditions were tested: (1) NG, (2) HG, (3) NG+NAC (antioxidant), (4) HG+NAC (5) CM from coculture angiogenesis assay, (6) CM from ASC monoculture. To further check HG-mediated effects, these CM media were obtained from angiogenesis coculture assays performed with ASC_{HG} in HG medium.

Indeed, NAC restored the angiogenic potential of HG HRMVEC to some extent (HRMVEC HG vs HG+NAC $p<0.0001$, Figure 21), but not to levels obtained in NG conditions (HRMVEC NG vs HG+NAC $p<0.05$, Figure 21).
CM of both ASC_{HG} mono- and coculture restored the impaired angiogenic potential of HG HRMVEC (HG HRMVEC vs CM_{HG}-ASC_{HG} coculture and ASC_{HG} monoculture $p<0.0001$, Figure 21). CM media-treated HG HRMVEC had a network length comparable to NG HRMVEC (NG HRMVEC vs CM_{HG} HRMVEC, not significant) and HG HRMVEC +NAC.
These data indicated that ASC could restore the HG-impaired angiogenic function of HRMVEC by the production of proangiogenic factors. The fact that NAC-treated and CM-treated HG HRMVEC displayed a similar network length, let us speculate about a not yet defined ROS scavenging/antioxidant potential of CM or an overruling effect of angiogenic factors within the CM.

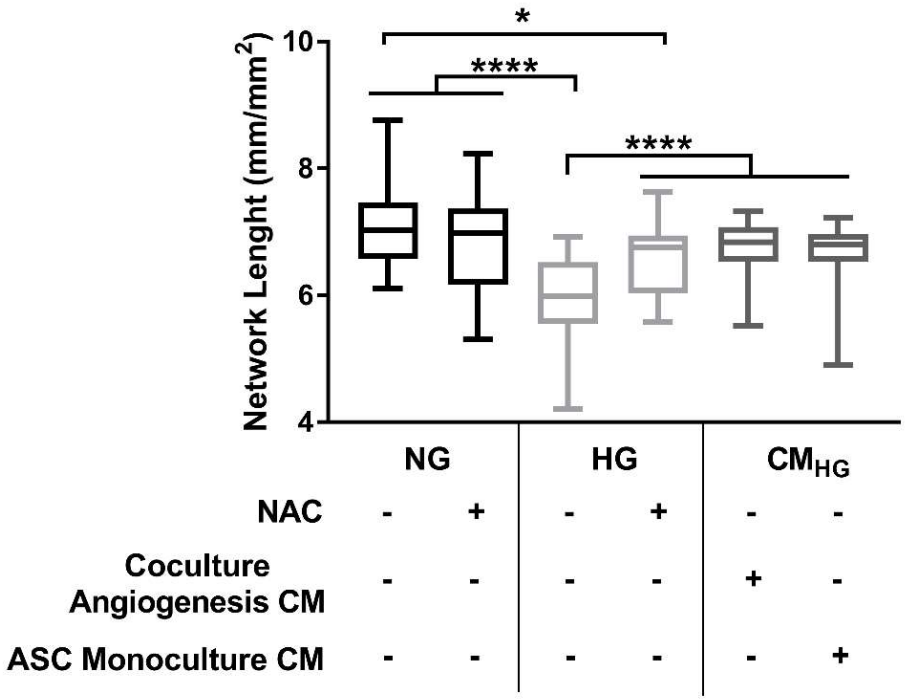

Figure 21 HG impairs the angiogenic potential of HRMVEC, which is restored by NAC, CM from ASC co- and monoculture assays. Tube forming potential of HRMVEC was tested in a BMA with NAC or pure CM, either from ASC_{HG} monoculture and ASC_{HG}:HRMVEC coculture in HG medium (CM_{HG}). To resemble culture condition of ROS measurement, the assay was run in RPMI1640 (supplemented with 2.5% FBS, 1% Penicillin/streptomycin and 2% Glutamine). Tube formation is reduced in HG HRMVEC compared to NG HRMVEC ($p<0.0001$ one-way ANOVA, multiple comparison). NAC treatment increases network length in HG ($p<0.0001$), but not to levels seen in NG HRMVEC ($p<0.05$, n=5, one-way ANOVA, multiple comparison). CM from co- and monoculture restored tube forming capacity of HG HRMVEC ($p<0.0001$) to levels seen in NG (CM_{HG} vs NG HRMVEC, not significant, one-way ANOVA, multiple comparison).

4.3 Evaluation of pericyte-like function of ASC in coculture

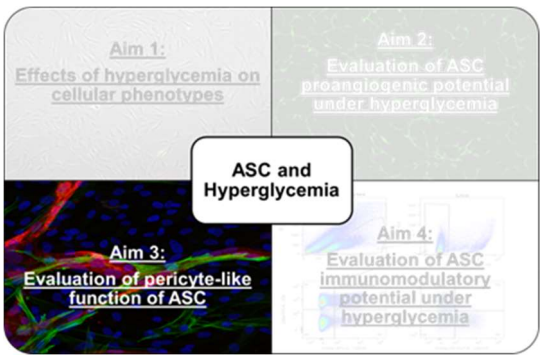

Pericytes are an important component in the microvasculature of the retina and many evidences sustain pericyte loss as one of the first sign of vessel degeneration. Their drop out would induce high microvascular instability [121]. As demonstrated by some studies in animals, MSC expressed pericyte-like markers once in the retinal microenvironment [125, 126]. In our third aim, we verified whether ASC might express pericyte-like markers when cocultured with HRMVEC. To

characterize the difference between ASC and HRMVPC, these were tested in coculture angiogenesis assays.

4.3.1 α-SMA positive ASC wrap around tube structures

To assess whether ASC could take over pericytes supporting function of vascular structures, we performed immunofluorescence staining on coculture angiogenesis assays and investigated the expression of two pericyte markers: α-SMA and NG-2.
In ASC:HUVEC cocultures, we observed that α-SMA positive $ASC_{NG\text{-}HG}$, were more concentrated around tube structures and in some cases, they even surrounded tubes reminiscent of pericytes wrapping around vessels (Figure 22). Notably, α-SMA had only a bare expression in ASC monoculture (not shown), suggesting that the contact with endothelial cells might induce a kind of pericyte-like differentiation in ASC.

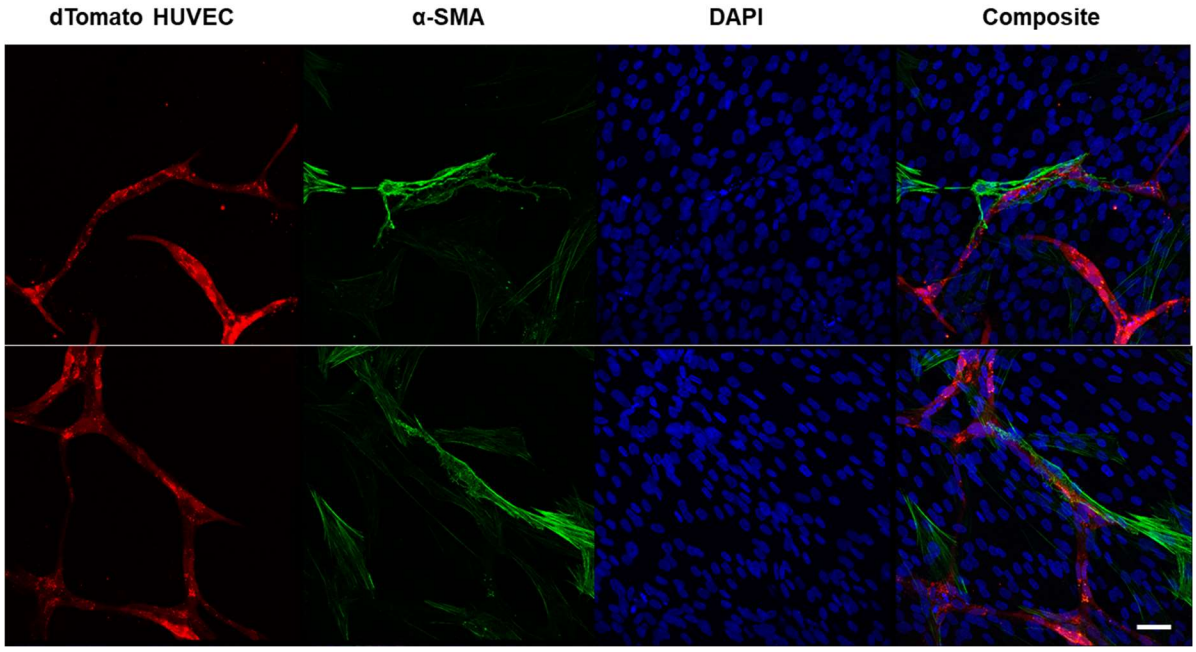

Figure 22 Representative confocal fluorescent images of α-SMA staining in coculture angiogenesis assays with ASC_{NG} (first line)/ASC_{HG} (second line) and dTomato HUVEC. α-SMA positive ASC (green) wrap around the tubular structures (red), resembling pericytes in normal physiology. Red: dTomato HUVEC; Green: anti-mouse Alexa Fluor 488 conjugated to anti-human α-SMA; Blue: DAPI. 50 µm scale bare; 40x oil immersion objective, images are a combination of 20 to 30 Z-stacks.

The same approach was applied to ASC:dTomato HRMVEC coculture angiogenesis assays. As previously observed in coculture with HUVEC, α-SMA positive ASC wrapped around HRMVEC (Figure 23). In line with previous results, ASC monoculture had only a weak expression of α-SMA (Figure 23, last line). These observations

confirmed that, independently of endothelial cell types, the proximity between ASC and endothelial cells induced in ASC a stronger α-SMA expression.

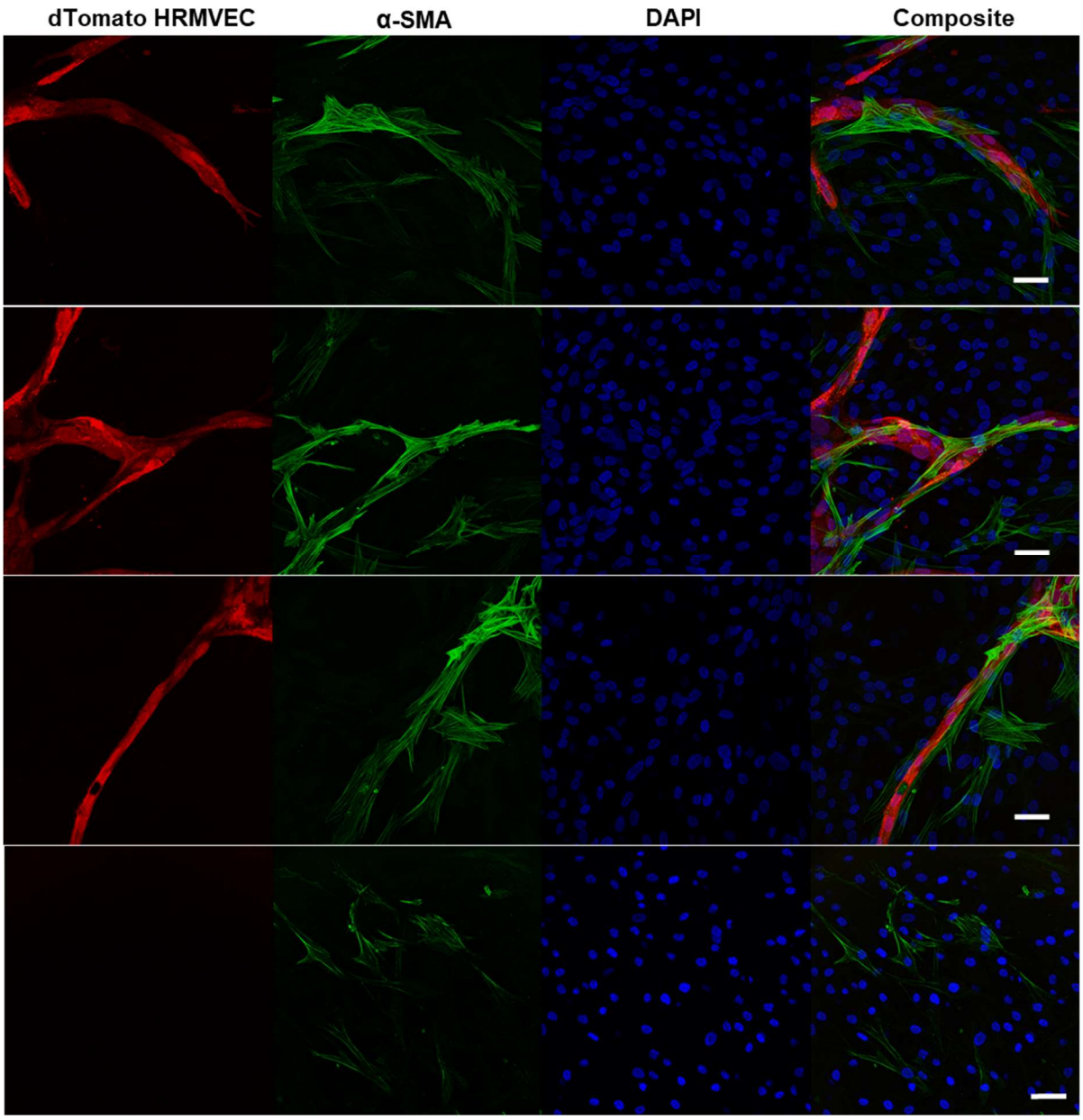

Figure 23 Representative confocal fluorescent images of α-SMA staining in coculture angiogenesis assays with ASC_{NG} and dTomato HRMVEC. α-SMA positive ASC (green) are concentrated around tube structures (red) and wrap around them (line 1, 2 and 3 are individual examples) . In ASC monoculture (last line), α-SMA is barely expressed. Red: dTomato HUVEC; Green: anti-mouse Alexa Fluor 488 conjugated to anti-human α-SMA; Blue: DAPI. 50 µm scale bare; 40x oil immersion objective; images in line 1,2 and 3 are a combination of 23 Z-stacks; last line, single plane image.

α-SMA is a very general pericyte marker; therefore, we performed a staining for NG-2 which is usually strongly expressed by capillary-associated pericytes [158]. In ASC: dTomato HRMVEC cocultures, we observed the whole ASC monolayer being positive

for NG-2 (Figure 24; line 1 and 2). In particular, no specific pattern of expression was found indicating that NG-2 expression was not aligned to tube-like structures. In ASC monolayer, NG-2 was similarly expressed as in coculture (Figure 24 last line). These observations suggested that, in contrast to α-SMA, NG-2 expression was constitutive in ACS and not related to endothelial cells and their tube formation.

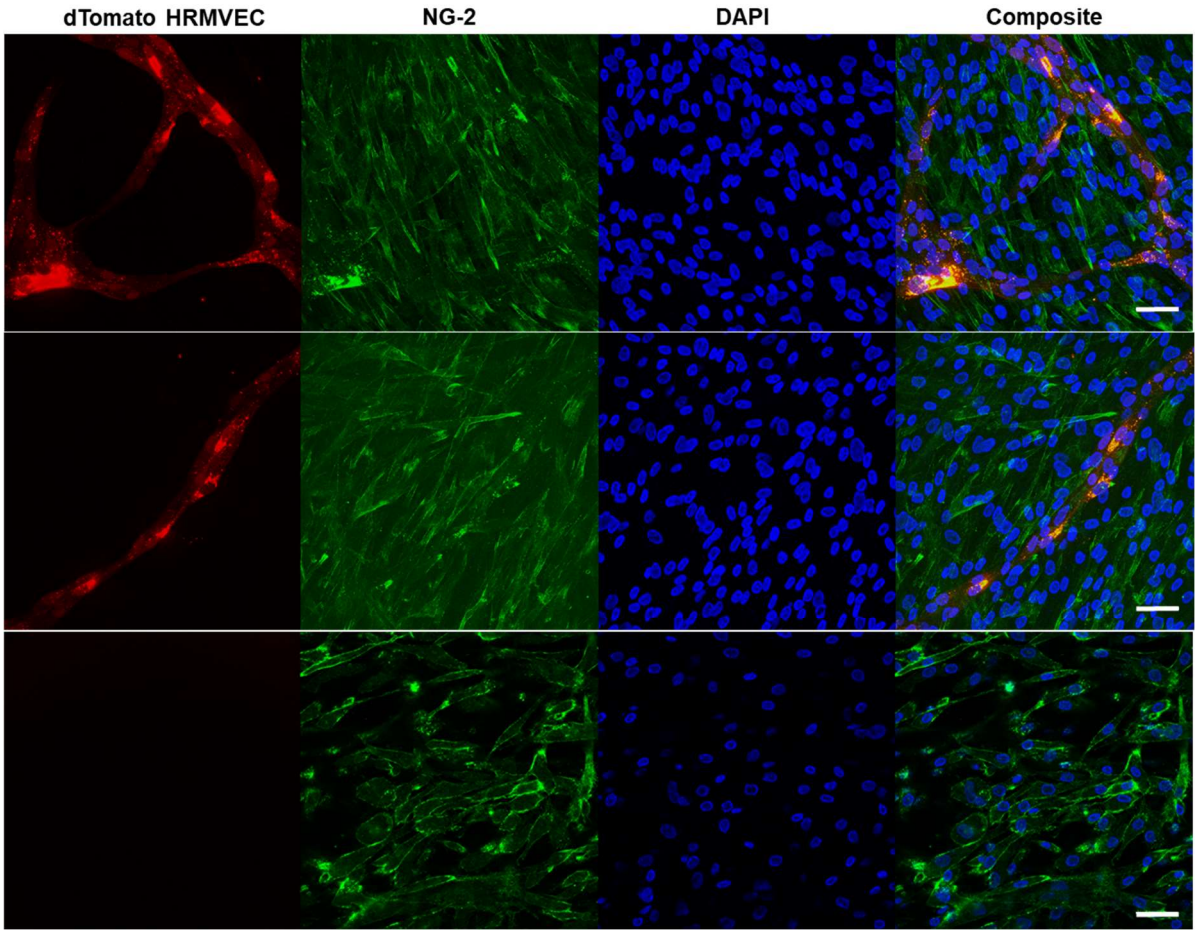

Figure 24 Representative confocal fluorescent images of NG-2 staining in coculture angiogenesis assays with ASC and dTomato HRMVEC. NG-2 (green) was uniformly expressed in the ASC monolayer of coculture (Line 1 and 2, two individual examples). A similar pattern was found in ASC monoculture (last line) Red: dTomato HUVEC; Green: anti-mouse Alexa Fluor 488 conjugated to anti-human NG-2; Blue: DAPI. 50 µm scale bare; 40x oil immersion objective; images in line 1 and 2 are a combination of 23 Z-stacks; last line, single plane image.

4.3.2 Pericytes have no angiogenic potential

So far, we demonstrated that ASC not only retained a strong angiogenic supportive potential, but also that they expressed pericyte marker such as α-SMA and NG-2. To further compare ASC to pericytes, we decided to test HRMVPC in a coculture angiogenic assay. We observed that HRMVPC cocultures with either HUVEC or

HRMVEC, did not support any tube formation in NG or HG culture media (Figure 25). Indeed, endothelial cells clustered together. This observation suggested thatHRMVPC, compared to ASC, do not retain a pro-angiogenic potential. This may be in line with their physiological role as modulator of vessels maturation, which stabilize and protect the vasculature.

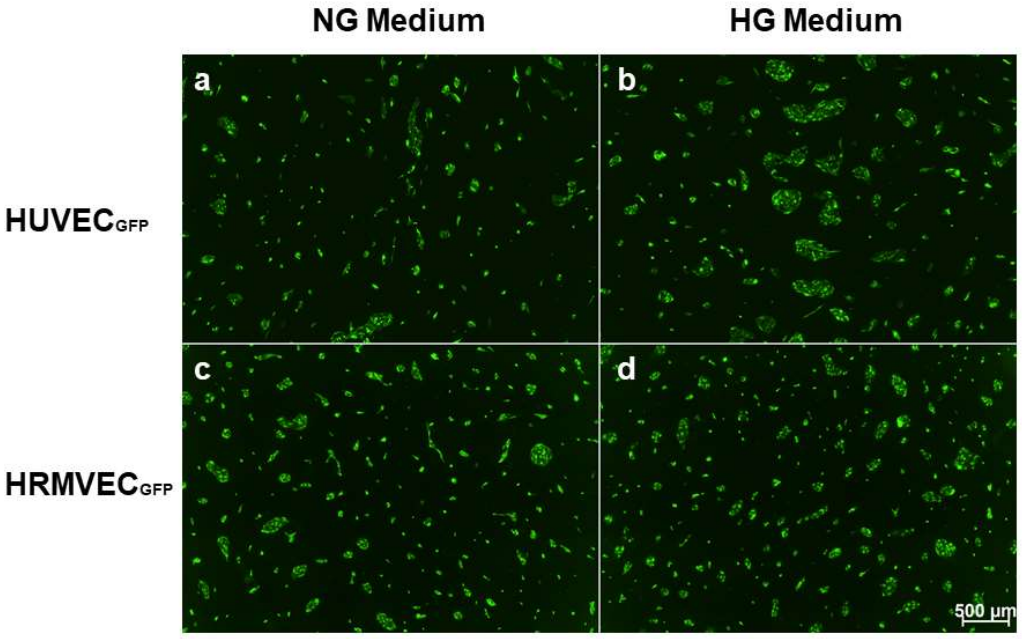

Figure 25 Representative pictures of coculture angiogenesis assay (n=3) with HRMVPC and HUVEC$_{GFP}$/ HRMVEC$_{GFP}$. Overall, no tube formation is observed. (a, b) Pericytes + HUVEC$_{GFP}$, in NG and HG media respectively; (c,d) pericytes + HRMVEC$_{GFP}$ in NG and HG media respectively.

As expected, HRMVPC expressed NG-2 both in coculture and monoculture. In cocultures, NG-2 expression pattern did not have any relation to HRMVEC, which were clustering together (Figure 26).

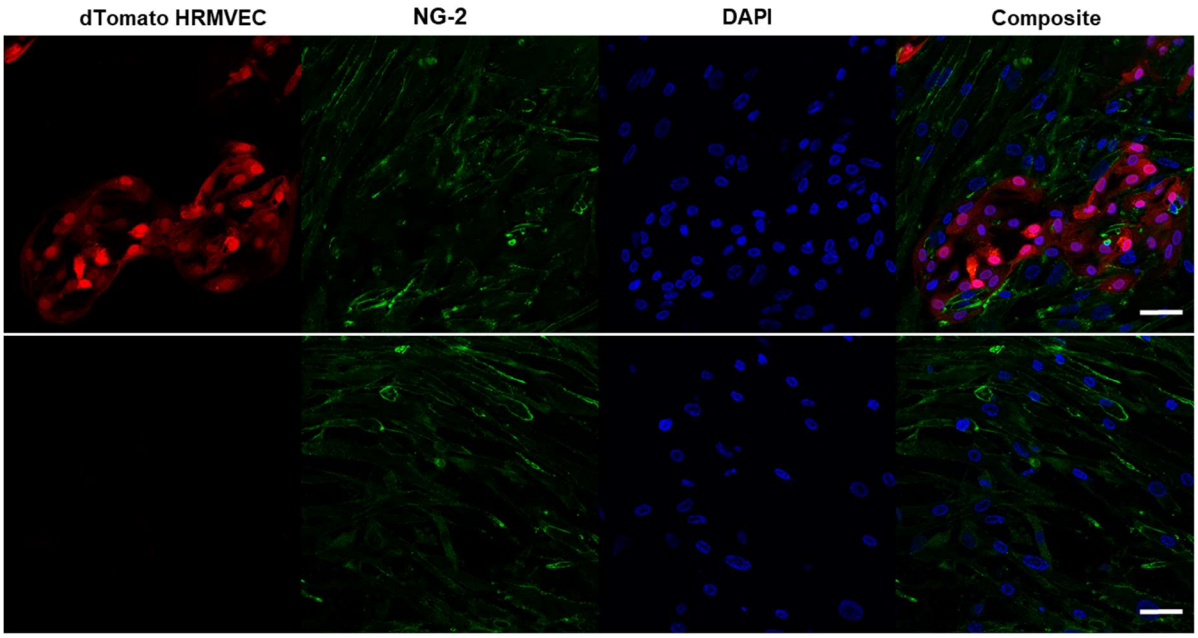

Figure 26 Representative confocal fluorescent images of NG-2 staining in coculture angiogenesis assays with HRMVPC and dTomato HRMVEC. dTomato HRMVEC (red) clustered together in cocultures with HRMVPC (Line 1). NG-2 (green) was expressed in the HRMVPC monolayer of coculture (Line 1). A similar NG-2 pattern was found in HRMVPC monoculture (Line 2). Red: dTomato HUVEC; Green: anti-mouse Alexa Fluor 488 conjugated to anti-human NG-2; Blue: DAPI. 50 µm scale bare; 40x oil immersion objective; single plane images.

Oppositely to NG-2, α-SMA expression in HRMVPC was very weak in coculture and almost absent in monoculture (Figure 27, Line 1 and 2), confirming the variability of α-SMA expression depending on pericyte location and origin [159, 160].

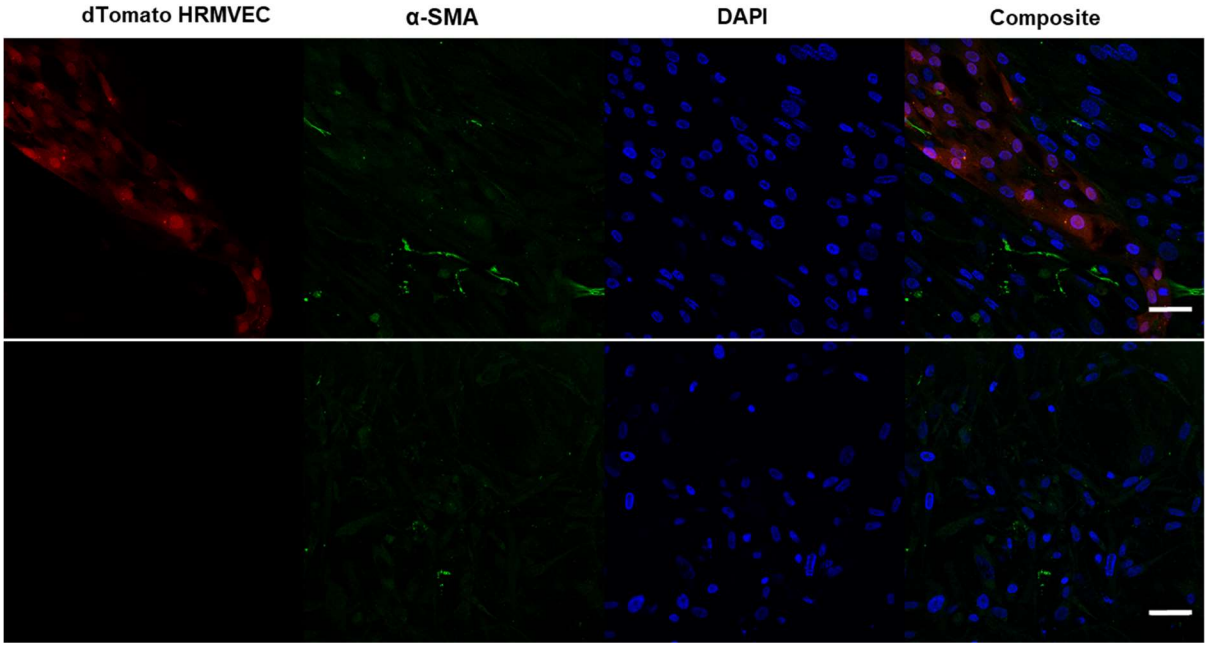

Figure 27 Representative confocal fluorescent images of α-SMA staining in coculture angiogenesis assays with HRMVPC and dTomato HRMVEC. dTomato HRMVEC (red) clustered together in cocultures with HRMVPC (Line 1). α-SMA (green) was weakly expressed in the HRMVPC monolayer of coculture (Line 1). In monoculture,

HRMVPC almost did not express α-SMA (Line 2). Red: dTomato HUVEC; Green: anti-mouse Alexa Fluor 488 conjugated to anti-human α-SMA; Blue: DAPI. 50 μm scale bare; 40x oil immersion objective; single plane images.

4.4 Evaluation of ASC immunomodulatory potential under hyperglycemia

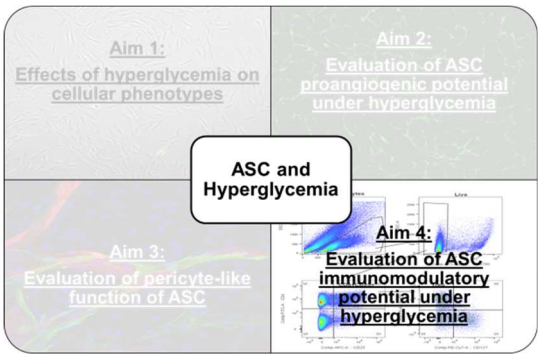

The fourth part of our project concerned the investigation of the immunomodulatory potential of ASC. As in the previous experiments, the distinction between ASC_{NG} and ASC_{HG} was kept, to evaluate potential hyperglycemia-mediated effects on ASC immunomodulation. Establishing ASC:PBMC direct and indirect (transwell) cocultures, we focused on the interaction between ASC and CD4 T cell subsets evaluating (1) the inhibitory effect of ASC on CD4 T cells, (2) the generation of Treg and (3) the soluble mediators involved. Two distinct conditions were evaluated: (a) stimulated cocultures, where PBMC were stimulated with CD3/CD28 beads and (b) not-stimulated cocultures, where resting PBMC were used.

4.4.1 ASC:PBMC stimulated coculture

4.4.1.1 ASC_{NG-HG} inhibit CD4 proliferation in coculture with stimulated PBMC

To verify ASC_{NG-HG} immunomodulatory capacity, direct and transwell cocultures with stimulated PBMC were established. As controls, stimulated PBMC monocultures placed in 6-well plate or in transwell inserts were used. After 7 days, CD4 cells highly proliferated in PBMC monocultures, as denoted by the high division index (Figure 28). In contrast, in both direct and transwell cocultures the division index significantly dropped (Figure 28), indicating that the presence of ASC, independently of cell-cell contact, was effective in inhibiting CD4 cell proliferation. Moreover, the extent of inhibition of CD4 proliferation was almost identical for ASC_{NG} and ASC_{HG}, suggesting that glucose did not interfere with ASC immunomodulatory potential.

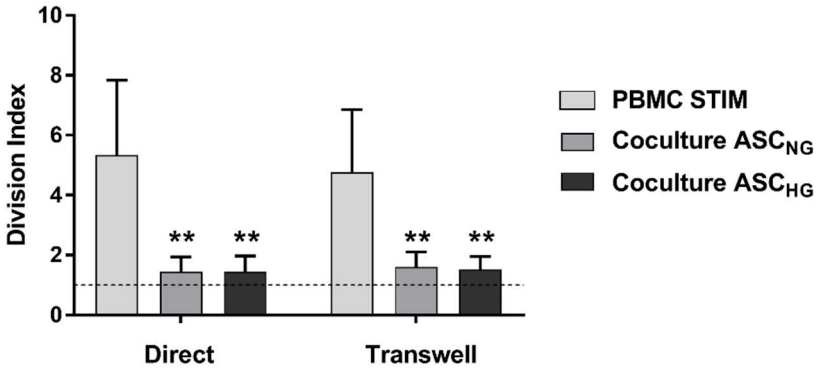

Figure 28 Direct and transwell coculture inhibit the proliferation of CD4 cells in stimulated PBMC. The inhibitory potential of ASC_{NG-HG} on stimulated PBMC was investigated in direct and transwell cocultures. After 7 days, cocultures and respective controls were harvested and analyzed. Division index of CD4 cells in stimulated PBMC monocultures and cocultures are reported. CD4 cells have similar division index in direct and transwell PBMC STIM monoculture (5.33±2.49 vs 4.76±2.08, respectively). ASC_{NG-HG}, either in direct or transwell cocultures, significantly inhibit CD4 cells proliferation, causing a reduction of the division index (direct: ASC_{NG} 1.45±0.4 and ASC_{HG} 1.45±0.5; transwell: ASC_{NG} 1.6±0.5 and ASC_{HG} 1.52±0.4; vs respective PBMC STIM controls: $p<0.01$). Data are normalized on division index of CD4 in not stimulated PBMC monoculture (division index =1). 2-way ANOVA multiple comparison, n=4.

4.4.1.2 The inhibition of T cell proliferation is based on IDO-mediated tryptophan depletion

Suppression of T cell proliferation is a well-established feature of the immunomodulatory potential of MSC and it has been related to IDO expression by MSC and the subsequent kynurenine production [161, 162].

To verify this mechanism to be relevant in our coculture, IDO levels were measured in cocultured ASC as well as kynurenine concentrations in coculture supernatants.

While IDO in ASC_{NG-HG} monocultures was not detectable, its level in ASC_{NG-HG} isolated from direct and transwell cocultures were considerably high and not affected by glucose (Figure 29 A). Notably, IDO was higher expressed in direct than in transwell cocultures ($p<0.05$) for both ASC_{NG} and ASC_{HG}. Despite this difference in IDO expression, kynurenine concentration in coculture supernatants was similar in all conditions (Figure 29 B). No kynurenine was detected in monocultures of stimulated PBMC, confirming that its production is to be allocated uniquely to ASC.

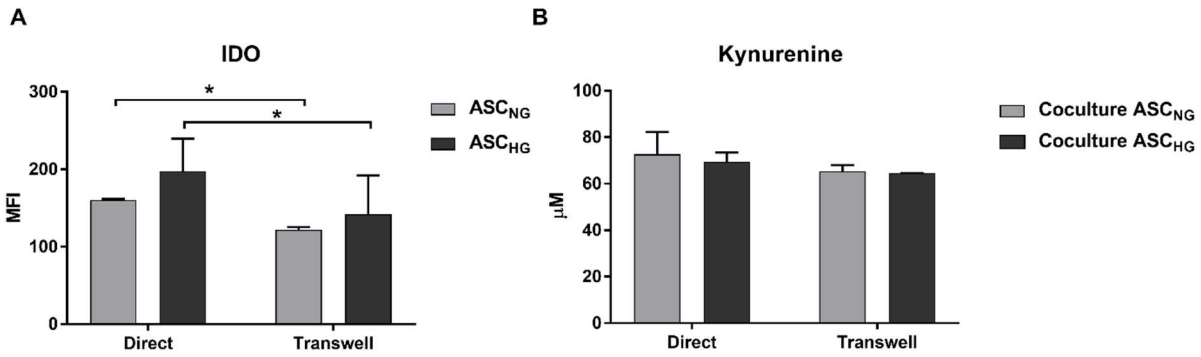

Figure 29 ASC-mediated inhibition of CD4 proliferation is regulated by induction of IDO and kynurenine production. A) IDO is highly induced in ASC_{NG-HG} of both cocultures when compared to ASC monoculture (not detectable, not shown); however, IDO induction is higher in ASC_{NG-HG} direct cocultures than transwell cocultures (MFI: direct ASC_{NG} 160.3±1.4 vs transwell ASC_{NG} 121.8±3.5, $p<0.05$ and transwell ASC_{HG} 197.8±42.4 vs transwell ASC_{HG} 141.8±50.2, $p<0.05$). No significant difference were found between ASC_{NG} and ASC_{HG}. 2-way ANOVA, n=3. B). Kynurenine production is similar in all conditions tested. No kynurenine was detected in ASC_{NG-HG} monoculture (not shown). 2-way ANOVA, n=3.

4.4.1.3 CD4 cells become activated in ASC cocultures

Having observed the significant suppression of CD4 cell proliferation in cocultures, we hypothesized that ASC might also inhibit their activation. Therefore, we dissected the CD4+ population looking for CD25 expression. CD25, known also as IL2RA (Interleukin-2 receptor alpha chain), is a type I transmembrane protein expressed on activated T cells and is considered one of the most prominent marker for cell activation [163].

The analysis of CD4+ viable cells revealed a similar degree of activation in PBMC monocultures in both direct and transwell conditions where CD4+CD25+ cells represented respectively 17.6±2.1% and 13.9±1.3% of the entire Live population (Figure 30 A). The fraction of CD4+CD25+ cells was increased in coculture with ASC_{NG-HG} in direct and transwell cultures. Although the increase was significant only in transwell cocultures (PBMC STIM vs ASC_{NG} and ASC_{HG}, $p<0.05$), a similar trend appeared also in direct cocultures (Figure 30 A). To understand whether the increase of CD4+CD25+ fractions in cocultures was related to their effective proliferation, we investigated the distribution of CD4+CD25+ cells in the proliferating (VPD-) and non-proliferating (VPD+) fractions (Figure 26 B). Despite the inhibition of CD4 proliferation previously documented in cocultures, we found a significant proliferation of CD4+CD25+ cells. Indeed, in the VPD- population, we observed a substantial increase

of CD4+CD25+ fractions in ASC_{NG-HG} cocultures compared to the PBMC STIM controls ($p<0.05$ in direct and $p<0.001$ in transwell). As already observed, no differences between ASC_{NG} and ASC_{HG} were found, again confirming that HG exerted no effects on ASC. In VPD+ fractions no major changes were detected in the CD4+CD25+ population, despite a small but significant increase in transwell ASC_{HG} coculture ($p<0.05$, Figure 30 B).

In conclusion, we found that despite the inhibition of CD4 cell proliferation, ASC induced their activation and proliferation in transwell and direct cocultures, exceeding the mere activation of CD3/CD28 beads.

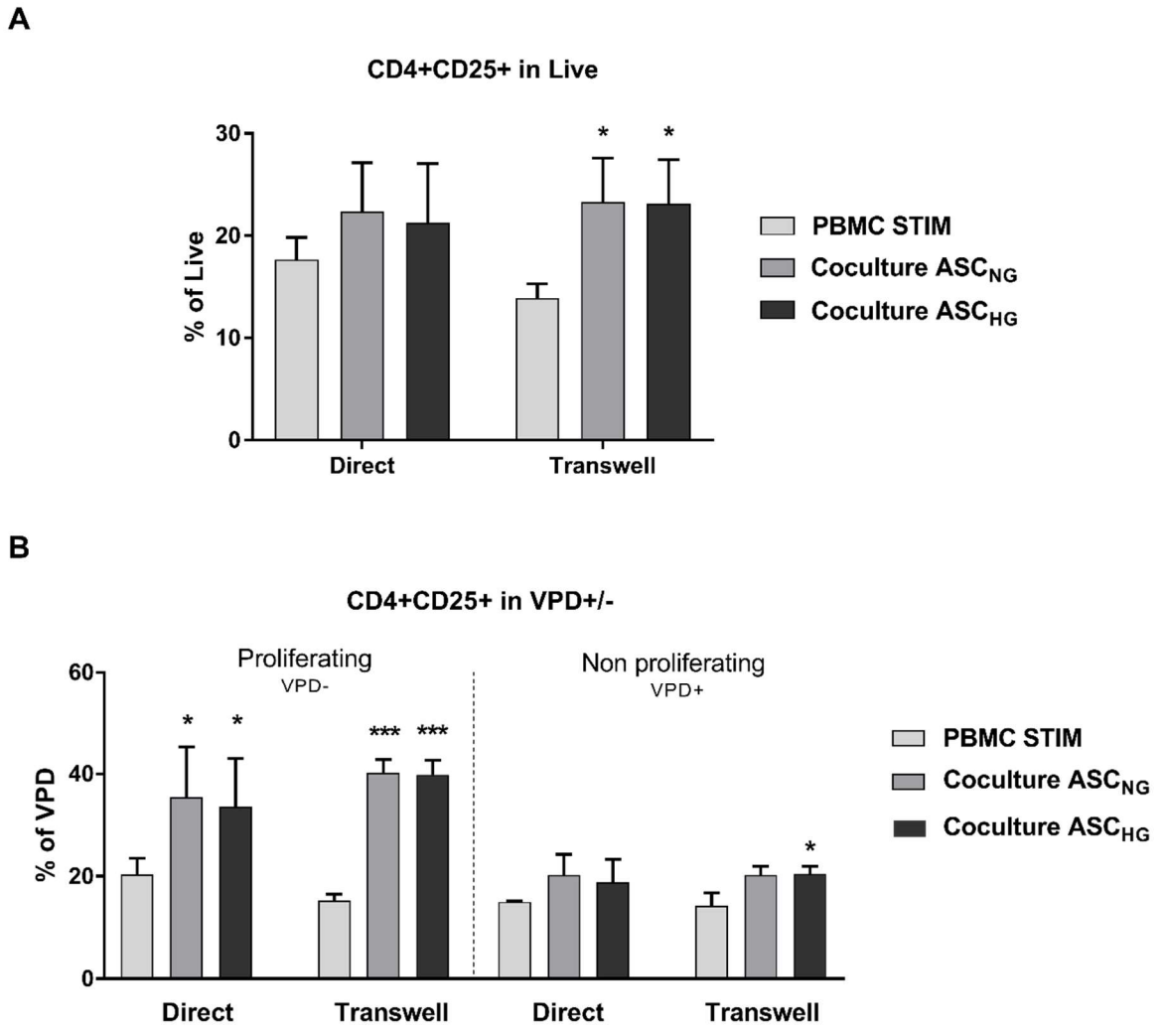

Figure 30 ASC promoted activation (CD25+) of CD4+ cells in coculture with stimulated PBMC. CD4+CD25+ population was analyzed in stimulated PBMC monocultures and cocultures after 7 days. A) Distribution of the CD4+CD25+ population in the Live population. In coculture, the CD4+CD25+ population is expanded compared to the PBMC monoculture (Direct: PBMC STIM 17.67±2.1% vs coculture ASC_{NG}: 22.3±4.7% and coculture ASC_{HG} 21.26±5.8, not significant; Transwell: PBMC 13.9±1.3% vs coculture ASC_{NG}: 23.2±4.3% and coculture ASC_{HG} 23.1±4.3%, $p<0.05$). 2-way ANOVA multiple comparison, n=3. B) Despite ASC inhibition on CD4+ cells proliferation,

CD4+CD25+ expansion is evident in both cocultures (VPD- direct: PBMC STIM 20.38±3.1% vs coculture ASC_{NG} 35.4±9.8% and coculture ASC_{HG} 33.55±9.4%, $p<0.05$; VDP- transwell: PBMC STIM 15.33±1.2% vs coculture ASC_{NG} 40.23±2.6% and coculture ASC_{HG} 39.84±2.8%, $p<0.001$). The VPD+ fraction remains constant in direct culture but it is slightly increased in transwell ASC_{HG} coculture compared to its control (PBMC STIM 14.3±2.4% vs coculture ASC_{HG} 20.47±1.5%, $p<0.05$). 2-way ANOVA multiple comparison, n=3.

4.4.1.4 The Treg fraction is unaffected by ASC coculture

Beyond being an activation marker, the expression of CD25 together with FoxP3 in CD4 cells is known to be a trademark for Treg (defined as CD4+CD25+FoxP3+). To investigate the distribution of Treg subpopulation in our cell cultures we compared direct and transwell cocultures as well as ASC_{NG-HG} to verify whether ASC could induce Treg.

Surprisingly, the Treg fractions in both direct and transwell, either ASC_{NG} or ASC_{HG} did not differ from the one observed in their control PBMC monocultures (Figure 31 A). We further checked the distributions of Treg in the VPD- and VPD+ populations (Figure 31 B). No difference was found between ASC_{NG-HG} direct coculture and its PBMC STIM control in the VPD- fractions. However, in transwell ASC_{NG} and ASC_{HG} cocultures, the Treg fraction was reduced compared to the transwell PBMC STIM control (PBMC STIM vs coculture ASC_{NG} $p<0.01$, PBMC STIM vs coculture ASC_{HG} $p<0.001$). Importantly, the reduction of Treg in VDP- fractions of ASC_{NG-HG} transwell cocultures was significant compared to the direct cocultures (direct coculture ASC_{NG} vs transwell coculture ASC_{NG} $p<0.01$ and direct coculture ASC_{HG} vs transwell coculture ASC_{HG}, $p<0.01$). The Treg distribution in VPD+ fractions was similar in all conditions (Figure 31 B).

In contrast to data in the literature, which mainly reported ASC-mediated induction of Treg, these data showed that direct or transwell cocultures did not modify the Treg balance in stimulated PBMC. Indeed, ASC seemed even to reduce Treg proliferation especially in transwell cocultures.

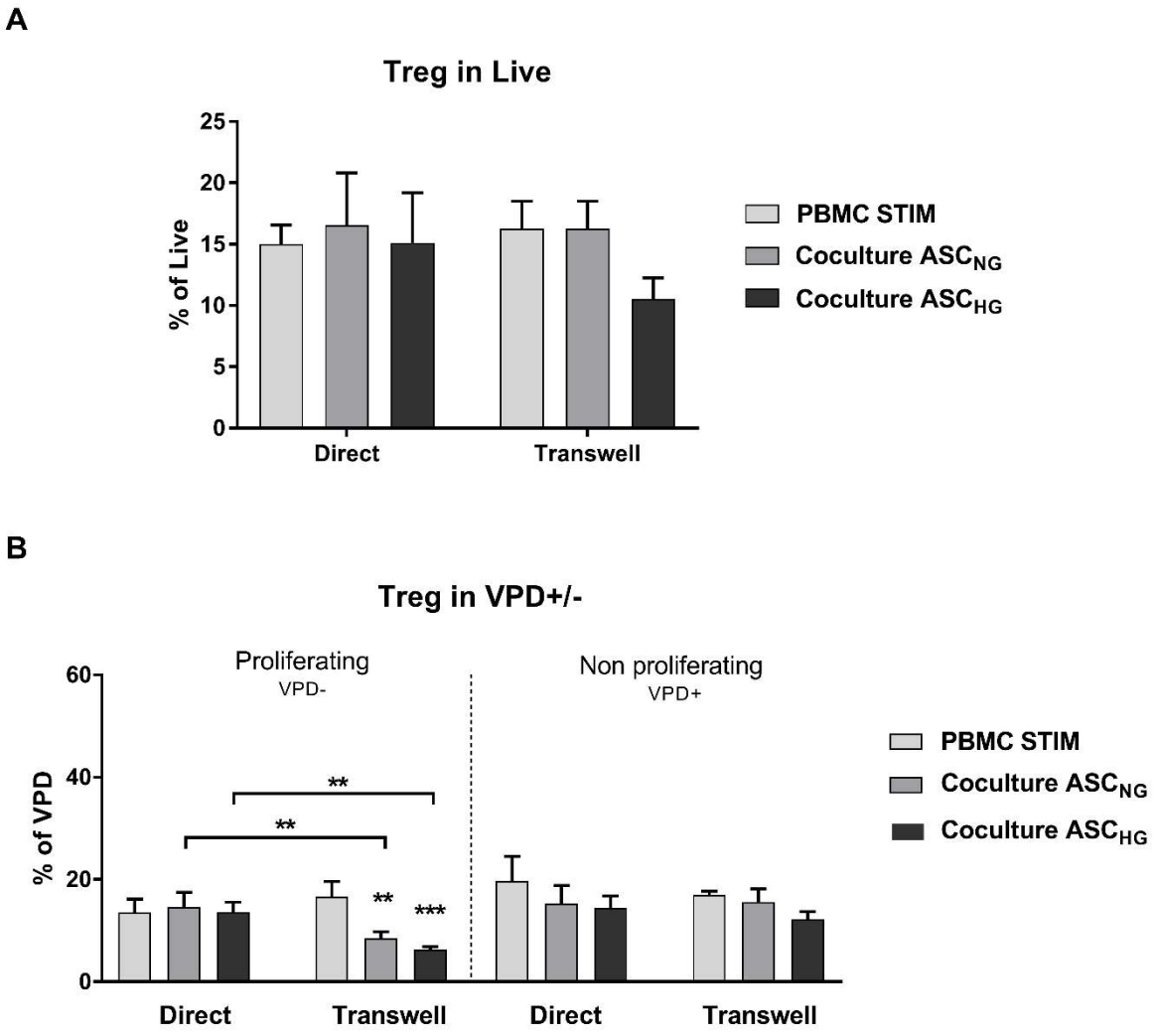

Figure 31 Distribution of the Treg population in the Live population (A) and in the VPD-/VDP+ group (B). A) The Treg fraction is equivalent in PBMC monocultures and ASC_{NG-HG} cocultures, in direct and transwell conditions. B) In direct cultures VDP-, Treg population is similar in all conditions. In transwell VPD-, T reg in ASC_{NG-HG} coculture are reduced compared to PBMC monoculture (transwell PBMC STIM 16.7±2.9% vs transwell coculture ASC_{NG} 8.5±1.2%, $p<0.01$ and vs transwell coculture ASC_{HG} 6.2±0.5% $p<0.001$). Moreover, in transwell ASC_{NG-HG} cocultures, Treg fraction was reduced compared to direct cocultures (direct coculture ASC_{NG} 14.5±2.8% vs transwell ASC_{NG} coculture 8.5±1.2%, $p<0.01$ and direct coculture ASC_{HG} 13.6±1.8% vs transwell ASC_{HG} coculture 6.2±0.5%, $p<0.01$). Overall, no differences were detected in the VPD+ fraction. 2-way ANOVA multiple comparison, n=3

4.4.1.5 ASC cocultures restrict cytokines secretion

We previously documented the inhibitory effect of ASC_{NG-HG} in coculture with T cells, independently of direct or indirect contact and independently of glucose. As the immunosuppressive potential of MSC has been reported to occur in parallel to polarization of Th subsets (which secrete specific set of cytokines) [73, 74], we

examined the CM of stimulated PBMC monocultures and ASC_{NG} cocultures for Th1/Th2 cytokines.

Overall, we found a reduction of analyzed cytokines in coculture in comparison to PBMC monoculture (Figure 32). Notably, IL-13 ($p<0.001$), IL-5 ($p<0.01$), IL-10 ($p<0.01$) and TNF-alpha ($p<0.01$) were significantly reduced in coculture. Similarly, although not significantly lowered, IL-9, IL-17a and IL-17f were also reduced, while IL-22 resulted unchanged.

These findings were in line with previous observations on the inhibitory effect of ASC on T cell proliferation. Indeed, it caused a reduction in number of cytokines producing cells and thus an overall reduction of cytokine levels. Moreover, we were not able to detect any specific Th1/Th2 polarization induced by ASC.

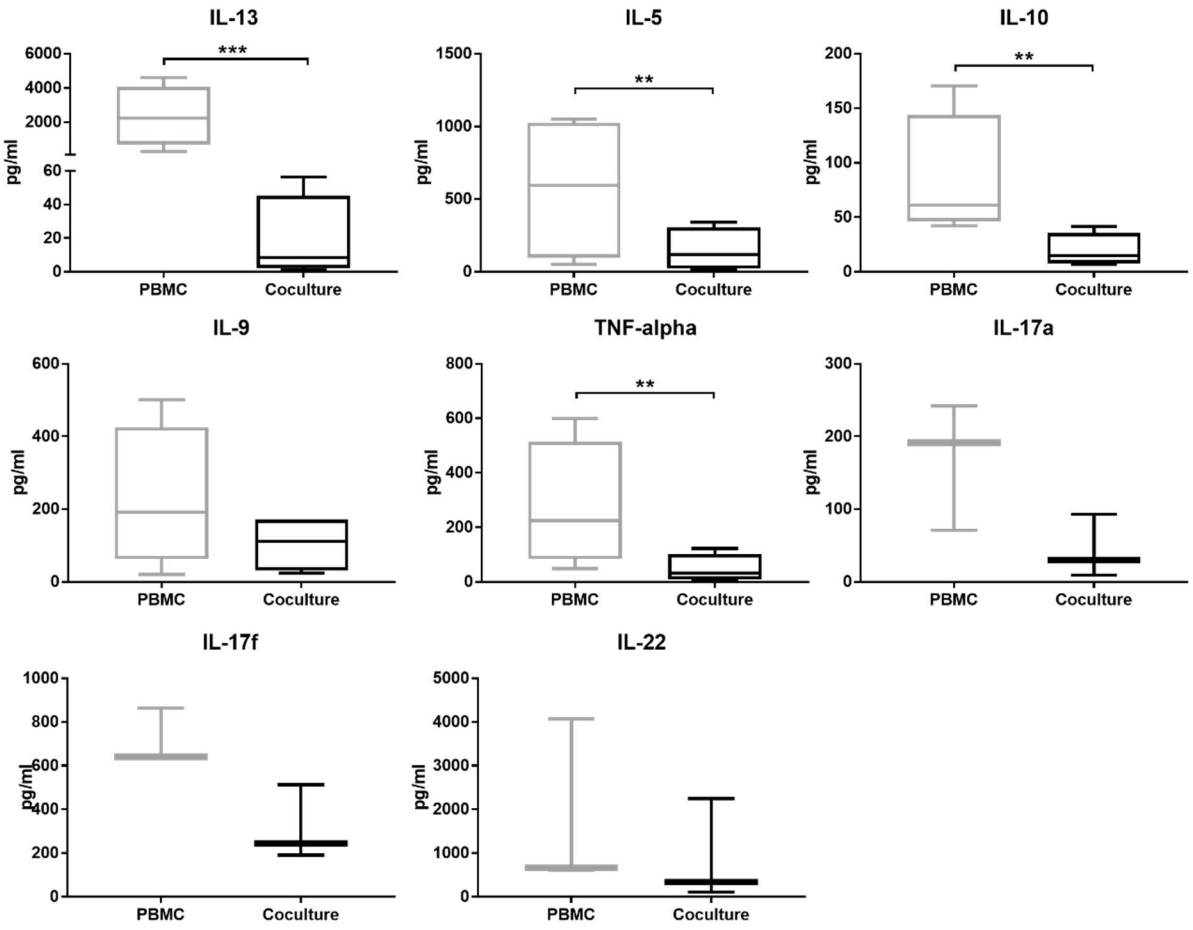

Figure 32 Th1/Th2 cytokines are decreased in stimulated coculture CM. Th1/Th2 cytokines (LEGENDplex™ Human Th1/Th2 Panel, Cat. n. 740730) were analyzed in CM of stimulated PBMC monoculture and coculture. Overall, coculture restricts cytokine secretion, notably: IL-5 ($p<0.01$), IL-10 ($p<0.01$), IL-13 ($p<0.001$) and TNF-alpha ($p<0.01$). Ratio paired T-test, n=4.

4.4.2 ASC:PBMC not stimulated coculture

4.4.2.1 ASC do not affect CD4 proliferation in resting PBMC

Having observed (1) the inhibiting effect of ASC on CD4 proliferation under CD3/CD28 stimulation, (2) induction of T cell activation marked by CD25 expression and (3) slight inhibition of Treg numbers, we established similar experiments in an not stimulated setting. Cocultures and their controls were set up using $ASC_{NH\text{-}HG}$ and not stimulated PBMC.

Because of their low immunogenicity, $ASC_{NG\text{-}HG}$ did not induce significant allogeneic proliferation of CD4 in both direct and transwell cultures (Figure 33). Intriguingly, CD4 in transwell PBMC control showed a slight but significant increase in the division index compared to PBMC in direct culture (PBMC direct vs PBMC transwell, $p<0.05$), suggesting a sort of auto-stimulation. The presence of $ASC_{NG\text{-}HG}$ did not affect this low level of proliferation within the transwell.

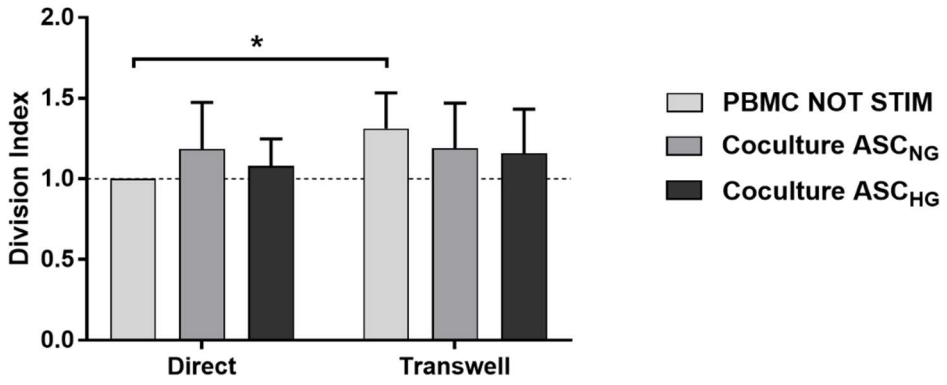

Figure 33 The inhibitory potential of $ASC_{NG\text{-}HG}$ in not-stimulated/resting PBMC coculture was investigated. $ASC_{NG\text{-}HG}$ do not affect not-stimulated PBMC (PBMC NOT STIM) in cocultures. However, some auto-stimulation of PBMC monoculture is observed in transwell culture when compared to direct ($p<0.05$). 2-way ANOVA multiple comparison, n=4.

4.4.2.2 IDO and kynurenine levels are low in coculture under not-stimulated conditions

We showed previously that IDO-mediated kynurenine production was observed in CD3/CD28-stimulated cocultures and was related to the immune suppressive action of ASC. In $ASC_{NG\text{-}HG}$:resting PBMC cocultures, both IDO and kynurenine were detectable

at low levels (Figure 34 A and B) while again no IDO was detected in ASC monocultures. Indeed, IDO levels in not stimulated ASC_{NG-HG} cocultures were more than halved compared to the one in stimulated cocultures (direct: stimulated ASC_{NG-HG} vs not stimulated ASC_{NG-HG}, $p<0.05$, not shown). In ASC_{NG} coculture with not stimulated PBMC, IDO was more expressed in ASC from transwell than in ASC from direct cocultures ($p<0.05$, Figure 34 A). Kynurenine concentrations were comparable in transwell and direct (Figure 34 B) but reduced when compared to stimulated cocultures (direct and transwell: stimulated coculture ASC_{NG-HG} vs not stimulated coculture ASC_{NG-HG}, $p<0.05$ not shown).

All together, these findings supported our previous observations, confirming that the ASC mediated IDO-kynurenine axis was actively involved in the inhibition of CD4 cell proliferation in a stimulated setting. However, in absence of CD3/CD8-mediated stimulation on PBMC, the IDO-kynurenine pathway was downregulated without any consequence on CD4 proliferation. CD4 proliferation did not occur in absence of CD3/CD28-stimulation.

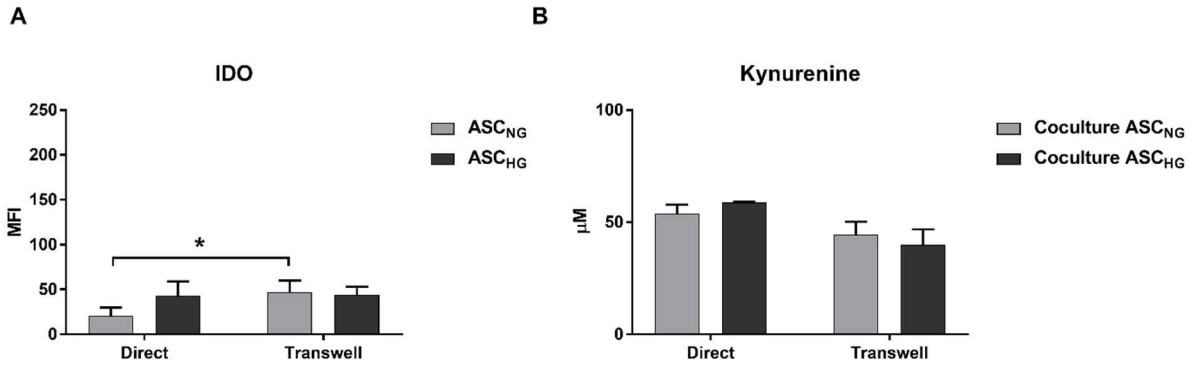

Figure 34 IDO, in cocultured $ASC_{NG.HG}$, and kynurenine, in cocultures CM, were measured. A) Low IDO levels are detected in both transwell and direct cocultured ASC_{NG-HG}. IDO is significantly higher in ASC_{NG} transwell coculture than direct coculture ($p<0.05$). Notably, IDO was not detectable in ASC monoculture. B) Kynurenine concentrations were low and comparable in both ASC_{NG-HG} transwell and direct cocultures. No kynurenine was detected in ASC monoculture or PBMC (not shown). 2-way ANOVA, n=3.

4.4.2.3 Unstimulated coculture do not activate CD4 cells

As stimulated coculture promoted CD4 activation, we evaluated CD25 expression on CD4 cells also in not stimulated cultures. The absence of CD3/CD28-mediated stimulation on PBMC strongly reduced the overall CD4+CD25+ population in ASC_{NG-HG} cocultures and controls (stimulated vs not stimulated in direct and transwell cultures

for PBMC and ASC_{NG-HG} coculture, from $p<0.05$ to $p<0.001$; not shown). In this case, no coculture-mediated activation of CD4 was detected (Figure 35 A). Zooming into the VPD- fractions (Figure 35 B), we found a similar trend in direct and transwell cultures, indicating a decrease of proliferating CD4+CD25+ cells in ASC_{NG-HG} cocultures when compared to PBMC monocultures (direct: PBMC vs ASC_{NG-HG} coculture, $p<0.05$; transwell: PBMC vs coculture, not significant, Figure 35 B). This indicated that despite the presence of ASC, in absence of CD3/CD28 stimulation, CD4 cells were not activated. No differences were detected in the distributions of CD4+CD25+ cells in VPD+ fraction.

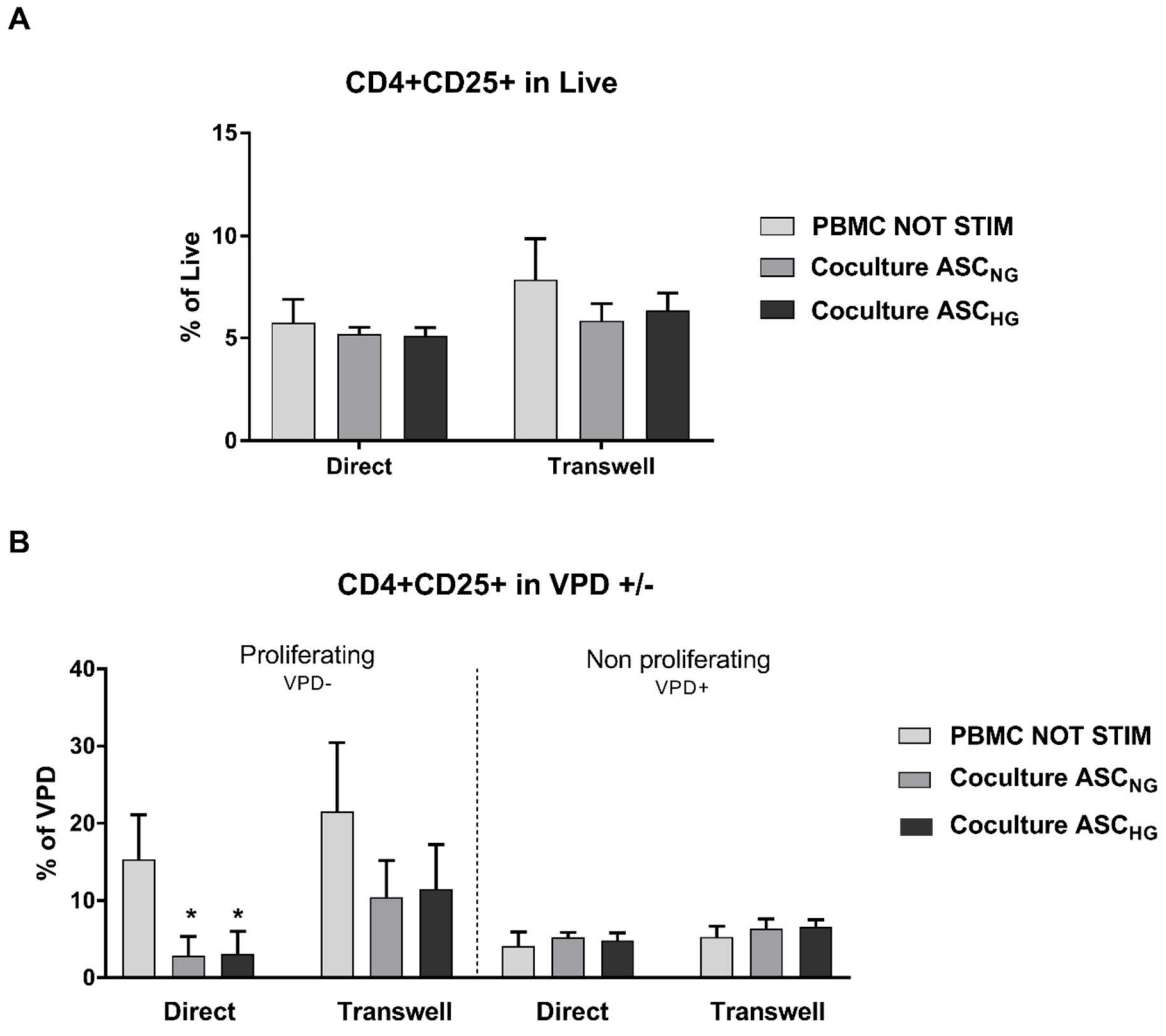

Figure 35 ASC do not induce activation (CD25+) of CD4+ cells under not-stimulated conditions. CD4+CD25+ population were analyzed in not-stimulated PBMC monoculture and coculture after 7 days. A) Distribution of the CD4+CD25+ population in the Live fraction. The CD4+CD25+ population is comparable in PBMC monoculture and ASC_{NG-HG} coculture in either direct and transwell. B) Distribution of CD4+CD25+ cells in the proliferating (VPD-)/non proliferating (VDP+) group. VPD- CD4+CD25+ population is reduced in direct ASC_{NG-HG} cocultures compared to PBMC (PBMC NOT STIM 15.37±5.7% vs coculture ASC_{NG} 2.83±2.5% and coculture ASC_{HG} 3.08±2.9%, $p<0.05$). A similar but not significant trend is observed in transwell (VPD- transwell: PBMC NOT STIM 21.5±8.9% vs coculture

ASC_{NG} 10.4±4.7% and coculture ASC_{HG} 11.52±5.7%, not significant). The proportion of the VPD+ CD4+CD25+ do not differ. 2-way ANOVA multiple comparison, n=3.

4.4.2.4 ASC_{NG-HG} cocultures promote Treg in not-stimulated setting

Subsequently, we evaluated the Treg distribution in the Live and in the VPD-/VPD+ population. The analysis of the Live population revealed that ASC_{NG} cocultures expanded the Treg fraction in both direct and transwell cocultures compared to PBMC monocultures ($p<0.05$). A similar but not significant trend was observed for ASC_{HG} cocultures (Figure 36 A). Overall, Treg fractions were higher in unstimulated conditions than stimulated (stimulated vs not stimulated in direct and transwell cultures for PBMC and ASC_{NG-HG} cocultures, from $p<0.05$ to $p<0.001$; not shown), suggesting that resting conditions might help in preserving Treg, which are further increased in presence of ASC.

These observations were further confirmed by dissecting the VPD-/VPD+ populations. Indeed, the proliferating fraction of Treg was increased in coculture, especially in direct cocultures (Figure 36 B). The VPD+ fraction did not vary upon culture conditions.

In summary, we observed that coculture between ASC and unstimulated PBMC did not promote CD4 cell activation. Instead, they promoted active proliferation of Treg.

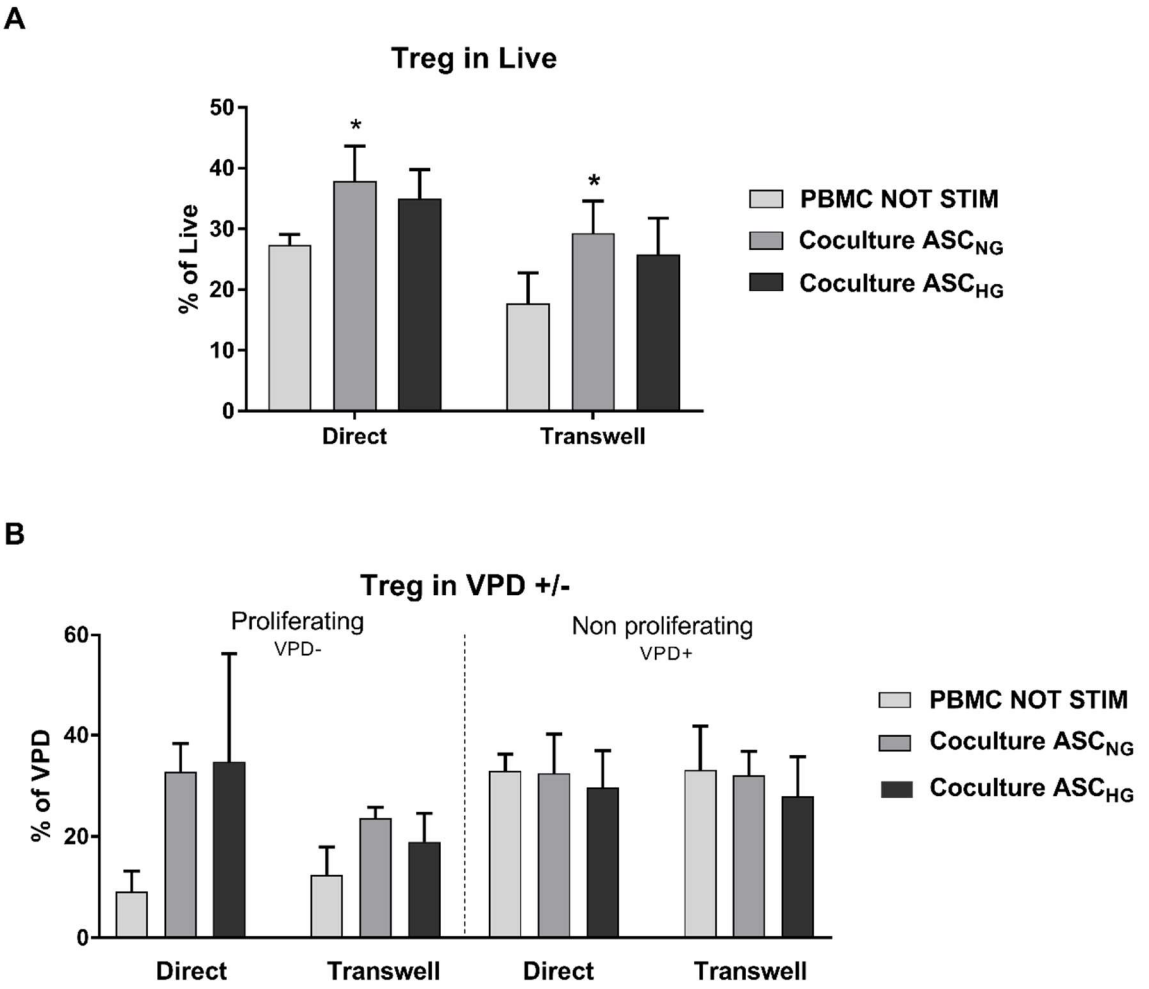

Figure 36 Distribution of Treg population in the Live fraction and in the VPD-/VDP+ fraction. A) The Treg fraction is increased in both cocultures compared to PBMC NOT STIM controls (direct: PBMC NOT STIM 27.35±1,7% vs ASC_{NG} coculture 37.9±5.6%, $p<0.05$; PBMC NOT STIM vs ASC_{HG} coculture 34.9±4.7%, not significant. Transwell: PBMC NOT STIM 17.7±5% vs ASC_{NG} coculture 29.3±5.2%, $p<0.05$; PBMC NOT STIM vs ASC_{HG} coculture 25.7±5.9%, not significant). 2-way ANOVA multiple comparison. B) Within the proliferated cell, the Treg fraction is increased in direct coculture (VPD- direct: PBMC NOT STIM 9.12±4% vs ASC_{NG} coculture 32.7±5.6% and ASC_{HG} coculture 34.7±21.5%, not significant). A similar trend is reported in transwell (VPD- transwell: PBMC NOT STIM 12.4±5.5% vs coculture 23.6.7±2.1% and ASC_{HG} coculture 18.9±5.6%, not significant). The distribution of Treg in the VPD+ population is similar in all condition. 2-way ANOVA multiple comparison, n=3.

4.4.2.5 ASC coculture reduces Th1/Th2 cytokine concentrations, while CCL-18 is highly concentrated in coculture

So far our data showed that cocultures between ASC_{NG-HG} and not-stimulated PBMC induced Treg proliferation independently of glucose, in contrast to cocultures with CD3/CD28-stimulated PBMC. As next step, we screened the CM of unstimulated cocultures for Th1/Th2 cytokines.

The analysis of Th1/Th2 showed a similar trend to the one observed in stimulated cultures. Indeed, all analyzed factors were reduced in coculture compared to PBMC monoculture (Figure 37). A significant reduction in coculture was found in the following factors: IL-5 ($p<0.05$), IL-9 ($p<0.05$), IL-10 ($p<0.05$) and IL-13 ($p<0.01$). On the contrary, IL-17f and IL-22 were similarly produced in PBMC monoculture and coculture while IL-17a and TNF-alpha were not detectable in coculture. To investigate whether CD3/CD28 mediated stimulation of PBMC influenced Th1/Th2 cytokine secretion, we compared unstimulated PBMC monoculture and coculture with their stimulated counterparts (not shown). We found that stimulated PBMC monocultures had generally higher level of cytokines compared to not stimulated PBMC. For instance, IL-10 ($p<0.001$), IL-13 ($p<0.01$), TNF-alpha ($p<0.01$), IL-17a ($p<0.05$) and IL-17f ($p<0.05$) were lower in not stimulated PBMC monoculture, in line with a quiescent not-activated state. Regarding cocultures comparison, a similar trend was detected within IL-10 ($p<0.01$), IL-9 ($p<0.05$), and IL-17f ($p<0.05$), which were lower in not stimulated coculture. These findings confirmed the immunosuppressive potential of coculture, which was detected in either unstimulated or stimulated coculture and proved that in absence of stimulation PBMC retained a different cytokine profile compared to stimulated PBMC.

In addition to the Th1/Th2 cytokine panels, we evaluated also IFN-gamma, IL-4 and CCL-18 (Figure 37). While IFN-gamma and IL-4 were substantially identical in PBMC and coculture, CCL-18 was highly concentrated in coculture ($p<0.05$).

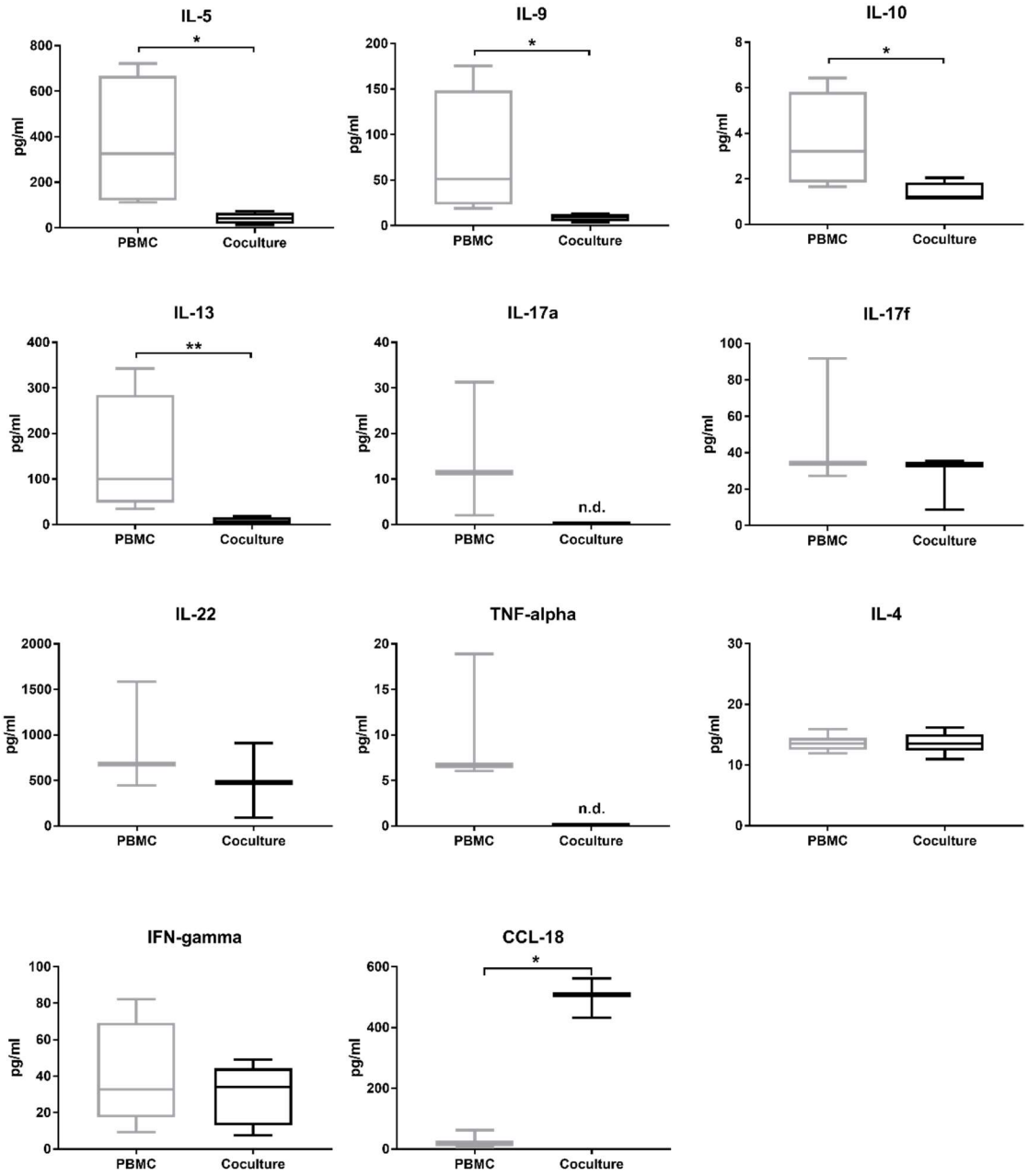

Figure 37 Th1/Th2 cytokines are inhibited in not stimulated coculture; IFN-gamma and IL-4 are unchanged. On the contrary, CCL-18 is highly produced in coculture. Th1/Th2 cytokines (LEGENDplex™ Human Th1/Th2 Panel, Cat. n. 740730) were analyzed in CM of stimulated PBMC monoculture and coculture. In addition, IFN-gamma, IL-4 and CCL-18 were also investigated. A) Overall, Th1/Th2 cytokines drop off in coculture, notably: IL-5, IL-9, IL-10 ($p<0.05$) and IL-13 ($p<0.01$). IFN-gamma and IL-4 have similar level in PBMC and coculture; CCL-18 is highly produced in coculture compared to not-stimulated PBMC monoculture ($p<0.05$). Ratio paired T-test n=3 to 4.

4.4.2.6 Coculture induces prolonged changes in the PBMC cytokine profile

Our early findings demonstrated that ASC mediated induction of Treg was evident only in coculture with resting PBMC. To explore whether the presence of ASC was sufficient

to activate a long lasting Treg expansion in resting PBMC, we further cultured pre-cocultured not stimulated PBMC in absence of ASC for further 7 days (a total of 14 days in culture). Afterwards, CD4+CD25+ and Treg populations were characterized as well as some selected cytokines analyzed in their CM.

The analysis of CD4+CD25+ cells in the Live population, revealed a similar distribution in control PBMC and PBMC from cocultures (ex-coculture; Figure 38 A). We found a higher percentage of Treg in control than in ex-coculture PBMC ($p<0.001$).

To assess whether the cytokine profile of PBMC was long-lastingly changed upon pre-treatment in coculture, we isolated CM from these PBMC cultures and analyzed selected cytokines (Figure 38 B). In contrast to previous observations, where cytokine concentrations were overall reduced in cocultures, ex coculture PBMC produced higher amounts of cytokines than their counterparts from monocultures (Figure 38 B). Specifically IL-10 ($p<0.01$), IFN-gamma ($p<0.01$), TNF-alpha ($p<0.05$) and CCL-18 ($p<0.01$) were increased in ex-coculture PBMC than control, only IL-4 was unchanged.

In conclusion, we observed that PBMC, which were cocultured with ASC, did not retain a long-lasting proliferation of Treg. Their cytokines profile indicated a high production of IL-10 and CCL-18, which was not observed during the coculture.

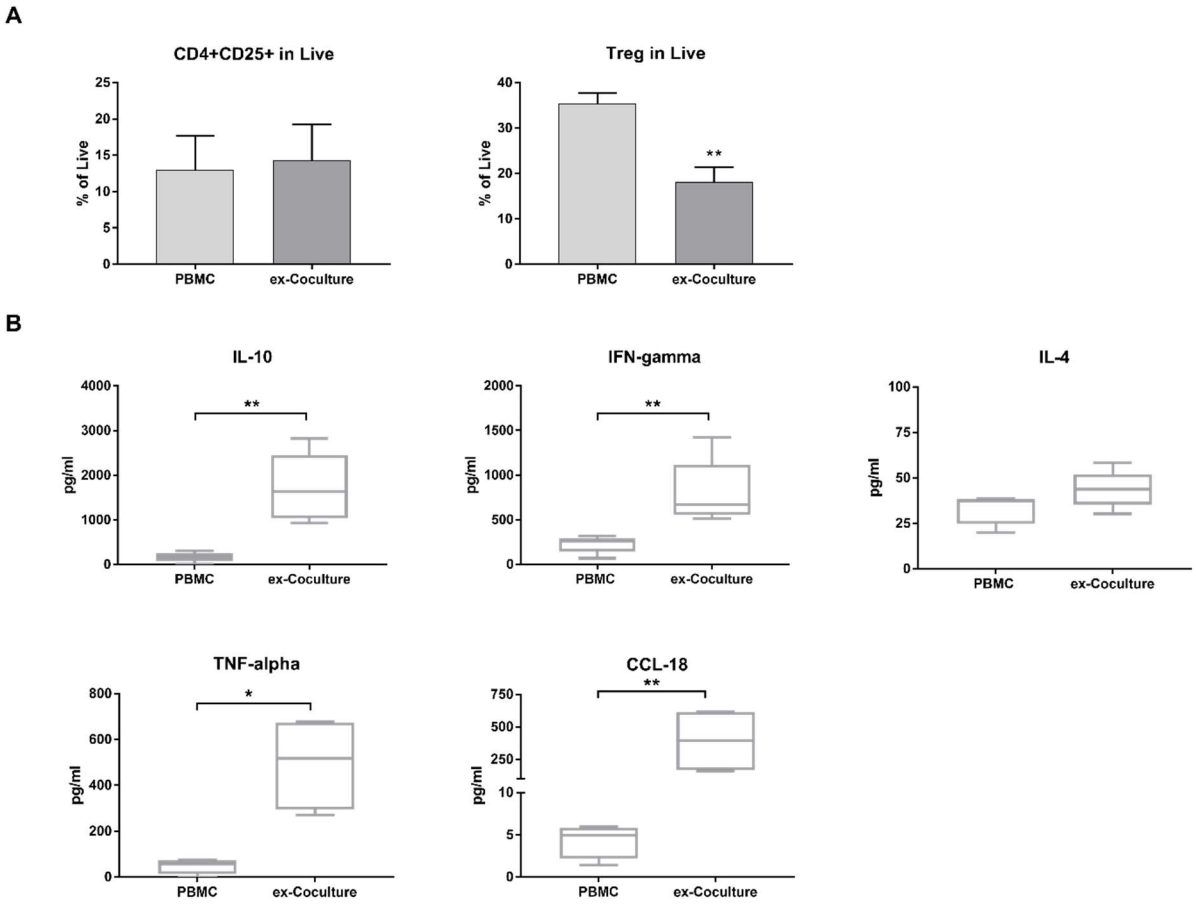

Figure 38 PBMC from coculture (ex-coculture) and control (PBMC) were cultured alone for further 7 days, CD4+CD25+ and Treg were measured in the Live population as well as cytokines in their CM. A) The CD4+CD25+ population is similarly detected in PBMC and ex-coculture PBMC (13±4.6% vs 14.3±4.9%, not significant). The Treg fraction in the Live population is higher in PBMC than ex-coculture PBMC (35.4±2.2% vs 18.1±3.1, $p<0.01$). Ratio paired T-test, n=4 to 5. B) IL-10, IFN-gamma and TNK-alpha are highly present in CM from ex-coculture PBMC than PBMC cultured alone (IL-10 and IFN-gamma $p<0.01$ and TNF-alpha $p<0.05$). IL-4 is equally present in both conditions. CCL-18 remains high in ex-coculture PBMC ($p<0.01$). Ratio paired T-test, n=4 to 5.

4.4.3 TGF-β is a mediator for Treg induction

Our findings generally denoted that glucose had no effect on the immunomodulatory potential of ASC. Moreover, we documented that cocultures induced Treg formation and proliferation only in resting conditions and that the same PBMC in culture for further 7 days were changed in their cytokine profile.

To confirm our observations on Treg induction in coculture, we investigated TGF-β production in direct and transwell cocultures as well as in stimulated and not stimulated settings. Indeed, TGF-β is considered a very important mediator in Treg generation being involved in their regulation [164].

Thus, we measured TGF-β in CM of direct and transwell cocultures of unstimulated PBMC and ASC, using ASC monoculture as control (Figure 39). All conditions produced more TGF-β than ASC alone (dotted line) and TGF-β was not found in CM from stimulated/not stimulated PBMC. These first findings suggested that TGF-β production was to be allocated uniquely to ASC. In not stimulated cocultures, we found that TGF-β was highly produced in direct coculture compared to transwell ($p<0.001$). In addition, comparing direct cocultures, not stimulated cocultures produced more TGF-β than stimulated one ($p<0.01$).

These data were in line with the observed increment of Treg in cocultures of unstimulated PBMC, especially in direct coculture, supporting the notion that TGF-β production was strongly related to Treg generation in our coculture and being dependent on both direct cell contact and resting condition of PBMC.

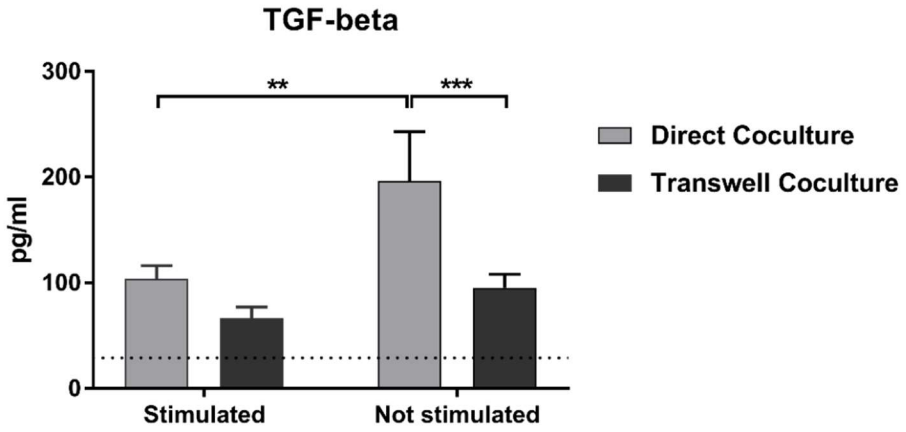

Figure 39 TGF-β was measured in CM of direct and transwell cocultures. TGF-β is more concentrated in direct and transwell cocultures than in the control (ASC monoculture, dotted line). In stimulated conditions, production of TGF-β is higher in direct than transwell cocultures (103.5±12.5 pg/ml and 66.5±10.6 pg/ml, respectively) but not significant. Whereas in not stimulated conditions, TGF-β is considerably more concentrated in CM of direct than transwell cocultures (196.2±46.7 pg/ml vs 95.2±12.8 pg/ml, $p<0.0001$). Moreover, comparing direct coculture, TGF-β is higher in not stimulated settings than stimulated ones ($p<0.001$). TGF-β was not detected in monoculture of stimulated/not-stimulated PBMC. 2-way ANOVA, n=4.

5 DISCUSSION

The rationale of this study was to evaluate whether ASC were affected by hyperglycemia in their basic characteristics and functional potentials. As mentioned in the introduction, hyperglycemia is considered one of the main factors driving cell damage in pathologies related to poor glycemic control such as diabetes and metabolic disorders. Glucose-mediated cell damage has been strongly related to microvascular complications and particularly to endothelial cell dysfunctions in secondary diabetic complication as DR [133]. MSC and especially ASC, have been recently proposed as potential cell-based treatment for DR and many studies on several animal models demonstrated the safety and efficacy of this approach. Indeed, ASC have been shown to interact within the retinal microenvironment through the following mechanisms: (1) secretion of proangiogenic factors and stimulation of neovascularization, (2) secretion of anti-inflammatory factors and reduction of inflammation/lymphocyte infiltration and (3) acquisition of a pericyte-like function giving support and stabilizing the retinal vasculature. All these studies proposed only allogenic application of MSC as many reports suggested that MSC isolated from diabetic donors, might be impaired in their potency and functions. In this context, (a) the evaluation of autologous MSC applications in hyperglycemia-related pathologies as well as (b) the investigation of diabetic/hyperglycemia-mediated effects that may occur once healthy MSC are in a diabetic/hyperglycemic environment, can give important insights on how MSC-mediated cell therapy can be improved in the particular pathological setting of DR.
In this study, we investigated hyperglycemia-mediated effects on ASC through a series of *in vitro* experiments

5.1 Does hyperglycemia affect ASC basic characteristics?

The first step in our study was to address “basic” effects of hyperglycemia on ASC, hypothesizing that potential HG-mediated effects would have been detected on cellular phenotype, differentiation and cell growth. As the vascular compartment represents the main target of MSC-based therapy in DR, we conduced similar analysis on HRMVEC.

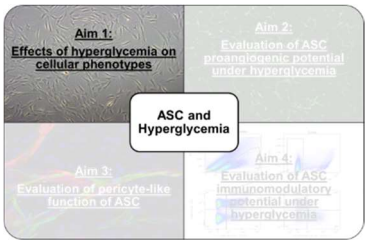

5.1.1 Hyperglycemia on ASC causes a transient increase of oxidative stress

Many studies already demonstrated the impairment of ASC isolated from diabetic patients/animals. Reduced therapeutic capacity in wound healing [145, 165] and even impaired ability to protect retinal vasculature in Akimba mice [148] were documented. However, none of them was uniquely focused on investigating potential cell damages mediated by hyperglycemia. In our study, we observed that hyperglycemic culture conditions had no major effect on (1) ASC basic characteristics (immunophenotype and differentiation potential), (2) nor their angiogenic supportive capacities, (3) nor their immunomodulatory properties. We speculate that this might be related to the capacity of ASC to regulate glucose uptake and thus, to control adverse intracellular events such as ROS formation and oxidative stress. Supporting our findings, Hajmousa et al. described that HG cultured ASC were largely refractory to hyperglycemia, despite an increased production of ROS and mitochondrial reorganization. Moreover, in presence of HG, ASC changed their metabolic profile decreasing oxygen consumption and glycolysis [151]. Taken together these findings suggested that ASC might have intrinsic regulatory mechanisms, to guarantee an efficient and rapid adaptation to metabolic changes in the surrounding microenvironment.

Since we cultured ASC in HG directly after isolation from lipoaspirate and kept this condition within experiments, we provided an even stronger evidence of ASC tolerance to HG, indicating that prolonged/long term HG cultures did not affect ASC. Only at the first passage after isolation, ASC_{HG} displayed a slower cell growth compared to ASC_{NG}, confirmed by an increase in doubling time and a reduction of cell doublings. The first phase of cell growth after isolation is the most delicate as cells face for the first time the *in vitro* culture. Therefore, being in contact with HG might have represented an additional obstacle for cells, which was then translated in a reduction of cell growth rate. Importantly, these effects were transient and restricted to the first passage, indicating and confirming that ASC could rapidly adapt to this culture condition. The measurement of intracellular oxidative stress (total ROS measurement) further supported this notion. Indeed, while ASC_{NG} and ASC_{HG} displayed similar and low levels of oxidative stress, in ASC_{NG} switched to HG (ASC_{NG} in HG) ROS levels increased and were sensitive and reduced upon antioxidant treatment. Again, in line with Hajmousa et al., only a transient effect of glucose was demonstrated.

Increased glucose influx in cells is defined by the unifying hypothesis as the main driving force of cellular destabilization as well as the principal cause of increased ROS

production [133]. Therefore, in parallel to measurement of intracellular oxidative stress, we evaluated glucose uptake in ASC_{NG} and ASC_{HG}. We found that both ASC_{HG} and ASC_{NG} in HG had a reduced glucose uptake compared to the one of ASC_{NG}. This was supported by similar observations provided by Hajmousa and colleagues. In $ASC_{HG,}$ glucose uptake levels were as low as those when applying a GLUT-1 inhibitor (WZB-117) on ASC_{NG}. These results are of crucial importance as, in contrast to the unifying hypothesis, they appear to disconnect ROS production from glucose uptake.

In our experimental setting, ROS production was not relatable to increased glucose influx. However, we cannot exclude that, at earlier time points of HG switching, a transient increase of glucose influx might have occurred together with an increase in oxidative stress, which could have been detectable even after several hours. Furthermore, our measurement of ROS may have been slightly imprecise, reflecting several cytoplasmic oxidative stressors rather than solely ROS. Indeed, as carboxy-H_2DFFDA penetrates in cells, it is subject to oxidation by several cytoplasmic ROS species such as hydrogen peroxide, organic hydroperoxides, nitric oxide and peroxynitrite, which turn it into being fluorescent. Moreover, its oxidation has been found to be influenced by glutathione (GSH) [154]. In light of this, we have to argue that our data: (1) could not be related to specific mitochondrial ROS production, which are the one effectively addressed in the unifying hypothesis, and (2) should be interpreted as a transient increase of oxidative stress index upon glucose switch.

In conclusion, our findings on ASC_{NG-HG}, were in line with the previous proposed by Hajmousa and colleagues, indicating a solely transient effect of glucose in increasing the oxidative state of cells, while other characterizing parameters were not affected. The absence of glucose-related damages on ASC appeared to be related to the restricted uptake of glucose, in virtue of their rapid metabolic adaptation to the hyperglycemic surrounding microenvironment.

5.1.2 Hyperglycemia induces an angiogenic dysfunction in HRMVEC

Considering ASC as potential therapy for DR, this study focused next to HRMVEC to investigate potential glucose toxicity. Hyperglycemia-mediated cell damage, especially for microvascular cells, is a well-established concept with multiple evidences confirmed *in vivo* and *in vitro* [135]. Loss of vascular permeability and induction of pro-inflammatory pathways are only some of the described indicators of HG toxicity [133, 166]. The common denominator triggering hyperglycemia-mediated injuries is ROS

overproduction. For metabolic reasons, mitochondrial ROS overproduction is the principal consequence of increased glucose influx inside endothelial cells. Indeed, ROS overproduction gives rise to a destabilizing cascade of detrimental events (increased polyol and hexosamine pathway, AGE production and PKC activation), which destabilize and damage endothelial cells [134]. Therefore, we first examined HG impact on HRMVEC growth rate and then, we focused on ROS production/oxidative state and glucose uptake. In last instance, we assessed whether hyperglycemia might affect their angiogenic potential

HRMVEC growth rate was not affected by HG. Thus, this first outcome was rather unexpected, as our rationale based on previous reports on pronounced glucose-toxicity in endothelial cells. We argued that optimal culture conditions, provided by the cell culture media, might potentially overrule detrimental effect of glucose. Indeed, the presence of growth factors in the culture media, such as VEGF, has been demonstrated to be protective for HG-mediated injuries [156, 157]. Therefore, cell growth monitoring was repeated in ¼ ECGM-2 medium (cell medium containing only ¼ of supplemented growth factors). Because of the lowered serum/growth factors provision, HRMVEC general growth rate diminished compared to ECGM-2. Only a slight reduction was caused by HG. Further readings revealed that, in fact, hyperglycemia-mediated effects on endothelial cell proliferation may vary. While some studies demonstrated hyperglycemia being effective in reducing endothelial cell growth [167, 168] and even promoting apoptosis [169], others found HG inducing their proliferation [170, 171]. We restricted our analysis on monitoring proliferation, thus, we cannot speculate on whether both findings might have occurred in parallel. Indeed, a feed forward mechanism in which dead cells were replaced by new proliferating ones, can be an explanation to an unchanged growth rate. To undercover this, a deeper analysis on cell cycle of HG exposed cells as well as apoptosis quantification could be performed.

Another aspect to be considered is the timing of hyperglycemic injury. Duration of HG exposure, especially a temporary switch from NG to HG (intermitted glucose) has been reported to cause a more pronounced proliferation than exposing cells to prolonged HG [170].

Similarly to ASC, where we observed that a transient switch to HG induced oxidative stress whilst glucose uptake became efficiently restricted, we performed similar experiments in HRMVEC. Here, HG caused an increase in intracellular oxidative stress. However, in contrast to many findings in the literature, this was not related to glucose uptake. Indeed HG HRMVEC showed a reduced glucose uptake compared to NG and the addition of the GLUT-1 inhibitor even lowered that uptake. We concluded that HG-mediated induction of oxidative stress (increased in detection of total ROS) was not related to glucose uptake. On one hand, our results are in line with findings in the literature (glucose-mediated oxidative stress induction), on the other, the fundamental milestone of intracellular hyperglycemia, as consequence of extracellular HG, is not corroborate. As ASC, HRMVEC restricted glucose uptake, however, in contrast to ASC they appeared to rely on at least some level of glucose uptake even in HG conditions. Thus, the fundamental link between extracellular hyperglycemia translating to intracellular hyperglycemia does not appear to be true in our study. Admittedly, similar shortcomings as discussed in the ASC section also apply to the HRMVEC, with respect to timing and kinetics of hyperglycemia exposure. Indeed, we can postulate an increased glucose uptake in the very first moments after HG application, which is later restricted. In support of our hypothesis, it was observed that chronical and acute glucose exposure resulted in different outcomes both *in vitro* and *in vivo* [170, 172].

In last instance, we assessed the proangiogenic potential of HRMVEC in regard of HG. In DR the first signs of the disease appear as microaneurysms and non-perfused capillaries. This degeneration is related not only to pericytes loss, but also to dysfunctions of the endothelium, which bring to an aberrant remodeling of the vasculature [121].To investigate whether hyperglycemia is directly involved in affecting angiogenic potential of HRMVEC, we set basement membrane angiogenesis (BMA) assays to monitor their tube formation potential upon glucose. The total tube network length as well as the number of junctions of HG HRMVEC was notably reduced compared to the one of NG HRMVEC. We concluded that HG induced angiogenic dysfunction of HRMVEC. Hyperglycemia is reported in many papers to reduce angiogenic potential of endothelial cells and VEGF transcription/production was found to be often involved in the process [135]. For instance, VEGF production by endothelial cells was diminished upon HG treatment resulting in reduced migration and tube

formation [173]. RasGRP1 was found to mediate these processes, since its overexpression rescued HG-mediated impairments [174]. The critical role of VEGF in protecting from apoptosis and ROS as well as regulating the angiogenic potential was also demonstrated [156]. Even miRNA were documented to be involved in the post-transcriptional regulation of VEGF. miR117 was found to be induced by hyperglycemia, reducing VEGF *in vivo* and *in vitro* and affecting endothelial cells' tube formation [175]. However, opposite findings observed also an HG-mediated induction of angiogenesis [176], which was usually related to an extended period of HG exposure [177, 178].

In conclusion, HG did not affect basic characteristics of ASC but it induced angiogenic dysfunction in HRMVEC. In both cell types, a transient increase of oxidative stress was reported upon HG exposure without being directly related to glucose uptake in our experimental settings. As suggested by literature, we found that hyperglycemia-mediated effects on ASC and HRMVEC relied on oxidative stress induction causing in the latter, a possible ROS-related functional impairment in the angiogenic potential.

5.2 Does glucose exposure influence ASC angiogenic supportive potential?

To fulfill our second aim we investigated hyperglycemia-mediated effects on ASC functions, asking whether (1) HG could affect ASC pro-angiogenic potential and if not, whether (2) ASC could rescue the HG-induced angiogenic dysfunction in HRMVEC.

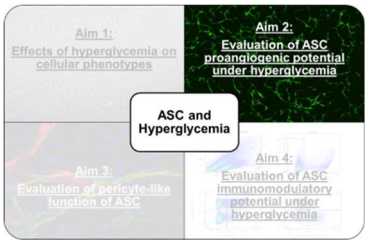

The supportive angiogenic potential of ASC was untouched by glucose. Not only ASC_{NG} and ASC_{HG} induced tube formation in coculture angiogenic assays with HUVEC and HRMVEC to a similar extent, but also the presence of glucose in the culture media did not affect the outcome. In contrast, in a similar assay, Hajmousa and colleagues observed reduced tube formation of HUVEC when cocultured with ASC in HG condition [151].

Similarly, HG in the medium as well as $ASC_{NG\text{-}HG,}$ did not alter significantly cytokine production in ASC monoculture and ASC cocultures. HG in culture medium was barely relevant in influencing cytokine production, with a few exceptions. CCL-7 surprisingly had a 2.8-fold increase in HG medium culture compared to NG. CCL-7, known also as

monocyte chemotactic protein 3 (MCP-3), is a chemokine mainly involved in the recruitment of monocytes [179]. It can be produced by several types of cells, including endothelial cells and MSC, especially upon inflammatory stimuli. On one side, CCL-7 acts as fundamental regulator in the management of the immune response, but on the other, its overexpression has been demonstrated being highly tumorigenic, contributing to the induction of a suitable tumor microenvironment as well as to tumor metastasis [180]. CCL-7 does not appear to be directly related to angiogenic processes; therefore, its high concentration in HG coculture was unexpected. In our assay, we cannot specify whether CCL-7 is produced by HUVEC, ASC or both. HUVEC-mediated CCL-7 secretion might be related to injury, maybe caused by hyperglycemia, possibly explaining the 2.8-fold increase in HG coculture. This would be in line with the 1.9-fold increase in soluble PECAM-1 (known also as CD31), a typical surface marker of endothelial cells, which might indicate increased endothelial cell damage and eventually death. Despite CCL-7 and PECAM-1 levels were increased in HG coculture, the outcome of vascular tube formation was not affected. This represented our first evidence that ASC angiogenic support could overcome any detrimental effect of glucose on endothelial cells.

When we compared $ASC_{NG\text{-}HG}$ in coculture and monoculture, all analyzed factors, except for VEGF, were increased in coculture and identical in ASC_{NG} and ASC_{HG}, confirming the proangiogenic milieu of cocultures and no effects of glucose on cytokine secretion.

VEGF concentrations were higher in ASC monoculture than coculture indicating that coculture might consume VEGF to support tube formation. In DR, especially in the proliferative stage, the combination of VEGF with Ang-1/Ang-2/Tie-2 signaling represents the driving force of hyperproliferation of retinal vessels [181]. Therefore, the detection of VEGF, Ang-1 and Ang-2 in coculture supernatants was carefully evaluated. Production of VEGF by ASC, together with other proangiogenic factors, is well known and largely documented [182]. However, little information is available regarding Ang-1/Ang-2. We found that $ASC_{NG\text{-}HG}$ produced considerable amounts of Ang-2 in monoculture, which were even increased in cocultures. Similarly, Ang-1 was found in monoculture and coculture but its level were generally lower in comparison to Ang-2. These findings let us speculate that the angiogenic process in the assay was sustained (1) by VEGF, produced mainly by ASC and (2) by Ang-2, which is produced by ASC in combination to VEGF activating the autocrine Ang-2/Tie2 signaling [183].

As Ang-1 is reported to be mainly involved in maintaining vessels quiescence and homeostasis [184], we argue that low level of Ang-1 did not contrast tube formation, but were fundamental in supporting the tube structure, which could last up to two weeks in coculture (not shown).
FGF is another well-known angiogenesis-related factor. It can combine with VEGF to promote endothelial cell proliferation and migration [185]. In our ASC_{NG} coculture, FGF was more concentrated than in ASC_{NG} monoculture as well as in ASC_{HG} coculture, confirming again the establishment of a proangiogenic microenvironment.
Interestingly, cytokine secretion was related to the extent of tube formation. Indeed, as the number of endothelial cells was always identical within experiments, these differences were attributed to ASC samples, indicating a donor-dependent angiogenic supportive capacity related to cytokine secretion.

To explain the rescuing capacity of ASC: HRMVEC cocultures, we considered also the possibility that MSC could rescue injured cells via mitochondrial transfer, as shown previously [186]. In an *in vitro* ischemia-reperfusion model, Liu et al. showed that mitochondrial transfer via tunneling nanotube like structures (TNT-like structures) was able to prevent endothelial cells apoptosis and promote aerobic respiration [187]. In addition, foreign-derived mitochondria from injured cells have been shown to sensitize MSC, inducing heme oxygenase-1 (HO-1), mitochondrial biogenesis and final mitochondrial transfer to injured cells. Interestingly, these results were even recapitulated in an *in vivo* model of myocardial infarction [188] and of middle cerebral artery occlusion [189]. Here, upon MSC engraftment on ischemia-reperfusion-damaged cerebral microvasculature, mitochondrial transfer from MSC was observed and promoted angiogenesis as well as amelioration of mitochondrial respiration in the microvasculature [189]. These studies clearly demonstrate the ROS-scavenging potential of MSC, especially in the interaction with endothelial cell. Therefore, we consider mitochondrial transfer via either TNT-like structure or microvescicles [186] as an option of interaction between hyperglycemia injured endothelial cells and ASC in our coculture system. Our data, however, showing that transfer of CM was sufficient to promote HG HRMVEC angiogenesis, favor secreted factors. However, future studies aim to investigate this putative mechanism by which ASC could rescue hyperglycemia injured endothelial cells, restoring their redox balance and reestablishing their angiogenic potential.

Overall, our analysis on supernatants of coculture angiogenesis assays corroborated our previous findings on glucose, which is not functionally affecting ASC in cytokine secretion. Moreover, ASC in combination with endothelial cells, created a proangiogenic microenvironment that sustained endothelial cell tube formation. In addition, the mechanism of mitochondrial transfer might be considered as an option for protection/restoration of endothelial cell angiogenic potential.

While HG induced a reduction of HRMVEC angiogenic potential, the treatment with the antioxidant NAC restored it to some degree. CM from angiogenesis assay cocultures and ASC monoculture restored HRMVEC tube formation similarly to NAC treatment. These findings fully confirmed our previous data on ASC/coculture growth factor profile analysis. The indirect presence of ASC (i.e. CM) overcame detrimental effects of hyperglycemia on the angiogenic potential of HRMVEC. Moreover, as NAC and CM treatments similarly restored HG HRMVEC angiogenic potential, the hypothesis of an additional oxidative stress/ROS scavenging potential (e.g. via mitochondrial transfer) of ASC CM becomes more concrete.
Although, we did not provide evidence to fulfill this last hypothesis, our preliminary findings raised the question about the importance of redox balance in angiogenesis. Indeed, the study of redox signaling in angiogenesis has been shown to be of importance. ROS, as a byproduct of the activity of several enzymes (such as mitochondrial enzymes, cyclooxygenase, myeloperoxidase), can be specifically produced by the family of NADPH oxidases (Nox). Nox are multiprotein complexes associated with membranes in cytoplasmic or intracellular locations, involved in the maintenance of redox balance in cells as well as in the mediation of intracellular signaling [190]. It has been demonstrated that ROS-derived Nox play a role in VEGF/VEGFR2 signaling by promoting cell mobilization (via tyrosine phosphorylation of VE-cadherin and beta catenin) as well as VEFGR2 activation itself (via tyrosine phosphorylation of the intracellular domain) [191]. Nox involvement in pathological angiogenesis has been demonstrated in several OIR animal models. While in the hyperoxia phase Nox2 was not changed, in the neovascularization phase (normoxia/hypoxia) of OIR increased expression of Nox2 as well as increased VEGF and ROS were documented. On the contrary, Nox2 knock-out animals and treatment wiht apocyanin (Nox inhibitor) reduced neovascularization [192, 193]. Similarly, the

Nox4 isoform led to pathological neovascularization in the OIR model and its knock-out reduced VEGFR2 phosphorylation (activation) as well as STAT3 activation [194]. Overall, these studies demonstrated that the ROS producer Nox proteins are involved in the regulation of angiogenesis in the retina suggesting that redox signaling is actually strongly related to angiogenesis. These observations, together with our findings propose a deep investigation on redox balance and angiogenesis in respect to ASC and HRMVEC interaction.

Our data in line with the published ones, suggest the following:

- Increased ROS production related to hyperglycemia exposure may interfere with the redox balance necessary for the angiogenic processing, resulting in reduction of the total tube length in the BMA assays.
- NAC as antioxidant may recover the angiogenic potential decreasing the total ROS content in the cell.
- CM from either ASC monoculture or coculture may restore angiogenic dysfunction providing the proangiogenic factors VEGF, Ang-1/Ang-2 and/or FGF (especially the VEGF/VEGFR2 pathway activation may be involved).
- CM may restore HRMVEC angiogenic dysfunction inducing a favorable redox balance potentially via mitochondrial transfer as the presence of mitochondrial containing vesicles in CM from ASC cannot be excluded.

In summary, we showed that while ASC are not affected by hyperglycemia in phenotype and proangiogenic function, it induced vascular dysfunction in HRMVEC, accompanied by an increase in oxidative stress. The direct (angiogenesis coculture) and indirect (CM from monocultures or cocultures) presence of ASC as well as antioxidant treatment restored the HG-mediated angiogenic dysfunction. A number of different pathways related to both redox balance and growth factor-mediated induction of angiogenesis may be involved and should be investigated in following studies.

All these evidences have to be carefully evaluated in the context of DR. Indeed, although ASC-mediated proangiogenic stimuli might be beneficial in early phases of DR to counteract early vasoregression, it might be highly detrimental if not accurately regulated/controlled. An overexpression of angiogenesis-related factors might open doors to diabetic vasoregression and even accelerate the progression to the proliferative stage. Indeed, recent data suggest that intravitreal ASC injection in a genetic animal model of DR worsened the pathological events [195]. These evidences

highlight the importance of deeper investigations on the role of ASC in the retinal microenvironment, with a focus on the long-term characterization of beneficial/dangerous trophic factors.

5.3 Do ASC retain a pericyte-like phenotype *in vitro* under hyperglycemic culture?

As an extension of the proangiogenic potential we investigated whether ASC could retain a pericyte-like phenotype *in vitro* under hyperglycemic culture.

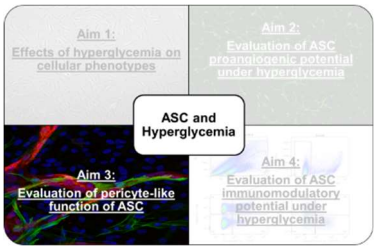

We finally investigated whether ASC could gain pericyte features in EC cocultures. Indeed, a variety of published studies showed that ASC acquired a pericyte-like location enwrapping EC and exerting vascular support, suggesting that ASC may undergo pericyte-like differentiation [196]. We detected α-SMA positive ASC wrapping around tubular structures of EC in cocultures. ASC in monolayer barely expressed a-SMA. α-SMA positive ASC were found in coculture with HUVEC [151] and ASC localization on retinal vessel was demonstrated after their intravitreal injection in mice model of ROP [126], in STZ rats [124] and in a murine model of OIR [125]. Activin-A signaling has been shown to be involved in α-SMA expression in ASC:EC cocultures suggesting that EC may initiate a smooth muscle cell differentiation in adjacent ASC [197]. In HRMVPC: HRMVEC cocultures, however, HRMVPC did not express α-SMA as well as their monoculture. Although α-SMA is often reported as pericytes marker, its expression has been demonstrated being variable depending on developmental stage and location [159, 160]. Therefore, in contrast to ASC, the lack of α-SMA expression in HRMVPC could be related to the differentiation stage of pericytes and it is not induced by EC.

We also evaluated NG-2 expression. As expected, NG-2 was highly expressed in HRMVPC mono- and cocultures. Surprisingly, ASC were constitutively positive for NG-2 without any specific pattern related to endothelial cell vessels. NG-2 was mainly expressed at the cytoplasmic membrane delineating cell´s shape. We did not expected this pattern of expression since, during flow cytometry characterization, ASC were always negative for this marker (not shown). It is important to underline that NG-2

expression on pericytes is not always homogeneous and it seems to be related to the nature of microvascular vessels (arterioles and venules) [198].
Separate investigations in our laboratory (not shown here), further evaluated pericyte marker expression in cocultures, focusing on RGS-5 and PDGFRβ [120]. RGS-5 (regulator of G-protein signaling) was defined as another pericyte marker, which expression varies upon pro/anti angiogenic stimuli [199]. Despite trying several different antibody clones, ASC resulted always negative in both monoculture and coculture. Similarly, PDGFRβ was also not detectable, even if ASC were found to be highly positive for this marker at flow cytometry (here not shown). We concluded that, despite the lack of complete overlap in terms of marker expression, as demonstrated by our and other results both *in vitro* and *in vivo*, ASC can acquire a pericyte-like phenotype when in contact with endothelial cells, supporting the formation and stability of vascular structures.

The fact that ASC did express NG-2 and α-SMA pericyte markers in coculture was highly indicative in confirming their “pericyte potential”. However, the distinction between ASC and pericytes is still a matter of debate [200]. Retinal pericytes have been demonstrated to be fundamental in the stabilization and regulation of adult retina as well as responsive to angiogenic signals during developmental angiogenesis [119]. Their drop-out in DR is considered one of the first signs of the retinal vasoregression and degeneration, suggesting that their loss might represent a starting signal for the pathological proliferation [121]. Overall, these findings provided evidences on their important role as “stabilizer” of the endothelium rather than “promoter” of angiogenesis. We also observed this phenotype in our angiogenesis assays, where HRMVPC, being positive for NG-2 lacked any supportive proangiogenic activity. In contrast, ASC showed profound angiogenic support. In regard of this, we hypothesize that proangiogenic potential might represent a distinctive criterion to characterize these two cell type. We, at least, argue that the coculture angiogenic assay could be used as potency test to discriminate ASC/MSC and pericytes.

With respect to the therapeutic concept, these finding are of utmost importance raising concerns about the potential risks of ASC therapy. Due to their angiogenic supportive activities, ASC application might represent a good preventive strategy in early DR to prevent vascular regression and obliteration. However, the proangiogenic potential

represents a concrete risk in later stages of DR and it might even promote and sustain the neovascularization.

In summary, being in line with *in vivo* experiments, we demonstrated that ASC acquired pericyte-like phenotype in EC cocultures expressing α-SMA. Besides that, having demonstrated that HRMVPC did not support EC angiogenesis, we propose the coculture angiogenesis assay as a potency test to better discriminate ASC/MSC and pericytes.

We auspicate in depth *in vitro* and *in vivo* analyses, to further characterize the differentiating potential of ASC towards the pericyte-like phenotype and to define functional efficacy of ASC-derived pericytes.

5.4 Are ASC affected in their immunomodulatory potential upon HG exposure?

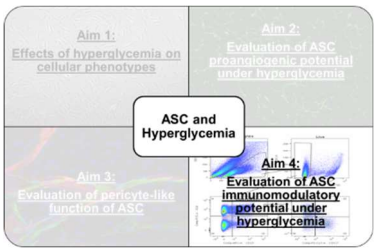

As our fourth aim, we assessed hyperglycemia-mediated effect on ASC immunomodulatory potential on T cell subtypes. Establishing $ASC_{NG\text{-}HG}$:PBMC cocultures, we investigated ASC-mediated effects on (1) CD4 activation and proliferation, (2) Treg generation and (3) PBMC Th1/Th2 cytokine profile. To mimic a local (direct contact) and systemic (indirect contact) environment, experiments were set in direct and transwell cocultures respectively. In addition, resting and CD3/CD28-stimulated PBMC were used to mimic homeostatic and inflammatory conditions.

As introduced earlier, ASC have been applied with differing success in models of DR. One aspect, which has not been addressed yet in these studies, is the effect on the immune system. In our opinion, the role of the immune response and its changes in presence of MSC, represents an intriguing topic even in DR. Because of retinal microvascular involvement as well as alteration/disruption of the BRB, we hypothesize that circulating immune cells might reach the vascular retina and modulate the local (para-) inflammation. Considering that after systemic MSC infusion, changes in the general skewing of immune response toward an anti-inflammatory milieu were observed, we can hypothesize that MSC-mediated anti-inflammatory immune cells might participate in the regulation of retinal vascular remodeling, even after local administration of MSC in the vascular retina. These aspects together, with recent

evidences on Treg involvement in DR [128] prompted us to investigate ASC:T cell interaction.

5.4.1 ASC and CD3/CD28-stimulated cocultures

Suppression of T-lymphocyte proliferation induced by cellular/non-specific stimuli was one of the first mechanism of MSC-mediated immunomodulation to be provided [201]. To verify whether hyperglycemia might affect ASC in this capacity, we established coculture between ASC_{NG-HG} and CD3/CD28-stimulated PBMC. We saw that ASC_{NG} and ASC_{HG} equally inhibited CD4 proliferation in either direct or transwell culture systems. In line with previous results on ASC refractory behavior towards hyperglycemia, we observed that HG did not affect ASC suppression capacity on stimulated T cells. To our knowledge, this is the first report having assessed glucose effects on ASC immunomodulatory potential.

MSC-mediated effects on T cells have been shown to be dependent on several mechanisms, which involve secretion of cytokines and growth factors as well as nitric oxide (NO) production or increased activity of indoleamine-2,3-dioxygenase (IDO) [202]. IDO is a catabolic enzyme which converts tryptophan to kynurenine [161]. Increased IDO activity in MSC has been related to suppression of T cell proliferation *in vitro*, indicating that tryptophan deprivation is a key mechanism in inhibiting T cell proliferation [162]. Our findings documented this mechanism to be key for the anti-proliferative effect as well. Kynurenine concentrations were similar in all cocultures and not detected in PBMC monoculture as well as in ASC monoculture. IDO levels were higher in direct than in transwell coculture for $ASC_{NG-HG.}$ As kynurenine levels were similar in all conditions we did not expect higher IDO levels in ASC from direct coculture than transwell. IDO induction was found to be dependent on IFN-γ stimulation [203], which is produced by stimulated PBMC. IFN-γ is a well-known and strong mediator of the immune response involved in both innate and adaptive immune responses [204]. The participation of IFN-γ in mediating the interaction between MSC and PBMC has been widely studied. Indeed, IFN-γ stimulated MSC displayed an enhanced immunosuppressive potential on T cells, often related to increased IDO expression [205]. To explain our observation, we speculate that the direct contact between ASC and PBMC might represent an additional or stronger activation stimulus, resulting in increased PBMC activation and IFN-γ production. IFN-γ levels have not been measured in this series of experiments, as previous findings documented rapid

induction of IFN-γ mRNA already after 3h of stimulation and IFN-γ protein expression to level up at 12-24 hours of stimulation (medical doctoral thesis P. Mattar). The ASC-IDO-mediated mechanism of inhibition of PBMC proliferation was further confirmed in separate experiments in our laboratory through tryptophan addition and IDO inhibition via Epacadostat (Torres Crigna, manuscript in preparation). These experiments corroborated our results showing that addition of tryptophan to ASC:PBMC cocultures resulted in abrogation of ASC inhibitory functions. Similarly, Epacadostat, a known inhibitor of IDO, blocked its activity (but not its expression in ASC), promoting PBMC proliferation.

Having confirmed the inhibitory potential of ASC on CD4 cells in stimulated PBMC, we zoomed into the CD4 T cell population investigating phenotypical changes related to activation (CD25+) and Treg induction (FoxP3+, CD127-). CD25 is defined as activation marker and its expression is highly induced in T cell upon CD3/CD28 stimulation, moreover, as part of the IL-2R, it is a mediator of the IL-2/IL-2R signaling [163]. Surprisingly, we found that, despite T cell inhibition of proliferation, in presence of $ASC_{NG\text{-}HG,}$ CD25 expression on CD4 T cells was significantly increased in both transwell and direct coculture compared to PBMC monoculture. This result was apparently in contrast with findings in literature, where ASC were previously documented to reduce CD25 expression when cocultured with stimulated PBMC [206, 207]. Moreover, addition of IL-2 to cocultures was able to abrogate MSC-mediated inhibitory effect on T cells [208]. Two main reasons could explain our different results. First, timing of the coculture; our cocultures lasted 7 days, while in all previously reported studies T cells analysis were performed after 48 or 72 hours. Second, IL-2 addition; to guarantee T cell survival over 7 days we added exogenous IL-2 to cocultures. Indeed, previous experiments in our laboratory revealed that after 7 days of coculture without IL-2, PBMC survival was highly compromised and cells numbers were not enough to perform cell surface analysis with flow-cytometry. We are aware that IL-2 addition might influence our results, however we previously assured the ASC inhibitory effect to occur in presence and absence of IL-2 upon CD3/CD28 stimulation. The increasing CD25 expression might be also explained by an additional PBMC-mediated IL-2 secretion due to CD3/CD28 stimulation.
We observed an even stronger increase in CD4+CD25+ cells in the proliferating fraction of cocultures. Thus, despite the general suppression of CD4 cell proliferation,

a significant proliferation of CD4+CD25+ cells was taking place, in contrast to what was observed in the not stimulated cocultures. This may suggest that some activation and proliferation of CD4+CD25+ cells may occur in presence of ASC and may not be inhibited, but even potentially induced by ASC themselves. Possibly, it can be an allogeneic stimulation or potential innate responses triggered by e.g. dying cells and occurrence of danger-associated molecular patterns (DAMPs).

MSC were reported to induce Treg generation in several studies. These Treg cells were functional in inhibiting T cell proliferation in a mixed lymphocyte reaction (MLR) [35, 83, 209]. We quantified Treg cells in mono- and coculture, defining them as CD4+CD25+FoxP3+CD127- cells [210]. Unexpectedly, we noticed that in the Live population, percentages of Treg fractions were similar in PBMC monoculture controls and $ASC_{NG\text{-}HG}$ cocultures.
There are different possible explanations for this difference to previously published data:

(1) Definition of Treg: previous reports, indicating an increase in Treg, used only CD4/CD25 as marker. We have previously discussed that we considered this as a sign of activation rather than indicative of a regulatory phenotype.
(2) Mode of stimulation [211-213].
(3) Timing of coculture. We cannot exclude Treg generation at earlier time point in our coculture, speculating that they might undergo apoptosis or lose FoxP3 expression after 7 days. A reduction of FoxP3 expression was indeed documented after 5 days in coculture with MSC [87].
(4) Presence of IL-2.

Finally, zooming in the VPD- fraction corroborated our previous observation of not changed Treg numbers observed in the general Live population. While in direct cultures, the amount of Treg was similar in $ASC_{NG\text{-}HG}$ coculture and PBMC monoculture, in transwell we found that Treg proportions were significantly reduced in $ASC_{NG\text{-}HG}$ coculture compared to PBMC. In addition, Treg were even reduced in comparison to direct coculture. Because of these findings, we hypothesized that the lack of direct cell-to-cell contact between ASC and PBMC might reduce the survival of naïve (naturally occurring) Treg. No differences were detected in the Treg VPD+ fraction.

To sum up this part, we observed that ASC exerted a strong anti-proliferative effect on CD4 cells; a fraction of these, however, became activated being marked by CD25 expression and proliferating. Treg numbers remained unchanged in direct coculture, but were reduced in transwell cultures. IDO was identified as key inhibitor of CD4 T cell proliferation.

The screening of Th1/Th2 cytokines revealed that all analyzed cytokines were reduced in coculture compared to PBMC monoculture. Significant reduction was found in IL-13, IL-5, IL-10 and TNF-α concentrations. Thus, not only pro-inflammatory cytokines (TNF-alpha, IL-17a, IL-17f and IL-22) but also anti-inflammatory ones (IL-13, IL-5, IL-10, IL-9) were reduced in coculture. These data partially fit to the overall suppression of CD4 T cell proliferation. Indeed, the ASC-mediated inhibition of CD4 T cells proliferation observed in cocultures might correlate with the reduction of pro-inflammatory cytokines. On the other hand, the reduction of anti-inflammatory factors might be related to the absence of Treg induction, resulting in an overall decrease of pro/anti-inflammatory factors. Once again, it has to be taken into account that we analyzed a single time point after 7 days and thus, we cannot speculate about expression kinetics. Indeed, ASC were often reported to induce increased IL-10 expression in T cells after few days of coculture [71, 83]. Further, the CD3/CD28-mediated stimulation and IL-2 have to be taken into account in the evaluation of these outcomes and comparison to literature.
The screening of Th1/Th2 cytokines in cocultures was not indicative of any T cell polarization suggesting that these events may occur at earlier time points [35, 73]. Our data underline the importance of a time-monitoring study on MSC:PBMC interaction, which might help in a better understanding of kinetics in T cell polarization and Treg induction.

Globally our findings on ASC and stimulated PBMC cocultures demonstrated that:

- ASC were not affected by hyperglycemia;
- ASC-mediated suppression of CD4 T cell proliferation occurred in both transwell and direct coculture denoting the central role of IDO-kynurenine axis;
- CD4+CD25+ cells were induced in coculture and actively proliferated despite the overall inhibition of CD4 T cell proliferation;
- No Treg induction as well as proliferation was detected in cocultures;

- Screening of Th1/Th2 cytokines did not suggest any T cell polarization, resulting in an overall reduction of all cytokines/growth factors tested.
- Direct and transwell coculture behaved almost identically in all tested parameters.

5.4.2 ASC and resting PBMC coculture

In the previous chapter, we focused on the analysis of stimulated cocultures. As controls, non-stimulated cultures were always run in parallel. The analysis of these data provided highly interesting results. As expected, CD4 cells within resting PBMC did not proliferate and the division index did not change in $ASC_{NG\text{-}HG}$ cocultures. Surprisingly, we denoted a slight but significant increase in CD4 proliferation in PBMC monoculture transwell compared to the direct control. We hypothesized that this difference was mainly related to the culture condition per se. Indeed, the culture surface of a transwell insert (4.5 cm^2) is reduced compared to a well of a 6-well plate (9.6 cm^2) and this might affect PBMC in terms of media availability and cell concentration/ml and cm^2 (even if the final volume of media in the well was the same in direct and transwell cultures). Moreover, transwell inserts and well plate differed in terms of material as they were made of polyethylene terephthalate (PET) and polystyrol, respectively. For these reasons we cannot exclude that PBMC in transwell might have been subject to slight auto-stimulation, causing an increased division index. Importantly, the auto-stimulation observed in transwell controls was slightly diminished in $ASC_{NG\text{-}HG}$ cocultures denoting somehow an inhibitory effect exerted by ASC. Similarly, Cuerquis and colleagues demonstrated that resting PBMC were not affected by MSC in terms of suppression of proliferation, but that MSC induced a slight activation of them (increased CD69 expression) in the first days of cocultures concluding that "..MSCs support a modest activation of initially resting PBMCs rather than a primary stimulatory full immune response followed with an inhibitory response." [214]. However, our and other results are openly in contrast with the study from Crop and colleagues [215]. They observed that ASC, despite the lack of expression of HLA-class I and co-stimulatory molecules, did actually promote expansion and proliferation of T cells in resting PBMC, suggesting that ASC induced an allogeneic response, like in a mixed lymphocyte reaction. These same cells underwent accelerated proliferation when cultured without ASC, but once cultured again in presence of ASC their

proliferation was almost abrogated [215]. Although this study confirmed the immunosuppressive capacity of ASC as well as their Treg induction, it indicated that under certain conditions ASC might promote and activate T cells. As coculture conditions were extremely similar to ours, we hypothesize that these contrasting results might be attributed to (1) the use of IL-2, which might provide in our case a stabilizing factor for PBMC survival when cocultured with ASC and (2) the source of ASC. In fact, while our ASC were isolated from lipoaspirate, the one used by Crop and colleagues were obtained from perirenal adipose tissue of living kidney donors. The well-known functional differences between diverse sources of MSC [216] as well as the peculiarity of perirenal fat pads [217] might be the reason of these opposing outcomes.

IDO expression in ASC_{NG-HG} from cocultures was very low, more than halved compared to ASC_{NG-HG} in cocultures with activated PBMC. Again, no IDO was detected in ASC and PBMC monocultures. This indicated that, despite the low ASC inhibitory function suggested by low IDO levels, the slight degree of activation of PBMC, especially in the transwell, was inducing a minimal increase in the expression of IDO in ASC. As, IDO induction has been found to be associated to secretion of IL-6 [218] and considering that very high level of IL-6 were found in coculture supernatants (not shown, because out of scale), we could also postulate that IL-6 might have mediated IDO induction. Yet, evidences of high IL-6 levels concomitant to IDO expression in ASC was provided [215]. Notably, IDO expression in ASC_{NG} from transwell cocultures was considerably higher than in ASC_{NG} from direct cocultures, most probably reflecting the low levels of PBMC auto-stimulation that we found in transwell cocultures. In line with that, kynurenine levels were significantly lower compared to stimulated cocultures and again no differences were found between all conditions tested.

As the previous data from ASC: stimulated-PBMC cocultures suggested that coculture induced CD25 expression in CD4 T cells, we expected to find here similar outcomes with a reduced extent. However, we saw that there was no difference between CD4+CD25+ fractions among all conditions and the percentage of activated CD4 was overall the same. The amount of CD4+CD25+ cells was reduced almost of one quarter in contrast to CD4+CD25+ cells in stimulated cocultures. This reduction was uniformly observed in coculture as well as in PBMC monoculture. Of note, the portion of

CD4+CD25+ in transwell PBMC monoculture was slightly higher than the one in direct monoculture, mirroring again a possible effect of auto-stimulation. Low degree of activation in PBMC monoculture as well as low IDO/kynurenine levels were related to the lack of inhibitory effects, being in line with the hypothesis about the requirement of pro-inflammatory stimuli (or priming factors) to induce MSC-mediated immunosuppression [219, 220]. Moreover, as mentioned in the previous chapter, the lack of CD3/CD28 stimulation might reduce IL-2 additional secretion from PBMC, resulting in an overall reduction of CD25 induction. In addition, we observed that in absence of stimulation, CD25 expression was not induced in PBMC monoculture neither in coculture with ASC, being in line with some results proposed by Le Blanc and colleagues [221]. However, in the same study, a significant reduction on CD25 expression is reported in stimulated cocultures [221], which is in contrast to our previous finings. Conflicting evidences are reported in another paper where CD3/CD28-activated lymphocytes did not changed CD25 expression upon cocultures [222]. These evidences suggest that CD25 expression on CD4 T cells might correlate not only with the CD3/CD28-mediated PBMC stimulation but also with the presence of ASC. The dual interpretation of CD25 expression on T cell as activation marker and/or Treg marker [223] is still generating confusing outcomes, highlighting the need of more detailed studies on kinetic changes in CD25 expression with/without stimulation and MSC.

CD4+CD25+ cells were then assessed for their FoxP3 expression to evaluate a potential induction of Treg in ASC:not-stimulated PBMC cocultures. Overall, the proportion of Treg were significantly increased in comparison to PBMC:stimulated PBMC cocultures. Resting PBMC monoculture had more Treg than stimulated PBMC and in not-stimulated setting cocultures promoted Treg proliferation. Similar outcomes were reported in resting cocultures of induced pluripotent stem cells MSC (iPSC-MSC) and PBMC where the percentage of FoxP3+CD4+ cells significantly increased in cocultures. Moreover, iPSC-MSC were found to cause an higher increase in FoxP3 mRNA levels in CD4 cells than BM-MSC did [224].

Overall, these results indicated that ASC were able to induce Treg expansion and proliferation in coculture with resting PBMC. As our investigation focused on the phenotypic characterization of CD4 T cells dissecting differences between proliferated and non-proliferated ones, we did not have enough Treg to functionally test whether

they exerted immunoregulatory functions. This was further hampered by the fact that we used FoxP3 for Treg characterization. FoxP3 is an intracellular marker, which detection is necessarily related to cell death. Despite several trials in using alternative markers (CD127, CD69, CD73, CD39) in order to select and sort Treg from our cocultures, we were not able to find a suitable candidate. However, as our outcomes reproduced findings provided also by others [82-84] not only in terms of cells (CD4 T cell inhibition and Treg induction) but also in terms of cytokine secretion (see below), we can reasonably infer that the Treg induced in our study would be functional in suppressing T cell proliferation.

Also for the resting condition, we analyzed the supernatant screening Th1/Th2 cytokines. The overall levels of Th1/Th2 cytokines (IL-5, IL-9, IL-10, IL-13, IL-17a, IL-17f, IL-22, TNF-α) were low compared to the ones in stimulated cultures in both PBMC monoculture and cocultures. However, also this screening confirmed that ASC cocultures, even in a resting condition and with no obvious CD4 inhibition, exerted a general suppressive effect in cytokines secretion. As discussed in previous paragraphs, our investigation on immunomodulatory cytokines might have a timing limitation suggesting that ASC-mediated effect of PBMC might be extended only few days after the beginning of the coculture.

Having observed that coculture induced the expansion and proliferation of the Treg fraction, being indicative of an anti-inflammatory microenvironment, we further checked the coculture supernatant for IL-4, IFN-γ and CCL-18 concentrations.

In our assays, we did not find differences between IL-4 in PBMC monoculture and in coculture, confirming the lack of any Th polarization. Indeed, IL-4 is produced by the subset Th2 of T cells in response to T receptor stimulation [225] and deregulation of its pathway has been linked to allergic diseases such as asthma [226]. MSC have been reported to favor the skewing of T cell response towards anti-inflammatory Th2 in an animal model of allergic encephalomyelitis and even in NOD mice [227, 228]. However, contrasting evidences from Kavanagh and colleagues, reported a suppression of allergen specific Th2 in a mouse model of airway inflammation denoted by inhibition of IL-4 production and reduction of eosinophil infiltration [229].

INF-γ was produced in both PBMC monoculture as well as in ASC cocultures but in a lower extent. The presence of IFN-γ in resting PBMC monoculture might be explained as the results of an auto-stimulation of PBMC for the long lasting culture. Importantly,

IFN-γ detected in coculture correlated with the low but increased level of IDO in cocultured ASC. Moreover, the reduction of IFN-γ in coculture in comparison to PBMC monoculture, could be an indication of immunosuppressive potential of ASC even in coculture with resting PBMC.
Inspired by findings provided by Melief and colleagues we also checked the presence of CCL-18 in coculture supernatants. Indeed, they reported CCL-18 being produced by monocytes as sign of MSC-mediated skewing of monocytes towards the anti-inflammatory type 2 [83, 230]. Moreover, as reported by other studies, the presence of CCL-18 as well as monocytes in PBMC:MSC coculture was fundamental for the generation of Treg [83, 231]. In line with these results, we found remarkably high levels of CCL-18 in cocultures, while it was almost absent in PBMC monocultures. This was indicative at least of an anti-inflammatory switch of monocytes, whose survival in the culture was probably sustained by ASC. In addition, the high concentration of CCL-18 correlated with the observed increased of Treg in coculture.
Also TGF-β is reported being one of the main soluble factors involved in Treg induction [164] and several paper documented this central role in ASC:PBMC cocultures [36, 82, 83]. Therefore, we compared TGF-β concentrations in stimulated and not stimulated, direct and transwell cocultures. Despite a low basal TGF-β level in ASC, our data showed a remarkable high concentration of TGF-β in direct non-stimulated coculture compared to transwell and its direct stimulated counterpart. These findings supported the Treg proliferation observed in resting direct coculture. However, we did not expect to find low and similar TGF-β levels in resting transwell coculture and stimulated ones. We hypothesized this being related to the auto-stimulation we observed in the resting transwell coculture. Overall, TGF-β quantification in supernatants of coculture demonstrated to be in line with the previous results and its high concentration in resting coculture denoted its involvement in Treg generation.

In conclusion, our data demonstrated that ASC were able to induce Treg proliferation and expansion when cocultured with resting PBMC. In parallel, ASC did not support activation of resting PBMC as demonstrated by the general low level of Th1/Th2 cytokines in coculture supernatant. Even if IL-10 was not increased in coculture, the reduction of IFN-γ together with a substantial increase of CCL-18 (and the general low level of Th1/Th2 cytokines) and TGF-β were indicative of an anti-inflammatory/pro-Treg microenvironment induced by ASC. Comparing our findings to the literature, we

identified the timing of the coculture as an important limiting factor for the evaluation of MSC-mediated effects on polarization of Th subsets.

In the last part of our study on the immunosuppressive capacity of ASC, we evaluated potential “long-term” effect of ASC on PBMC, asking whether ASC might “prime” PBMC in term of Treg induction and changing in their cytokine profile. No differences were found in the CD4+CD25+ fractions of control PBMC and ex-coculture PBMC, indicating that both resting and ex-coculture PBMC did not undergo activation. Surprisingly, we found a prominent reduction in Treg from ex-coculture PBMC in comparison with controls. These results displayed that, despite a previous Treg induction at day 7 and the provision of IL-2 in the culture medium, Treg did not survive and expand further. These outcomes were partially in contrast with previous reports, which accounted Treg proliferation as well as an increased inhibitory potential of these population [83, 215]. As a very prominent indicator of Treg induction and functionality, we found markedly high concentrations of IL-10 and CCL-18 in ex-coculture PBMC, exceeding values measured after 7 days. A similar concomitant production of Treg and monocyte-derived IL-10 and CCL-18 was also reported by Melief et al. [83]. There were no changes in IL-4 concentrations, suggesting that no skewing towards Th2 phenotype in both conditions occurred. IFN-γ and TNF-α were considerably increased ex-coculture PBMC. The presence of these cytokines, traditionally coming from CD8 T cells and NK cells, was unexpected at these high levels. However, as separate experiments in our lab denoted an increase in NK cells after 1 week of coculture, we might postulate an expansion of CD8 and NK cells in the second week of cultures producing high level of these cytokines.

In summary, the analysis on ASC:resting PBMC cocultures showed that:

- ASC did not affect resting PBMC in terms of inhibition of proliferation and activation;
- Cocultures induced Treg expansion in both transwell and direct cultures;
- Cocultures caused a general reduction in secretion of Th1/Th2 cytokines without any specific polarization of Th subsets;
- CCL-18 and TGF-β were highly concentrated in cocultures denoting (a) the participation of monocytes in driving Treg induction as well as (b) ASC-dependent TGF-β secretion as reported by Melief et al [83];

- Cocultures induced prolonged changes in PBMC cytokine profile towards an anti-inflammatory phenotypes with high secretion of IL-10 and CCL-18. However, concomitant high concentrations of IFN-γ and TNF-α might indicate an expansion of CD8 and NK cells.

In conclusion, our data demonstrated the immunomodulatory potential of ASC being strictly dependent on the activation state of PBMC. This is in line with the hypothesis about the requirement of priming factors to induce MSC-mediated immunosuppression [219, 220]. These assumptions have to be taken into consideration in the development of MSC-mediated therapies together with the specific diseased context. In the case of DR, our data support the concept that an early MSC treatment would be preferred to increase circulating Treg which might act in the retina. Importantly, this has been documented in an animal model of OIR [128]. These promising findings still need to be fully elucidate especially *in vivo*. Further investigations on Treg involvement in MSC-mediated therapy for DR will take place.

6 SUMMARY

Hyperglycemia and poor glycemic controls are two marked features of metabolic disorders, such as diabetes or metabolic syndrome. Patients affect by these pathologies often develop secondary complications, which involve the vascular system. Besides macrovascular complications at the expense of the cardiovascular system, microvascular disorders can seriously affect quality and, in some cases, duration of life. This is the case of diabetic complications such as DR, diabetic nephropathy and diabetic neuropathy. Hyperglycemia represents a connection point between all these secondary complications since high glucose has been identified as one of the causes mediating cell damage. Through years, clear evidences on hyperglycemia-mediated cell damage have been produced, leading to the elaboration of the “unifying hypothesis”. Here, glucose-mediated cell damage is explained as the result of a deleterious increase of oxidative stress in cells, which induces cell dysfunction and death. This mechanism has been demonstrated in several cell types from endothelial to neuronal cells, however, some aspects of hyperglycemia-mediated cell damages still need to be elucidated. This is the case of the cell/stem cell-mediated therapeutic approach.

The application of cell/stem cell-mediated therapies in diabetes and diabetic complications already gave some positive outcomes. In particular, MSC-mediated therapies demonstrated to be safe and efficient. Thanks to their trophic, differentiation and immunomodulatory potential MSC promoted reconstitution of β-cell islets in the pancreas, wound healing in diabetic foot and an overall reduction of inflammation. However, the majority of studies used an allogenic approach proposing the application of MSC from healthy donors. Indeed, MSC from diabetic donors often revealed to be impaired by the disease which caused reduction of their potency and even affecting their survival. In this context, specific investigations focused on possible effects of diabetes/hyperglycemia on MSC are lacking.

Our study proposes an investigation of possible hyperglycemia-mediated effects on ASC through *in vitro* experiments. In particular, we assessed effects of hyperglycemia on (1) cellular phenotype, (2) ASC proangiogenic potential, (3) ASC pericyte-like function and (4) immunomodulatory potential.

Overall, we observed that hyperglycemia did not affect any of the evaluated aspects. Indeed, ASC demonstrated as strong refractory behavior towards HG exposure resulting only in a transient increase of intracellular oxidative stress. This was corroborated by observing that, when exposed to HG, ASC reduced glucose uptake. On the contrary, HRMVEC appeared sensitive to HG and glucose uptake resulted to be not only GLUT-1 dependent. In HRMVEC, hyperglycemia increased the level of oxidative stress and affected the angiogenic potential suggesting a possible connection between the two aspects.

ASC proangiogenic potential was not affected by glucose and ASC sustained HRMVEC angiogenesis giving structural support and secreting proangiogenic growth factors. Moreover, conditioned media form ASC monoculture and ASC:HRMVEC cocultures reproduced the effect of antioxidant application on HG treated HRMVEC, rescuing their angiogenic potential. This observation not only confirmed the proangiogenic potential of ASC but also indicated a possible antioxidant effect exerted by ASC.

ASC pericyte-like function was detected being unaffected by HG. α-SMA positive ASC clearly wrapped around tubular structures reminding pericytes in normal physiology. In contrast to ASC, pericytes did not support the angiogenesis of EC, confirming their role in supporting homeostasis in the vascular department. Importantly, because of the still ongoing discrepancies in distinguishing MSC from pericytes, this finding indicates that the coculture angiogenesis assay might be used as a potency assay to functionally discriminate the two cell types.

Finally, we found that glucose did not affect the immunomodulatory potential of ASC, which was evaluated in terms of (1) inhibition of CD4 proliferation, (2) induction of CD25 expression and Treg and (3) production of immunomodulatory cytokines. Actually, the major discriminant in the outcomes of the experiments was represented by the presence of CD3/CD28-stimulated or not stimulated (resting) PBMC. In simulated cocultures, ASC strongly inhibited CD4 proliferation via IDO-kynurenine. Despite this, cocultures strongly enlarged the CD4+CD25+ positive fractions, promoting CD4 activation but not Treg expansion. Cytokines analysis showed and overall cytokines reduction in cocultures compared to PBMC monocultures but did not reveal specific polarization towards specific Th subsets.

In resting cocultures, IDO and kynurenine were also measured at low levels but ASC-inhibiting effect of CD4 was not detectable. Here, CD4+CD25+ were even reduced

compared to the control. Although, Treg highly proliferated in cocultures. Cytokines analysis was similar to the stimulated coculture having overall general lower concentrations. Having observed Treg formation in this condition, we further analyzed CCL-18, IL-4, INF-γ and TGF-β to eventually confirm the anti-inflammatory skewing of CD4. No distinction between IL-4 and INF-γ were found and CCL-18 resulted to be highly produced in cocultures, suggesting the involvement of monocytes in Treg induction. Also TGF-β, which is produced by ASC and drive Treg induction, was detected in high concentration in resting direct coculture confirming Treg proliferation. Contrarily, low TGF-β levels were detected in stimulated cocultures. Further, cocultures induced a long-term priming of PBMC, which after 14 days in culture secreted high levels of IL-10, TNF-α, IFN-γ and CCL-18. The analysis of the immunomodulatory potential of ASC confirmed ASC-mediated immunosuppression on activated PBMC and ASC-mediated Treg induction, highlighting how much the activation/resting condition of PBMC might be determinant in affecting the direction of the ASC-mediated immune response.

In relation to DR and the eventual application of MSC-based cell therapy our study provides the important evidence that hyperglycemia does not affect ASC in their basic characteristics, proangiogenic and immunomodulatory potential. However, some separate considerations have to be done for MSC from diabetic patients. It is worth to mention that several papers described impaired therapeutic capacity of diabetic-MSC, especially in terms of reduced angiogenic potential and secretion of angiogenic factors [145, 148, 232]. Dysfunction of diabetic-MSC were observed in proliferation, mitochondrial activity, signaling pathway and secretome profile [144, 233, 234]. We also had the chance to perform some experiments with diabetic ASC, but the restricted number of samples limited us in collecting significant amount of data. In our hand, these ASC were not different from healthy ASC in terms of growth rate and immunophenotype but their differentiation potential to adipogenic lineages was reduced. Notably, their proangiogenic potential in coculture angiogenesis assays resulted slightly reduced in comparison to healthy ASC, while the immunosuppressive function on CD4 proliferation as well as Treg induction was not changed. From these assumptions, we hypothesize that diabetic-MSC might indeed have alterations in some of their functions, which are not mediated exclusively by hyperglycemia, as it is reported by our experiments.

Our data on the proangiogenic function of ASC suggest a careful evaluation of ASC application in the context of DR. Indeed, proangiogenic stimuli might be beneficial in the early phases of the disease to prevent vasoregression and even to replace pericytes. However, a prolonged proangiogenic stimuli might cause highly detrimental effects if not accurately regulated/controlled, promoting hyperproliferation of retinal vessels and accelerating the progression to the proliferative stage. This highlights the importance of deeper investigations on the role of ASC in the retinal microenvironment, with a focus on the long-term characterization of beneficial/dangerous trophic factors.
In addition to the proangiogenic potential, we hypothesize that ASC may retain a ROS scavenging potential, acting as a second potential mechanisms to rescue damaged endothelial cells. As the redox signaling has been demonstrated to be involved in the regulation of angiogenic processes, we propose ASC-ROS scavenging potential as a new aspect to be further investigated in the modulation of retinal dysfunction.
Lastly, having demonstrated the strong immunomodulatory effect of ASC *in vitro* and because of the recent publication on Treg involvement in the retina, we auspicate that *in vivo* experimentations may clarify and characterize this mechanism, which may represent a real novelty in DR treatment.

7 REFERENCES

1. Friedenstein, A.J., R.K. Chailakhjan, and K.S. Lalykina, *The development of fibroblast colonies in marrow and spleen cells monolayer cultures of guinea-pig bone.* Cell Tissue Kinet., 1970. **3**: p. 11.
2. Gartner, S. and H.S. Kaplan, *Long-term culture of human bone marrow cells.* Proceedings of the National Academy of Sciences, 1980. **77**: p. 4756-4759.
3. Friedenstein, A.J., R.K. Chailakhyan, and U.V. Gerasimov, *Bone marrow osteogenic stem cells: in vitro cultivation and transplantation in diffusion chambers.* Cell Tissue Kinet, 1987. **20**: p. 10.
4. Berebichez-Fridman, R. and P.R. Montero-Olvera, *Sources and Clinical Applications of Mesenchymal Stem Cells: State-of-the-art review.* Sultan Qaboos University medical journal, 2018. **18**(3): p. e264-e277.
5. Bajek, A., et al., *Adipose-Derived Stem Cells as a Tool in Cell-Based Therapies.* Arch Immunol Ther Exp (Warsz), 2016. **64**(6): p. 443-454.
6. Kern, S., et al., *Comparative Analysis of Mesenchymal Stem Cells from Bone Marrow, Umbilical Cord Blood, or Adipose Tissue.* STEM CELLS, 2006. **24**(5): p. 1294-1301.
7. Bieback, K., et al., *Critical parameters for the isolation of mesenchymal stem cells from umbilical cord blood.* Stem Cells, 2004. **22**: p. 625-634.
8. Perry, B.C., et al., *Collection, cryopreservation, and characterization of human dental pulp-derived mesenchymal stem cells for banking and clinical use.* Tissue Eng Part C Methods, 2008. **14**(2): p. 149-56.
9. Joerger-Messerli, M.S., et al., *Mesenchymal Stem Cells from Wharton's Jelly and Amniotic Fluid.* Best Pract Res Clin Obstet Gynaecol, 2016. **31**: p. 30-44.
10. Stanko, P., et al., *Comparison of human mesenchymal stem cells derived from dental pulp, bone marrow, adipose tissue, and umbilical cord tissue by gene expression.* 2014. **158**(3): p. 373-377.
11. Phinney, D.G. and L. Sensebe, *Mesenchymal stromal cells: misconceptions and evolving concepts.* Cytotherapy, 2013. **15**(2): p. 140-5.
12. Dominici, M., et al., *Minimal criteria for defining multipotent mesenchymal stromal cells. The International Society for Cellular Therapy position statement.* Cytotherapy, 2006. **8**(4): p. 315-7.
13. Horwitz, E.M., et al., *Clarification of the nomenclature for MSC: The International Society for Cellular Therapy position statement.* Cytotherapy, 2005. **7**(5): p. 393-5.
14. Bourin, P., et al., *Stromal cells from the adipose tissue-derived stromal vascular fraction and culture expanded adipose tissue-derived stromal/stem cells: a joint statement of the International Federation for Adipose Therapeutics and Science (IFATS) and the International Society for Cellular Therapy (ISCT).* Cytotherapy, 2013. **15**(6): p. 641-8.
15. Heathman, T.R.J., et al., *Characterization of human mesenchymal stem cells from multiple donors and the implications for large scale bioprocess development.* Biochemical Engineering Journal, 2016. **108**: p. 14-23.
16. Mushahary, D., et al., *Isolation, cultivation, and characterization of human mesenchymal stem cells.* Cytometry Part A, 2018. **93**(1): p. 19-31.
17. Blogowski, W., T. Bodnarczuk, and T. Starzynska, *Concise Review: Pancreatic Cancer and Bone Marrow-Derived Stem Cells.* Stem Cells Transl Med, 2016. **5**(7): p. 938-45.

18. Cammarota, F. and M.O. Laukkanen, *Mesenchymal Stem/Stromal Cells in Stromal Evolution and Cancer Progression.* Stem Cells Int, 2016. **2016**: p. 4824573.
19. Koliaraki, V., et al., *Mesenchymal Cells in Colon Cancer.* Gastroenterology, 2017. **152**(5): p. 964-979.
20. Gaur, M., M. Dobke, and V.V. Lunyak, *Mesenchymal Stem Cells from Adipose Tissue in Clinical Applications for Dermatological Indications and Skin Aging.* Int J Mol Sci, 2017. **18**(1).
21. Kim, K.H., et al., *Mesenchymal stromal cells: properties and role in management of cutaneous diseases.* J Eur Acad Dermatol Venereol, 2017. **31**(3): p. 414-423.
22. Grégoire, C., et al., *Comparison of Mesenchymal Stromal Cells From Different Origins for the Treatment of Graft-vs.-Host-Disease in a Humanized Mouse Model.* Frontiers in immunology, 2019. **10**: p. 619-619.
23. Fang, B., et al., *Human adipose tissue-derived mesenchymal stromal cells as salvage therapy for treatment of severe refractory acute graft-vs.-host disease in two children.* Pediatric Transplantation, 2007. **11**(7): p. 814-817.
24. Krasowska-Kwiecien, A., et al., *Mesenchymal Stem Cells as a Salvage Treatment for Severe Refractory Graft-vs-Host Disease in Children After Bone Marrow Transplantation.* Transplantation Proceedings, 2019. **51**(3): p. 880-889.
25. Rad, F., et al., *Mesenchymal stem cell-based therapy for autoimmune diseases: emerging roles of extracellular vesicles.* Molecular Biology Reports, 2019. **46**(1): p. 1533-1549.
26. Liou, Y.-M., et al., *Differential effects of mesenchymal stem cells on T cells isolated from childhood allergies and autoimmune diseases.* Allergy, 2019. **74**(10): p. 2006-2010.
27. Oh, D.Y., et al., *Potently Immunosuppressive 5-Fluorouracil–Resistant Mesenchymal Stromal Cells Completely Remit an Experimental Autoimmune Disease.* The Journal of Immunology, 2012. **188**(5): p. 2207.
28. Moreira, A., S. Kahlenberg, and P. Hornsby, *Therapeutic potential of mesenchymal stem cells for diabetes.* Journal of molecular endocrinology, 2017. **59**(3): p. R109-R120.
29. Eric, L.M., R.-M. Luis, and V.B. Evangelos, *Role of Mesenchymal Stem Cells in Dermal Repair in Burns and Diabetic Wounds.* Current Stem Cell Research & Therapy, 2017. **12**(1): p. 61-70.
30. Qi, Y., et al., *Applicability of adipose-derived mesenchymal stem cells in treatment of patients with type 2 diabetes.* Stem cell research & therapy, 2019. **10**(1): p. 274-274.
31. Salgado, A.J., et al., *Adipose tissue derived stem cells secretome soluble factors and their roles in regenerative medicine.* Current Stem Cell Research & Therapy, 2010. **5**: p. 103-110.
32. Doorn, J., et al., *Therapeutic applications of mesenchymal stromal cells: paracrine effects and potential improvements.* Tissue Eng Part B Rev, 2012. **18**(2): p. 101-15.
33. Yin, K., S. Wang, and R.C. Zhao, *Exosomes from mesenchymal stem/stromal cells: a new therapeutic paradigm.* Biomarker Research, 2019. **7**(1): p. 8.
34. Haddad, R. and F. Saldanha-Araujo, *Mechanisms of T-cell immunosuppression by mesenchymal stromal cells: what do we know so far?* Biomed Res Int, 2014. **2014**: p. 216806.
35. Luz-Crawford, P., et al., *Mesenchymal stem cells generate a CD4+CD25+Foxp3+ regulatory T cell population during the differentiation*

process of Th1 and Th17 cells. Stem Cell Research & Therapy, 2013. **4**(65): p. 1-12.
36. Yan, Z., et al., *Immunomodulation of mesenchymal stromal cells on regulatory T cells and its possible mechanism.* Exp Cell Res, 2014. **324**(1): p. 65-74.
37. Luby, A.O., et al., *Stem Cells for Bone Regeneration: Current State and Future Directions.* Journal of Craniofacial Surgery, 2019. **30**(3): p. 730-735.
38. Mamidi, M.K., et al., *Mesenchymal stromal cells for cartilage repair in osteoarthritis.* Osteoarthritis and Cartilage, 2016. **24**(8): p. 1307-1316.
39. Urrutia, D.N., et al., *Comparative study of the neural differentiation capacity of mesenchymal stromal cells from different tissue sources: An approach for their use in neural regeneration therapies.* PLOS ONE, 2019. **14**(3): p. e0213032.
40. Bhonde, R.R., et al., *Making surrogate β-cells from mesenchymal stromal cells: Perspectives and future endeavors.* The International Journal of Biochemistry & Cell Biology, 2014. **46**: p. 90-102.
41. Tao, H., et al., *Proangiogenic Features of Mesenchymal Stem Cells and Their Therapeutic Applications.* Stem Cells Int, 2016. **2016**: p. 1314709.
42. Bhang, S.H., et al., *Efficacious and clinically relevant conditioned medium of human adipose-derived stem cells for therapeutic angiogenesis.* Molecular therapy : the journal of the American Society of Gene Therapy, 2014. **22**(4): p. 862-872.
43. Boomsma, R.A. and D.L. Geenen, *Mesenchymal stem cells secrete multiple cytokines that promote angiogenesis and have contrasting effects on chemotaxis and apoptosis.* PloS one, 2012. **7**(4): p. e35685-e35685.
44. Kwon, H.M., et al., *Multiple paracrine factors secreted by mesenchymal stem cells contribute to angiogenesis.* Vascular Pharmacology, 2014. **63**(1): p. 19-28.
45. Timmers, L., et al., *Human mesenchymal stem cell-conditioned medium improves cardiac function following myocardial infarction.* Stem Cell Research, 2011. **6**(3): p. 206-214.
46. Karantalis, V., et al., *Autologous mesenchymal stem cells produce concordant improvements in regional function, tissue perfusion, and fibrotic burden when administered to patients undergoing coronary artery bypass grafting: The Prospective Randomized Study of Mesenchymal Stem Cell Therapy in Patients Undergoing Cardiac Surgery (PROMETHEUS) trial.* Circulation research, 2014. **114**(8): p. 1302-1310.
47. Lee, J.-W., et al., *A randomized, open-label, multicenter trial for the safety and efficacy of adult mesenchymal stem cells after acute myocardial infarction.* Journal of Korean medical science, 2014. **29**(1): p. 23-31.
48. Hare, J.M., et al., *Comparison of allogeneic vs autologous bone marrow–derived mesenchymal stem cells delivered by transendocardial injection in patients with ischemic cardiomyopathy: the POSEIDON randomized trial.* JAMA, 2012. **308**(22): p. 2369-2379.
49. Nassiri, S.M. and R. Rahbarghazi, *Interactions of mesenchymal stem cells with endothelial cells.* Stem Cells Dev, 2014. **23**(4): p. 319-32.
50. Zacharek, A., et al., *Angiopoietin1/Tie2 and VEGF/Flk1 induced by MSC treatment amplifies angiogenesis and vascular stabilization after stroke.* Journal of cerebral blood flow and metabolism : official journal of the International Society of Cerebral Blood Flow and Metabolism, 2007. **27**(10): p. 1684-1691.
51. Lai, R.C., et al., *Exosome secreted by MSC reduces myocardial ischemia/reperfusion injury.* Stem Cell Research, 2010. **4**(3): p. 214-222.

52. Huang, P., et al., *Combinatorial treatment of acute myocardial infarction using stem cells and their derived exosomes resulted in improved heart performance.* Stem cell research & therapy, 2019. **10**(1): p. 300-300.
53. Ding, J., et al., *Exosomes Derived from Human Bone Marrow Mesenchymal Stem Cells Stimulated by Deferoxamine Accelerate Cutaneous Wound Healing by Promoting Angiogenesis.* BioMed research international, 2019. **2019**: p. 9742765-9742765.
54. Dimova, I., G. Popivanov, and V. Djonov, *Angiogenesis in cancer – general pathways and their therapeutic implications.* Journal of B.U.O.N., 2014. **19**(1): p. 7.
55. Huang, W.H., et al., *Mesenchymal stem cells promote growth and angiogenesis of tumors in mice.* Oncogene, 2013. **32**(37): p. 4343-4354.
56. Yang, K.-Q., et al., *Bone marrow-derived mesenchymal stem cells induced by inflammatory cytokines produce angiogenetic factors and promote prostate cancer growth.* BMC cancer, 2017. **17**(1): p. 878-878.
57. Suzuki, K., et al., *Mesenchymal stromal cells promote tumor growth through the enhancement of neovascularization.* Molecular medicine (Cambridge, Mass.), 2011. **17**(7-8): p. 579-587.
58. Ishii, G., A. Ochiai, and S. Neri, *Phenotypic and functional heterogeneity of cancer-associated fibroblast within the tumor microenvironment.* Advanced Drug Delivery Reviews, 2016. **99**: p. 186-196.
59. Santi, A., F.G. Kugeratski, and S. Zanivan, *Cancer Associated Fibroblasts: The Architects of Stroma Remodeling.* Proteomics, 2018. **18**(5-6): p. e1700167-e1700167.
60. Timar, J., et al., *Angiogenesis-Dependent Diseases and Angiogenesis Therapy.* Pathology Oncology Reserach, 2001. **7**(2): p. 10.
61. Gonzalez-Rey, E., et al., *Human adipose-derived mesenchymal stem cells reduce inflammatory and T cell responses and induce regulatory T cells in vitro in rheumatoid arthritis.* Annals of the Rheumatic Diseases, 2010. **69**(01): p. 241.
62. González, M.A., et al., *Adipose-Derived Mesenchymal Stem Cells Alleviate Experimental Colitis by Inhibiting Inflammatory and Autoimmune Responses.* Gastroenterology, 2009. **136**(3): p. 978-989.
63. Mohammadzadeh, A., et al., *Immunomodulatory effects of adipose-derived mesenchymal stem cells on the gene expression of major transcription factors of T cell subsets.* Int Immunopharmacol, 2014. **20**(2): p. 316-21.
64. Nicola, M.D., et al., *Human bone marrow stromal cells suppress T-lymphocyte proliferation induced by cellular or nonspecific mitogenic stimuli.* Blood, 2002. **99**(10): p. 3838-3843.
65. Yan, Z., et al., *Mesenchymal stem cells suppress T cells by inducing apoptosis and through PD-1/B7-H1 interactions.* Immunol Lett, 2014. **162**(1 Pt A): p. 248-55.
66. Benvenuto, F., et al., *Human mesenchymal stem cells promote survival of T cells in a quiescent state.* Stem Cells, 2007. **25**(7): p. 1753-60.
67. Najar, M., et al., *Mesenchymal stromal cells promote or suppress the proliferation of T lymphocytes from cord blood and peripheral blood: the importance of low cell ratio and role of interleukin-6.* Cytotherapy, 2009. **11**(5): p. 570-583.
68. Yang, S.H., et al., *Soluble mediators from mesenchymal stem cells suppress T cell proliferation by inducing IL-10.* Exp Mol Med, 2009. **41**(5): p. 315-24.

69. Liang, C., et al., *Interferon-γ mediates the immunosuppression of bone marrow mesenchymal stem cells on T-lymphocytes in vitro.* Hematology, 2018. **23**(1): p. 44-49.
70. Ryan, J.M., et al., *Interferon-gamma does not break, but promotes the immunosuppressive capacity of adult human mesenchymal stem cells.* Clinical and experimental immunology, 2007. **149**(2): p. 353-363.
71. Duffy, M.M., et al., *Mesenchymal stem cell effects on T-cell effector pathways.* Stem Cell Research & Therapy, 2011. **2**(34): p. 9.
72. Raphael, I., et al., *T cell subsets and their signature cytokines in autoimmune and inflammatory diseases.* Cytokine, 2015. **74**(1): p. 5-17.
73. Carrion, F., et al., *Opposing effect of mesenchymal stem cells on Th1 and Th17 cell polarization according to the state of CD4+ T cell activation.* Immunol Lett, 2011. **135**(1-2): p. 10-6.
74. Aggarwal, S. and M.F. Pittenger, *Human mesenchymal stem cells modulate allogeneic immune cell responses.* Blood, 2005. **105**(4): p. 1815-1822.
75. Ezquer, M., et al., *Intravitreal administration of multipotent mesenchymal stromal cells triggers a cytoprotective microenvironment in the retina of diabetic mice.* Stem Cell Res Ther, 2016. **7**: p. 42.
76. Favaro, E., et al., *Human mesenchymal stem cell-derived microvesicles modulate T cell response to islet antigen glutamic acid decarboxylase in patients with type 1 diabetes.* Diabetologia (2014), 2014. **57**: p. 10.
77. Boumaza, I., et al., *Autologous bone marrow-derived rat mesenchymal stem cells promote PDX-1 and insulin expression in the islets, alter T cell cytokine pattern and preserve regulatory T cells in the periphery and induce sustained normoglycemia.* Journal of Autoimmunity, 2009. **32**(1): p. 33-42.
78. Wan, Y.Y. and R.A. Flavell, *How diverse--CD4 effector T cells and their functions.* Journal of molecular cell biology, 2009. **1**(1): p. 20-36.
79. Sakaguchi, S., et al., *Immunologic self-tolerance maintained by activated T cells expressing IL-2 receptor alpha-chains (CD25). Breakdown of a single mechanism of self-tolerance causes various autoimmune diseases.* The Journal of Immunology, 1995. **155**(3): p. 1151.
80. Rodríguez-Perea, A.L., et al., *Phenotypical characterization of regulatory T cells in humans and rodents.* Clinical and experimental immunology, 2016. **185**(3): p. 281-291.
81. Yu, N., et al., *CD4+CD25+CD127low/− T Cells: A More Specific Treg Population in Human Peripheral Blood.* Inflammation, 2012. **35**(6): p. 1773-1780.
82. English, K., et al., *Cell contact, prostaglandin E(2) and transforming growth factor beta 1 play non-redundant roles in human mesenchymal stem cell induction of CD4+CD25(High) forkhead box P3+ regulatory T cells.* Clin Exp Immunol, 2009. **156**(1): p. 149-60.
83. Melief, S.M., et al., *Multipotent stromal cells induce human regulatory T cells through a novel pathway involving skewing of monocytes toward anti-inflammatory macrophages.* Stem Cells, 2013. **31**(9): p. 1980-91.
84. Engela, A.U., et al., *Human adipose-tissue derived mesenchymal stem cells induce functional de-novo regulatory T cells with methylated FOXP3 gene DNA.* Clin Exp Immunol, 2013. **173**(2): p. 343-54.
85. Ge, W., et al., *Regulatory T-Cell Generation and Kidney Allograft Tolerance Induced by Mesenchymal Stem Cells Associated With Indoleamine 2,3-Dioxygenase Expression.* Transplantation, 2010. **90**(12): p. 1312-1320.
86. Casiraghi, F., et al., *Pretransplant Infusion of Mesenchymal Stem Cells Prolongs the Survival of a Semiallogeneic Heart Transplant through the*

Generation of Regulatory T Cells. The Journal of Immunology, 2008. **181**(6): p. 3933.
87. Khosravi, M., et al., *Induction of CD4(+)CD25(+)FOXP3(+) regulatory T cells by mesenchymal stem cells is associated with modulation of ubiquitination factors and TSDR demethylation.* Stem Cell Res Ther, 2018. **9**(1): p. 273.
88. Xv, J., et al., *Mesenchymal stem cells moderate immune response of type 1 diabetes.* Cell Tissue Res, 2017. **368**(2): p. 239-248.
89. Aali, E., et al., *A comparative study of mesenchymal stem cell transplantation with its paracrine effect on control of hyperglycemia in type 1 diabetic rats.* Journal of Diabetes & Metabolic Disorders, 2014. **13**(76): p. 10.
90. Dong, Q., et al., *Allogeneic diabetic mesenchymal stem cells transplantation in streptozotocin-induced diabetic rat.* Clin Invest Med, 2008. **31**(6): p. 10.
91. Kota, D.J., et al., *TSG-6 Produced by hMSCs Delays the Onset of Autoimmune Diabetes by Suppressing Th1 Development and Enhancing Tolerogenicity.* Diabetes, 2013. **62**: p. 10.
92. Carlsson, P., et al., *Preserved β-cell function in type 1 diabetes by mesenchymal stromal cells.* Diabetes, 2015. **64**: p. 6.
93. Bhansali, A., et al., *Efficacy and safety of autologous bone marrow-derived stem cell transplantation in patients with type 2 diabetes mellitus: a randomized placebo-controlled study.* Cell Transplant, 2014. **23**(9): p. 1075-85.
94. Cantu-Rodriguez, O.G., et al., *Long-Term Insulin Independence in Type 1 Diabetes Mellitus Using a Simplified Autologous Stem Cell Transplant.* J Clin Endocrinol Metab, 2016. **101**(5): p. 2141-8.
95. Cai, X. and J.F. McGinnis, *Diabetic Retinopathy: Animal Models, Therapies, and Perspectives.* J Diabetes Res, 2016. **2016**: p. 3789217.
96. El-Bab, M.F., et al., *Retinopathy and risk factors in diabetic patients from Al-Madinah Al-Munawarah in the Kingdom of Saudi Arabia.* Clin Ophthalmol, 2012. **6**: p. 269-76.
97. Flaxel, C.J., et al., *Diabetic Retinopathy Preferred Practice Pattern®.* Ophthalmology, 2019.
98. Daruich, A., et al., *Mechanisms of macular edema: Beyond the surface.* Prog Retin Eye Res, 2018. **63**: p. 20-68.
99. Antonetti, D.A., R. Klein, and T.W. Gardner, *Diabetic Retinopathy.* New England Journal of Medicine, 2012. **366**(13): p. 1227-1239.
100. Kern, T.S. and A.J. Barber, *Retinal ganglion cells in diabetes.* The Journal of physiology, 2008. **586**(18): p. 4401-4408.
101. Park, S.-H., et al., *Apoptotic death of photoreceptors in the streptozotocin-induced diabetic rat retina.* Diabetologia, 2003. **46**(9): p. 1260-1268.
102. Sohn, E.H., et al., *Retinal neurodegeneration may precede microvascular changes characteristic of diabetic retinopathy in diabetes mellitus.* Proceedings of the National Academy of Sciences of the United States of America, 2016. **113**(19): p. E2655-E2664.
103. Coughlin, B.A., D.J. Feenstra, and S. Mohr, *Müller cells and diabetic retinopathy.* Vision research, 2017. **139**: p. 93-100.
104. Kern, T.S., *Contributions of inflammatory processes to the development of the early stages of diabetic retinopathy.* Experimental diabetes research, 2007. **2007**: p. 95103-95103.
105. Boss, J.D., et al., *Assessment of Neurotrophins and Inflammatory Mediators in Vitreous of Patients With Diabetic Retinopathy.* Investigative ophthalmology & visual science, 2017. **58**(12): p. 5594-5603.

106. Doganay, S., et al., *Comparison of serum NO, TNF-α, IL-1β, sIL-2R, IL-6 and IL-8 levels with grades of retinopathy in patients with diabetes mellitus.* Eye, 2002. **16**(2): p. 163-170.
107. Jain, A., et al., *Status of serum VEGF and ICAM-1 and its association with external limiting membrane and inner segment-outer segment junction disruption in type 2 diabetes mellitus.* Molecular vision, 2013. **19**: p. 1760-1768.
108. Antonetti, D.A., et al., *Diabetic retinopathy: seeing beyond glucose-induced microvascular disease.* Diabetes, 2006. **55**(9): p. 2401-11.
109. Joussen, A.M., et al., *Leukocyte-mediated endothelial cell injury and death in the diabetic retina.* Am J Pathol., 2001. **158**(1): p. 147-152.
110. Joussen, A.M., et al., *Retinal vascular endothelial growth factor induces intercellular adhesion molecule-1 and endothelial nitric oxide synthase expression and initiates early diabetic retinal leukocyte adhesion in vivo.* The American journal of pathology, 2002. **160**(2): p. 501-509.
111. Chen, W., et al., *Anti-inflammatory effect of docosahexaenoic acid on cytokine-induced adhesion molecule expression in human retinal vascular endothelial cells.* Investigative ophthalmology & visual science, 2005. **46**(11): p. 4342-4347.
112. Miyamoto, K., et al., *Prevention of leukostasis and vascular leakage in streptozotocin-induced diabetic retinopathy via intercellular adhesion molecule-1 inhibition.* Proceedings of the National Academy of Sciences, 1999. **96**: p. 10836-10841.
113. Costagliola, C., et al., *TNF-alpha levels in tears: a novel biomarker to assess the degree of diabetic retinopathy.* Mediators of inflammation, 2013. **2013**: p. 629529-629529.
114. Croll, S.D., et al., *VEGF-mediated inflammation precedes angiogenesis in adult brain.* Experimental Neurology, 2004. **187**(2): p. 388-402.
115. Lee, T.H., et al., *Vascular endothelial growth factor modulates neutrophil transendothelial migration via up-regulation of interleukin-8 in human brain microvascular endothelial cells.* J Biol Chem, 2002. **277**(12): p. 10445-51.
116. Bergers, G. and S. Song, *The role of pericytes in blood-vessel formation and maintenance.* Neuro-oncology, 2005. **7**(4): p. 452-464.
117. Ferland-McCollough, D., et al., *Pericytes, an overlooked player in vascular pathobiology.* Pharmacology & therapeutics, 2017. **171**: p. 30-42.
118. Gerhardt, H. and C. Betsholtz, *Endothelial-pericyte interactions in angiogenesis.* Cell and Tissue Research, 2003. **314**(1): p. 15-23.
119. Pfister, F., et al., *Pericytes in the eye.* Pflugers Arch, 2013. **465**(6): p. 789-96.
120. Trost, A., et al., *Pericytes in the Retina*, in *Pericyte Biology in Different Organs*, A. Birbrair, Editor. 2019, Springer International Publishing: Cham. p. 1-26.
121. Hammes, H.P., *Pericytes and the pathogenesis of diabetic retinopathy.* Horm Metab Res, 2005. **37 Suppl 1**: p. 39-43.
122. Semeraro, F., et al., *Diabetic retinopathy, a vascular and inflammatory disease: Therapeutic implications.* Diabetes & Metabolism, 2019.
123. Fiori, A., et al., *Mesenchymal stromal/stem cells as potential therapy in diabetic retinopathy.* Immunobiology, 2018. **223**(12): p. 729-743.
124. Rajashekhar, G., et al., *Regenerative therapeutic potential of adipose stromal cells in early stage diabetic retinopathy.* PLoS One, 2014. **9**(1): p. e84671.
125. Mendel, T.A., et al., *Pericytes derived from adipose-derived stem cells protect against retinal vasculopathy.* PLoS One, 2013. **8**(5): p. e65691.
126. Hajmousa, G., et al., *Human adipose tissue-derived stromal cells act as functional pericytes in mice and suppress high-glucose-induced*

proinflammatory activation of bovine retinal endothelial cells. Diabetologia, 2018. **61**(11): p. 2371-2385.
127. Terlizzi, V., et al., *The Pericytic Phenotype of Adipose Tissue-Derived Stromal Cells Is Promoted by NOTCH2.* Stem Cells, 2018. **36**(2): p. 240-251.
128. Deliyanti, D., et al., *Foxp3(+) Tregs are recruited to the retina to repair pathological angiogenesis.* Nat Commun, 2017. **8**(1): p. 748.
129. Baena-Díez, J.M., et al., *Risk of Cause-Specific Death in Individuals With Diabetes: A Competing Risks Analysis.* Diabetes Care, 2016. **39**: p. 1987-1995.
130. Forbes, J.M. and M.E. Cooper, *Mechanisms of diabetic complications.* Physiol Rev, 2013. **93**(1): p. 137-88.
131. Chawla, A., R. Chawla, and S. Jaggi, *Microvasular and macrovascular complications in diabetes mellitus: Distinct or continuum?* Indian journal of endocrinology and metabolism, 2016. **20**(4): p. 546-551.
132. Fowler, M.J., *Microvascular and Macrovascular Complications of Diabetes.* Clinical Diabetes, 2008. **26**(2): p. 77.
133. Brownlee, M., *The pathobiology of diabetic complications: a unifying mechanism.* Diabetes, 2005. **54**(6): p. 11.
134. Brownlee, M., *Biochemistry and molecular cell biology of diabetic complications.* Nature, 2001. **414**: p. 8.
135. Gero, D., *Hyperglycemia-Induced Endothelial Dysfunction.* 2018.
136. Sonneville, R., et al., *Impact of hyperglycemia on neuropathological alterations during critical illness.* J Clin Endocrinol Metab, 2012. **97**(6): p. 2113-23.
137. Grohova, A., et al., *Cell Based Therapy for Type 1 Diabetes: Should We Take Hyperglycemia Into Account?* Front Immunol, 2019. **10**: p. 79.
138. Bieback, K., et al., *Replicative aging and differentiation potential of human adipose tissue-derived mesenchymal stromal cells expanded in pooled human or fetal bovine serum.* Cytotherapy, 2012. **14**(5): p. 570-83.
139. Wuchter, P., et al., *Standardization of Good Manufacturing Practice–compliant production of bone marrow–derived human mesenchymal stromal cells for immunotherapeutic applications.* Cytotherapy, 2015. **17**(2): p. 128-139.
140. Liping, L. and L. Meilian, *Adipose tissue in control of metabolism.* Journal of Endocrinology, 2016. **231**(3): p. R77-R99.
141. Davies, L.C., et al., *Type 1 Diabetes Mellitus Donor Mesenchymal Stromal Cells Exhibit Comparable Potency to Healthy Controls In Vitro.* Stem cells translational medicine, 2016. **5**(11): p. 1485-1495.
142. Yaochite, J.N., et al., *Therapeutic efficacy and biodistribution of allogeneic mesenchymal stem cells delivered by intrasplenic and intrapancreatic routes in streptozotocin-induced diabetic mice.* Stem Cell Res Ther, 2015. **6**: p. 31.
143. Zhang, D., et al., *High glucose induces the aging of mesenchymal stem cells via Akt/mTOR signaling.* Molecular medicine reports, 2017. **16**(2): p. 1685-1690.
144. Kornicka, K., J. Houston, and K. Marycz, *Dysfunction of Mesenchymal Stem Cells Isolated from Metabolic Syndrome and Type 2 Diabetic Patients as Result of Oxidative Stress and Autophagy may Limit Their Potential Therapeutic Use.* Stem Cell Rev Rep, 2018. **14**(3): p. 337-345.
145. Cianfarani, F., et al., *Diabetes impairs adipose tissue-derived stem cell function and efficiency in promoting wound healing.* Wound Repair Regen, 2013. **21**(4): p. 545-53.
146. Rennert, R.C., et al., *Diabetes impairs the angiogenic potential of adipose-derived stem cells by selectively depleting cellular subpopulations.* Stem Cell Research & Therapy, 2014. **5**(79): p. 1-12.

147. Inoue, O., et al., *Diabetes impairs the angiogenic capacity of human adipose-derived stem cells by reducing the CD271+ subpopulation in adipose tissue.* Biochemical and Biophysical Research Communications, 2019. **517**(2): p. 369-375.
148. Cronk, S.M., et al., *Adipose-derived stem cells from diabetic mice show impaired vascular stabilization in a murine model of diabetic retinopathy.* Stem Cells Transl Med, 2015. **4**(5): p. 459-67.
149. Peng, Z., et al., *Glyoxalase-1 Overexpression Reverses Defective Proangiogenic Function of Diabetic Adipose-Derived Stem Cells in Streptozotocin-Induced Diabetic Mice Model of Critical Limb Ischemia.* STEM CELLS Translational Medicine, 2017. **6**(1): p. 261-271.
150. Mehrabani, M., et al., *Deferoxamine preconditioning to restore impaired HIF-1α-mediated angiogenic mechanisms in adipose-derived stem cells from STZ-induced type 1 diabetic rats.* Cell Proliferation, 2015. **48**(5): p. 532-549.
151. Hajmousa, G., et al., *Hyperglycemia induces bioenergetic changes in adipose-derived stromal cells while their pericytic function is retained.* Stem Cells Dev, 2016. **25**(19): p. 9.
152. Rharass, T. and S. Lucas, *High Glucose Level Impairs Human Mature Bone Marrow Adipocyte Function Through Increased ROS Production.* Frontiers in endocrinology, 2019. **10**: p. 607-607.
153. Kong, Y., et al., *Norepinephrine protects against apoptosis of mesenchymal stem cells induced by high glucose.* Journal of Cellular Physiology, 2019. **234**(11): p. 20801-20815.
154. Jakubowski, W. and G. Bartosz, *2,7-dichlorofluorescin oxidation and reactive oxygen species: what does it measure?* Cell Biol Int, 2000. **24**(10): p. 757-60.
155. Bieback, K., et al., *Cord blood derived endothelial colony forming cells emerge from a CD45dim CD31+ circulating precursor.* Cytotherapy, 2014. **16**(4): p. S71.
156. Yang, Z., et al., *Critical effect of VEGF in the process of endothelial cell apoptosis induced by high glucose.* Apoptosis, 2008. **13**(11): p. 1331-43.
157. Amato, R., et al., *VEGF as a Survival Factor in Ex Vivo Models of Early Diabetic Retinopathy.* Investigative Ophthalmology & Visual Science, 2016. **57**(7): p. 3066-3076.
158. Smyth, L.C.D., et al., *Markers for human brain pericytes and smooth muscle cells.* J Chem Neuroanat, 2018. **92**: p. 48-60.
159. Hughes, S. and T. Chan-Ling, *Characterization of Smooth Muscle Cell and Pericyte Differentiation in the Rat Retina In Vivo.* Investigative Ophthalmology & Visual Science, 2004. **45**(8): p. 2795-2806.
160. Nehls, V. and D. Drenckhahn, *Heterogeneity of microvascular pericytes for smooth muscle type alpha-actin.* The Journal of cell biology, 1991. **113**(1): p. 147-154.
161. Cervenka, I., L.Z. Agudelo, and J.L. Ruas, *Kynurenines: Tryptophan's metabolites in exercise, inflammation, and mental health.* Science, 2017. **357**(6349).
162. Francois, M., et al., *Human MSC suppression correlates with cytokine induction of indoleamine 2,3-dioxygenase and bystander M2 macrophage differentiation.* Mol Ther, 2012. **20**(1): p. 187-95.
163. Fehervari, Z., T. Yamaguchi, and S. Sakaguchi, *The dichotomous role of IL-2: tolerance versus immunity.* Trends Immunol, 2006. **27**(3): p. 109-11.
164. Hadaschik, E.N. and A.H. Enk, *TGF-beta1-induced regulatory T cells.* Hum Immunol, 2015. **76**(8): p. 561-4.

165. Shin, L. and D.A. Peterson, *Impaired therapeutic capacity of autologous stem cells in a model of type 2 diabetes.* Stem Cells Transl Med, 2012. **1**(2): p. 125-35.
166. Rubsam, A., S. Parikh, and P.E. Fort, *Role of Inflammation in Diabetic Retinopathy.* Int J Mol Sci, 2018. **19**(4).
167. Nakamura, N., et al., *High glucose impairs the proliferation and increases the apoptosis of endothelial progenitor cells by suppression of Akt.* J Diabetes Investig, 2011. **2**(4): p. 262-70.
168. Varma, S., et al., *Hyperglycemia alters PI3k and Akt signaling and leads to endothelial cell proliferative dysfunction.* Am J Physiol Heart Circ Physiol., 2005 **284**(4): p. 7.
169. Li, A.F. and S. Roy, *High glucose-induced downregulation of connexin 43 expression promotes apoptosis in microvascular endothelial cells.* Invest Ophthalmol Vis Sci, 2009. **50**(3): p. 1400-7.
170. Sun, J., et al., *Intermittent high glucose enhances cell proliferation and VEGF expression in retinal endothelial cells: the role of mitochondrial reactive oxygen species.* Mol Cell Biochem, 2010. **343**(1-2): p. 27-35.
171. Premanand, C., et al., *Effect of curcumin on proliferation of human retinal endothelial cells under in vitro conditions.* Investigative Ophthalmology & Visual Science, 2006. **45**(5): p. 6.
172. Xu, G., et al., *Contradictory effects of short- and long-term hyperglycemias on ischemic injury of myocardium via intracellular signaling pathway.* Exp Mol Pathol, 2004. **76**(1): p. 57-65.
173. Xing, Y., et al., *Netrin-1 restores cell injury and impaired angiogenesis in vascular endothelial cells upon high glucose by PI3K/AKT-eNOS.* J Mol Endocrinol, 2017. **58**(4): p. 167-177.
174. Xu, J., et al., *RasGRP1 is a target for VEGF to induce angiogenesis and involved in the endothelial-protective effects of metformin under high glucose in HUVECs.* IUBMB Life, 2019. **71**(9): p. 1391-1400.
175. Yan, M., et al., *Glucose impairs angiogenesis and promotes ventricular remodelling following myocardial infarction via upregulation of microRNA-17.* Exp Cell Res, 2019. **381**(2): p. 191-200.
176. Yu, Z., et al., *Erianin inhibits high glucose-induced retinal angiogenesis via blocking ERK1/2-regulated HIF-1α-VEGF/VEGFR2 signaling pathway.* Scientific Reports, 2016. **6**: p. 34306.
177. Yoon, C.H., et al., *High glucose-induced jagged 1 in endothelial cells disturbs notch signaling for angiogenesis: a novel mechanism of diabetic vasculopathy.* J Mol Cell Cardiol, 2014. **69**: p. 52-66.
178. Madonna, R., et al., *High glucose-induced hyperosmolarity contributes to COX-2 expression and angiogenesis: implications for diabetic retinopathy.* Cardiovasc Diabetol, 2016. **15**: p. 18.
179. Cheng, J.W., et al., *The role of CXCL12 and CCL7 chemokines in immune regulation, embryonic development, and tissue regeneration.* Cytokine, 2014. **69**(2): p. 277-83.
180. Liu, Y., et al., *Crucial biological functions of CCL7 in cancer.* PeerJ, 2018. **6**: p. e4928.
181. Hammes, H.P., et al., *Diabetic retinopathy: targeting vasoregression.* Diabetes, 2011. **60**(1): p. 9-16.
182. Murohara, T., S. Shintani, and K. Kondo, *Autologous adipose-derived regenerative cells for therapeutic angiogenesis.* Curr Pharm Des., 2009. **15**(24): p. 6.

183. Scharpfenecker, M., et al., *The Tie-2 ligand angiopoietin-2 destabilizes quiescent endothelium through an internal autocrine loop mechanism.* J Cell Sci, 2005. **118**(Pt 4): p. 771-80.
184. Fagiani, E. and G. Christofori, *Angiopoietins in angiogenesis.* Cancer Letters, 2013. **328**(1): p. 18-26.
185. Rusnati, M. and M. Presta, *Fibroblast growth factorsfibroblast growth factor receptors as targets for the development of anti-angiogenesis strategies.* Current Pharmaceutical Design, 2007. **12**(20): p. 20.
186. Paliwal, S., et al., *Regenerative abilities of mesenchymal stem cells through mitochondrial transfer.* J Biomed Sci, 2018. **25**(1): p. 31.
187. Liu, K., et al., *Mesenchymal stem cells rescue injured endothelial cells in an in vitro ischemia-reperfusion model via tunneling nanotube like structure-mediated mitochondrial transfer.* Microvasc Res, 2014. **92**: p. 10-8.
188. Mahrouf-Yorgov, M., et al., *Mesenchymal stem cells sense mitochondria released from damaged cells as danger signals to activate their rescue properties.* Cell Death Differ, 2017. **24**(7): p. 1224-1238.
189. Liu, K., et al., *Mesenchymal stem cells transfer mitochondria into cerebral microvasculature and promote recovery from ischemic stroke.* Microvasc Res, 2019. **123**: p. 74-80.
190. Prieto-Bermejo, R. and A. Hernandez-Hernandez, *The Importance of NADPH Oxidases and Redox Signaling in Angiogenesis.* Antioxidants (Basel), 2017. **6**(2).
191. Craige, S.M., S. Kant, and J.F. Keaney, Jr., *Reactive oxygen species in endothelial function - from disease to adaptation.* Circ J, 2015. **79**(6): p. 1145-55.
192. Chan, E.C., et al., *Involvement of Nox2 NADPH oxidase in retinal neovascularization.* Invest Ophthalmol Vis Sci., 2013. **54**: p. 7.
193. Al-Shabrawey, M., et al., *Inhibition of NAD(P)H Oxidase Activity Blocks Vascular Endothelial Growth Factor Overexpression and Neovascularization during Ischemic Retinopathy.* The American Journal of Pathology, 2005. **167**(2): p. 599-607.
194. Wang, H., et al., *Endothelial NADPH oxidase 4 mediates vascular endothelial growth factor receptor 2–induced intravitreal neovascularization in a rat model of retinopathy of prematurity.* Molecular Vision 2014. **20**: p. 10.
195. Huang, H., et al., *Intravitreal injection of mesenchymal stem cells evokes retinal vascular damage in rats.* The FASEB Journal, 2019: p. fj.201901500R.
196. Merfeld-Clauss, S., et al., *Adipose stromal cells differentiation toward smooth muscle cell phenotype diminishes their vasculogenic activity due to induction of activin A secretion.* Journal of Tissue Engineering and Regenerative Medicine, 2017. **11**(11): p. 3145-3156.
197. Merfeld-Clauss, S., et al., *Adipose Stromal Cells Differentiate Along a Smooth Muscle Lineage Pathway Upon Endothelial Cell Contact via Induction of Activin A.* Circulation Research, 2014. **115**(9): p. 800-809.
198. Crisan, M., et al., *Perivascular cells for regenerative medicine.* J Cell Mol Med, 2012. **16**(12): p. 2851-60.
199. Mitchell, T.S., et al., *RGS5 expression is a quantitative measure of pericyte coverage of blood vessels.* Angiogenesis, 2008. **11**(2): p. 141-51.
200. de Souza, L.E., et al., *Mesenchymal Stem Cells and Pericytes: To What Extent Are They Related?* Stem Cells Dev., 2016. **15**(25): p. 10.

201. Di Nicola, M., et al., *Human bone marrow stromal cells suppress T-lymphocyte proliferation induced by cellular or nonspecific mitogenic stimuli.* Blood, 2002. **99**(10): p. 6.
202. Shi, Y., et al., *Immunoregulatory mechanisms of mesenchymal stem and stromal cells in inflammatory diseases.* Nat Rev Nephrol, 2018. **14**(8): p. 493-507.
203. Du, M.X., W.D. Sotero-Esteva, and M.W. Taylor, *Analysis of transcription factors regulating induction of indoleamine 2,3-dioxygenase by IFN-gamma.* Journal of Interferon & Cytokine Research 2000. **20**(2): p. 10.
204. Schroder, K., et al., *Interferon-gamma: an overview of signals, mechanisms and functions.* J Leukoc Biol, 2004. **75**(2): p. 163-89.
205. De Miguel, M.P., et al., *Immunosuppressive Properties of Mesenchymal Stem Cells: Advances and Applications.* Current Molecular Medicine, 2012. **12**: p. 18.
206. Le Blanc, K., et al., *Mesenchymal stem cells inhibit the expression of CD25 (interleukin-2 receptor) and CD38 on phytohaemagglutinin-activated lymphocytes.* Scandinavian Journal of Immunology, 2004. **60**: p. 8.
207. Yoo, H.S., et al., *Mesenchymal stromal cells inhibit CD25 expression via the mTOR pathway to potentiate T-cell suppression.* Cell Death Dis, 2017. **8**(2): p. e2632.
208. Bartholomew, A., et al., *Mesenchymal stem cells suppress lymphocyte proliferation in vitro and prolong skin graft survival in vivo.* xperimental Hematology, 2002. **30**: p. 7.
209. Prevosto, C., et al., *Generation of CD4+ or CD8+ regulatory T cells upon mesenchymal stem cell-lymphocyte interaction.* Haematologica, 2007. **92**(7): p. 8.
210. Hori, S. and S. Sakaguchi, *Foxp3: a critical regulator of the development and function of regulatory T cells.* Microbes Infect, 2004. **6**(8): p. 745-51.
211. Guo, F., et al., *CD28 controls differentiation of regulatory T cells from naive CD4 T cells.* Journal of immunology (Baltimore, Md. : 1950), 2008. **181**(4): p. 2285-2291.
212. Valencic, E., et al., *T cells stimulated in vitro have a suppressive function but do not contain only regulatory T cells.* Clinical and experimental immunology, 2007. **150**(3): p. 561-566.
213. Wang, H., et al., *Differences in the Induction of Induced Human CD4+ CD25+ FoxP3+ T-Regulatory Cells and CD3+ CD8+ CD28− T-Suppressor Cells Subset Phenotypes In Vitro: Comparison of Phorbol 12-Myristate 13-Acetate/Ionomycin and Phytohemagglutinin Stimulation.* Transplantation Proceedings, 2013. **45**(5): p. 1822-1831.
214. Cuerquis, J., et al., *Human mesenchymal stromal cells transiently increase cytokine production by activated T cells before suppressing T-cell proliferation: effect of interferon-gamma and tumor necrosis factor-alpha stimulation.* Cytotherapy, 2014. **16**(2): p. 191-202.
215. Crop, M.J., et al., *Human Adipose Tissue-Derived Mesenchymal Stem Cells Induce Explosive T-Cell Proliferation.* Stem Cells and Development, 2010. **19**(12): p. 11.
216. Mattar, P. and K. Bieback, *Comparing the Immunomodulatory Properties of Bone Marrow, Adipose Tissue, and Birth-Associated Tissue Mesenchymal Stromal Cells.* Front Immunol, 2015. **6**: p. 560.
217. Liu, B.X., W. Sun, and X.Q. Kong, *Perirenal Fat: A Unique Fat Pad and Potential Target for Cardiovascular Disease.* Angiology, 2019. **70**(7): p. 584-593.

218. Li, F., et al., *Indoleamine-2,3-dioxygenase and Interleukin-6 associated with tumor response to neoadjuvant chemotherapy in breast cancer.* Oncotarget, 2017. **8**(64): p. 15.
219. English, K., A. French, and K.J. Wood, *Mesenchymal stromal cells: facilitators of successful transplantation?* Cell Stem Cell, 2010. **7**(4): p. 431-42.
220. Ren, G., et al., *Mesenchymal stem cell-mediated immunosuppression occurs via concerted action of chemokines and nitric oxide.* Cell Stem Cell, 2008. **2**(2): p. 141-50.
221. Le Blanc, K., et al., *Mesenchymal Stem Cells Inhibit the Expression of CD25 (Interleukin-2 Receptor) and CD38 on Phytohaemagglutinin-Activated Lymphocytes.* Scandinavian Journal of Immunology, 2004. **60**(3): p. 307-315.
222. Castro-Manrreza, M.E., et al., *Human mesenchymal stromal cells from adult and neonatal sources: a comparative in vitro analysis of their immunosuppressive properties against T cells.* Stem cells and development, 2014. **23**(11): p. 1217-1232.
223. Maccario, R., et al., *Interaction of human mesenchymal stem cells with cells involved in alloantigen-specific immune response favors the differentiation of CD4+ T-cell subsets expressing a regulatory/suppressive phenotype.* Haematologica, 2005. **90**(4): p. 516-525.
224. Fan, X.-L., et al., *Induced pluripotent stem cell-derived mesenchymal stem cells activate quiescent T cells and elevate regulatory T cell response via NF-κB in allergic rhinitis patients.* Stem Cell Research & Therapy, 2018. **9**(1): p. 170.
225. Kelly-Welch, A., E.M. Hanson, and A.D. Keegan, *Interleukin-4 (IL-4) Pathway.* Science Signaling 2005. **293**: p. 2.
226. Bagnasco, D., et al., *A Critical Evaluation of Anti-IL-13 and Anti-IL-4 Strategies in Severe Asthma.* Int Arch Allergy Immunol, 2016. **170**(2): p. 122-31.
227. Bai, L., et al., *Human bone marrow-derived mesenchymal stem cells induce Th2-polarized immune response and promote endogenous repair in animal models of multiple sclerosis.* Glia, 2009. **57**(11): p. 1192-203.
228. Fiorina, P., et al., *Immunomodulatory function of bone marrow-derived mesenchymal stem cells in experimental autoimmune type 1 diabetes.* J Immunol, 2009. **183**(2): p. 993-1004.
229. Kavanagh, H. and B.P. Mahon, *Allogeneic mesenchymal stem cells prevent allergic airway inflammation by inducing murine regulatory T cells.* Allergy, 2011. **66**(4): p. 523-31.
230. Mosser, D.M., *The many faces of macrophage activation.* J Leukoc Biol, 2003. **73**(2): p. 209-12.
231. Chang, Y., et al., *The chemokine CCL18 generates adaptive regulatory T cells from memory CD4+ T cells of healthy but not allergic subjects.* FASEB J, 2010. **24**(12): p. 5063-72.
232. Rennert, R., et al., *Diabetes impairs the angiogenic potential of adipose-derived stem cells by selectively depleting cellular subpopulations.* Stem Cell Res Ther, 2014. **5**(79): p. 12.
233. Alicka, M., et al., *Adipose-Derived Mesenchymal Stem Cells Isolated from Patients with Type 2 Diabetes Show Reduced "Stemness" through an Altered Secretome Profile, Impaired Anti-Oxidative Protection, and Mitochondrial Dynamics Deterioration.* J Clin Med, 2019. **8**(6).
234. Deng, X., et al., *Effects of Type 2 Diabetic Serum on Proliferation and Osteogenic Differentiation of Mesenchymal Stem Cells.* J Diabetes Res, 2018. **2018**: p. 5765478.

8 APPENDIX

8.1 Generation of fluorescent cells

8.1.1 Plasmids

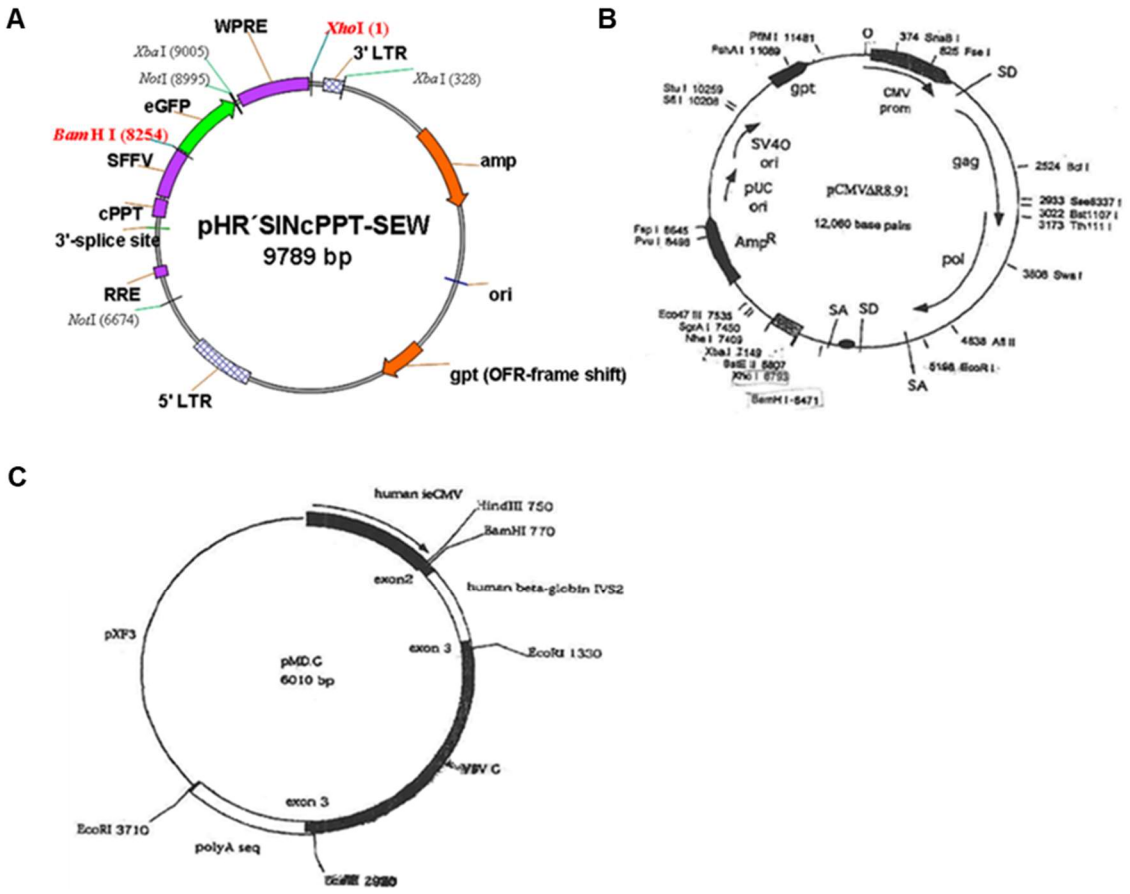

Figure 40 Plasmid maps. A) GFP plasmid; dTomato plasmid has the same backbone with dTomato gene replacing GFP ; B) pCMVDR8.91; C) pMD.G plasmid.

8.1.2 Enzymatic restriction

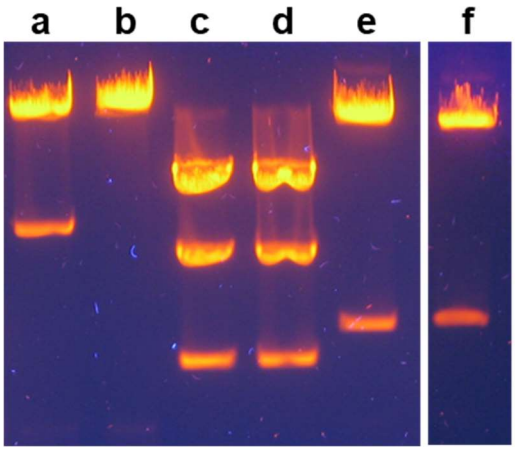

Figure 41 Representative agarose gel loaded with enzymatically restricted plasmids: a) pCMVDR8.91 Mix 1; b) pCMVDR8.91 Mix 2; c) pMD.G Mix 1; d) pMD.G Mix 2; e) dTomato; f) GFP.

8.1.3 Sort gating strategy

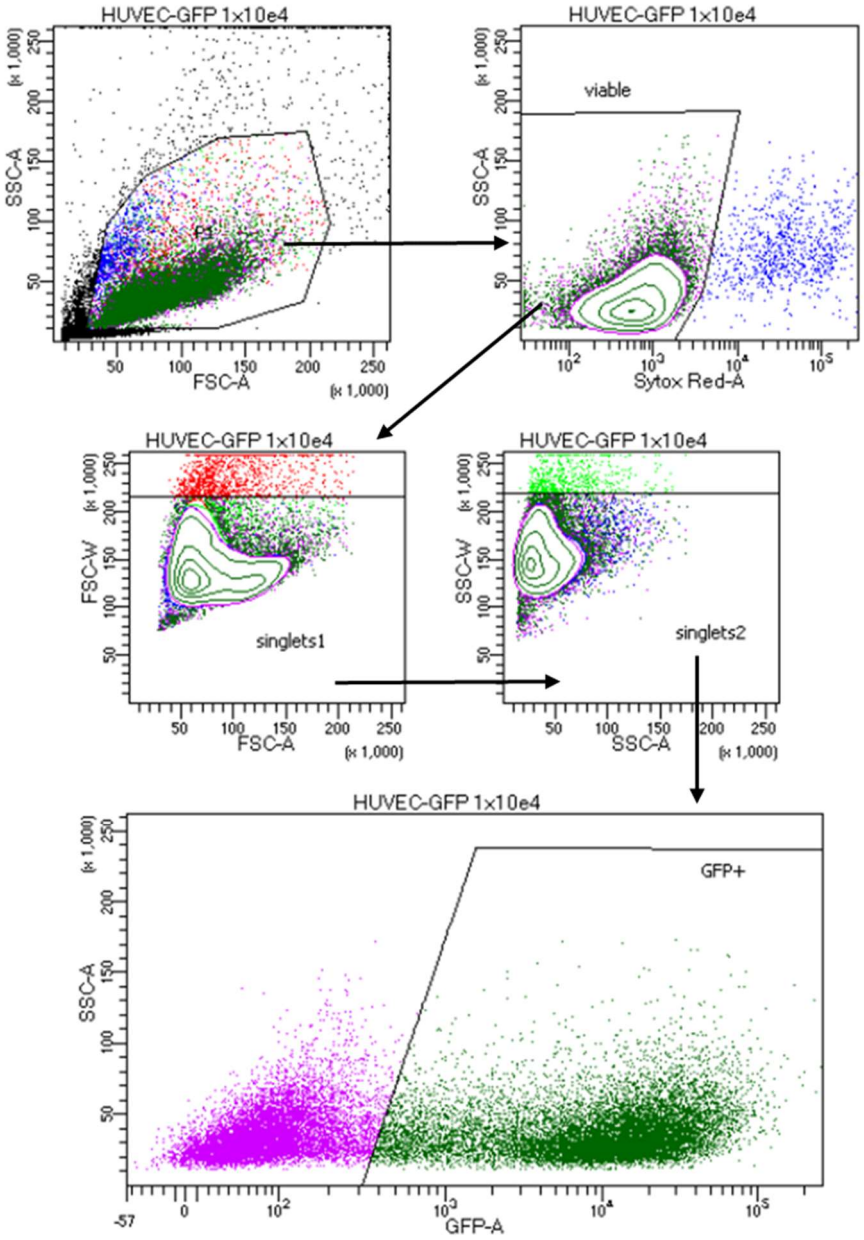

Figure 42 Representative gating strategy to sort fluorescent cells. HUVEC were first morphologically selected on the SSC and FSC. Viable cells were then gated and further selected after duplets discrimination. Then GFP positive HUVEC (green population) were gated and sorted.

9 CURRICULUM VITAE

PERSONALIEN

Name und Vorname:	Agnese Fiori
Geburtsdatum:	26.11.1990
Geburtsort:	Sassuolo (Modena, Italy)
Familienstand:	Ledig
Vater:	Alberto Fiori
Mutter:	Maria Grazia Salerno

SCHULISCHER WERDEGANG

2004 – 2009	High School leaving certificate in science Liceo Scientifico “Alessandro Tassoni”, Modena (Italy) Certificate in science 91/100 (26.08.2009)

UNIVERSITÄRER WERDEGANG

10/2009 – 12/2012	**1st Level Degree (Bachelor´s Degree) in Biotechnology** University of Modena and Reggio Emilia
10/2011 – 12/2012	• **Research Internship, Bachelor´s Degree** Thesis title: “Interaction Between Tumor and Stroma by Spectrophotometric and Flow-Cytometry Analysis: The Model of Ewing Sarcoma”. (Supervisor: Prof. Massimo Dominici / Co-supervisor: Dr. Giulia Grisendi) Final degree mark: 107/110 (11.12.2012)
11/2012 – 12/2014	**2nd Level Degree (Master´s Degree) in Medical and Pharmaceutical Biotechnology** University of Modena and Reggio Emilia

01/2014 – 12/2014	• **Research Internship, Master´s Degree** Thesis title: “Mesenchymal Stromal Cells Interaction with Ewing Sarcoma: Between Insights on Tumor Microenvironment and a Therapeutic Strategy”. (Supervisor: Prof. Massimo Dominici / Co-supervisor: Dr. Giulia Grisendi) Final degree mark: 110/110 cum laude (10.12.2014)
01/2015 – 07/2015	**Postgraduate Internship** University of Modena and Reggio Emilia
10/2015 – 12/2015	**Post graduated specialization course: Stem Cells in Neuromuscular and Neurodegenerative diseases** University of Milano
12/2015	**Qualifying examination to practice as Biologist** University of Modena and Reggio Emilia
01/2016 – Current	**Promotion, Dr. sc. Hum (scientiarum humanarum)** DIAMICOM graduate school; Institute of Transfusion Medicine and Immunology, Medical Faculty Mannheim, Heidelberg University; Title: “Effects of hyperglycemia on adipose-derived mesenchymal stromal cells: a study on their proangiogenic and immunomodulatory potential”. Supervisor: Prof. Karen Bieback

PUBLICATIONS

Fiori A., Terlizzi V., Kremer H., Gebauer J., Hammes HP., Harmsen M.C., Bieback K., *Mesenchymal stromal/stem cells as potential therapy in diabetic retinopathy.* Immunobiology, 2018. **223**(12): p. 729-743

Fiori A., Hammes HP., Bieback K. *Adipose derived mesenchymal stromal cells reverse hyperglycemia-induced deficiency of angiogenesis in human retinal microvascular endothelial cells*. In preparation.

Fiori A., Uhlig S., Klüter H., Bieback K. *Human adipose-derived mesenchymal stromal cells target different T cell subpopulations depending on the activation of PBMC.* In preparation.

Kremer H., Gebauer J., Helvers-Hornung S., Uhlig S., Beltramo E., Steeb L., Hammes HP., Bieback K., Fiori A., *Pro-angiogenic activity discriminates human adipose-derived*

stromal cells and retinal pericytes: a potential risk in diabetic retinopathy. In preparation.

POSTER/ORAL PRESENTATIONS

June 2017	**1st Heidelberger Young Scientist Meeting, Heidelberg (Germany).** Poster presentation: *Impact of adipose-derived stromal cells (ASC) on diabetic and proliferative retinopathy.*
May 2018	**Deutsche Diabetes Gesellschaft (DDG) 2018, Berlin (Germany).** Oral presentation: *Therapeutic potential of Stem Cell in Diabetic Retinopathy.*
September 2018	**International Society for Cell and Gene Therapy (ISCT) Europe 2018 Regional Meeting, Firenze (Italy).** Poster presentation: *Impact of adipose-derived mesenchymal stromal cells in diabetic retinopathy.*
October 2018	**International Summer School for doctoral students "Vascular cell function in health and in diseases", Santiago de Chile (Chile).** Poster and oral presentation: *Impact of Adipose derived Stromal Cells on Diabetic and Proliferative Retinopathy.*
November 2018	**DRK Forschungsseminar 2018, Tübingen (Germany).** Poster presentation: *Impact of Adipose derived Stromal Cells on Diabetic and Proliferative Retinopathy.*
September 2019	**Deutschen Gesellschaft für Transfusionsmedizin und Immunhämatologie (DGTI) 2019, Mannheim (Germany).** Poster presentation: *High glucose does not affect the angiogenic properties of human adipose stromal cells as potential therapeutics for diabetic retinopathy.*
DIAMICOM Spring/Autumn Schools (2016-2019)	Posters and oral presentations.

REWARDED FUNDINGS

December 2019	**Abschlussstipendium der Graduiertenakademie, Heidelberg University.**

ACCOMPLISHMENTS

January 2016	Enrolled in DIAMICOM graduate school (International Research Training Group 1874/1-2)
May 2018	Invited for oral presentation at Deutsche Diabetes Gesellschaft (DDG) 2018, Berlin (Germany).
October 2018	Selected for the International Summer School for doctoral students “Vascular cell function in health and in diseases”, Santiago de Chile (Chile).

10 AKNOWLEDGEMENTS

This project as part of the DIAMICOM graduate school (International Research Training Group 1874/1-2) was funded by the DFG (Deutsche Forschungsgemeinschaft). As essential contributors to the dissertation and manuscripts, I would like to acknowledge the FlowCore facility (Mannheim Medical faculty) and the Live Cell Imaging facility (LIMA; Center for Biomedicine and Medical Technology Mannheim – CBTM; Mannheim University).
An important mention goes to the Institute of Transfusion Medicine and Immunology (Mannheim) for the efficient provision of buffy coats and serum.

I would like to thank Prof. Hans-Peter Hammes and Prof. Jens Kroll for my enrollment in the DIAMICOM graduate school. I am very grateful for all the courses, teachings and experiences I could attend throughout this program.
My gratitude goes also to Prof. Harald Klüter for having enrolled me in the Institute of Transfusion Medicine and Immunology, providing the financial support for the last period of my PhD.

I sincerely thank Prof. Karen Bieback for her constant presence and support during these years of hard work. Your guidance has been fundamental for my personal development as a person, scientist and researcher. I am very thankful for all the advices, comments and suggestions as well as for all the opportunities you gave me. Thank you for having constantly encouraged and stimulated my passion for research and science, making me more and more aware on how much I love this work. Unfortunately, there are not enough words to express my gratitude but I ensure you I will keep forever your teachings and all experiences of these years tightly in my heart.

Furthermore, very special thanks go to Stefanie Uhlig. I deeply thank you for your work and personal support during these years. It has been a pleasure working with such a competent and brilliant person. Your help has been fundamental from the very beginning to the real end of my time here. I would like to thank you for your excellent assistance in the lab (and in life) and all the countless hours of help in upcoming questions and problems (obviously not only related to work). I will never forget the time

(too much) spent together at the FACS as well as our conversations and backing sessions.

I would like thank Susanne Elvers-Hornung, for having introduced me to the lab and for the support, especially in the very first years of my PhD. I am really grateful for your help and for always having been so patient with me. Besides the lab life, I sincerely thank you for having pushed me in studying German and for the many experiences and conversations shared together.

Moreover, some special thanks go to my homologous counterpart, Adriana Torres Crigna. It has been a pleasure and a great help to share with you these years. Being together through this long life/work journey has been really helpful in facing all the goods and bads. They say, “There is strength in unity”, and I actually think, this is the case. Our discussions and experiences will be always part of my best memories, thank you again for having been my “sister in PhD”.

There are still so many people to thank and their participation not only supported this work but actively contributed to my personal/career development. I would like to thank Christina Schmuttermaier for having been always so helpful and joyful. A special thank goes to my friends Marije Mossel and Utsho Ali Haider for the support and friendship we developed in these years. Thanks to Katrin Widmann for the kind welcoming in Germany and in the lab. In addition, I deeply thank Prama Pallavi for the collaboration and for having been so patient and accommodating in teaching me plasmid production and bacteria transformation. I thank also Frau Ina Schäfer for having introduced me to the confocal microscopy and having been so kind every time I asked for help. I would like to thank Adriana Grbenicek for having introduced me to cell transfection and virus production. My special gratitude goes also to Prof. Jens Kroll for having been the promoter of the Summer School in Santiago de Chile, which allowed me to live one of the best experiences in my life. In last instance, I would like to thank Eleonora Scaccia and Erika for having brought fresh air and energy in the lab. Your enthusiasm has been really helpful in facing the last period of my PhD and I wish you all the best for yours.

Great and deep thanks go to Prof. Massimo Dominici who was the very first person to make all this possible.

Moving to more personal acknowledgments, I sincerely would like to thank all the new and the old Kampfstörche of the VSG Mannheim-Damen 1 volleyball team and the whole Verein, which represented here my second family. You cannot imagine how much this experience in our team enriched me as athlete and person. I am sorry for all the time I have been too rude or too much “Italian”. Despite this, you always gave me so much love that I have never perceived in any team I have played before. I would have like to be able to give back that love. Unfortunately, I know that this was always not easy to perceive because of my temperament. But trust me, I keep closely in my heart these years of trainings and matches, victories and defeats, they are all unforgettable and wonderful memories. Thank you for having been my fresh air in work-related hard moments and for having allowed me to continue playing my beloved sport. I am not mentioning you all here name by name just because I am afraid to forget someone and this would be a mistake. You have been ALL important for me and you ALL contributed to render this experience unforgettable, I will bring each of you in my best and deepest memories.

Ed infine veniamo ai ringraziamenti per voi che con tanto affetto mi avete accompagnato in questo percorso nonostante la distanza.

Un grazie ai miei amici, pochi ma buoni, che ad ogni visita mi hanno sempre accolto con entusiasmo ed allegria. La distanza e il tempo non sono certo fattori che favoriscono questo tipo di rapporti, ma io non mi sono mai sentita abbandonata e non vi ho mai dimenticato. La voglia di ritrovarvi e vedervi è stata parte delle emozioni che mi hanno guidata durante questo percorso ed ha costituito una spinta fondamentale nei momenti di difficoltà.

Ed ora veniamo a te Dani, che sicuramente ti lamenterai di essere stato messo così in fondo. Questa avventura l´abbiamo percorsa insieme, senza sapere bene come fosse iniziata e tantomeno dove avrebbe portato. E dopo quattro anni siamo ancora qua. Per quanto possa essere ovvio, anche tu meriti i tuoi personali ringraziamenti. Grazie per avermi accompagnata in questo percorso, per non avermi mai lasciato sola e per avermi sostenuto in qualunque momento. Grazie per l´amore che mi dai ogni giorno e

per farmi sentire importante. Grazie, perché mi aiuti ad essere una persona migliore, non solo con gli altri ma soprattutto con me stessa.
Alla fine non è del tutto vero che non sappiamo come sia iniziata. Io ho scelto te, tu hai scelto me, è stato ed è super efficace ♥. Gyaradors.

In ultimo, il ringraziamento più grande, che va alla mia famiglia. Cara Mina, caro Pino il successo di questo percorso è anche il vostro. Quello che sono, quello che faccio lo devo a voi, ai vostri insegnamenti e al vostro sostegno. Questi non sono stati anni facili per voi, vedervi soffrire e non potervi aiutare mi ha fatto stare tanto male. Nonostante questo e la distanza, il vostro sostegno e la vostra presenza non mi sono mai mancate. Ho avuto modo di pensare tanto al passato in questi anni, mi avete regalato un´infanzia indimenticabile e mi avete reso la bella persona che mi sento oggi. Tutto questo senza di voi non sarebbe stato possibile, spero di riuscire a rendervi orgogliosi di me il più al lungo possibile. Grazie, vi voglio bene.

Caro Diddo, noi lo sappiamo che non ci sarebbe bisogno di scrivere nessuna parola. Ma questa volta penso che vada scritta. Grazie per le piccole cose (una gif, un messaggio vocale, un link di video, di una canzone) di cui solo noi sappiamo il significato, che hanno fatto/fanno sorridere e hanno illuminato/illuminano anche le giornate più buie. Grazie per l´ammirazione e l´amore che mi trasmetti, un po' a modo tuo, ma ti assicuro, riesco sempre a cogliere. Non sono speciale, non sono migliore/più intelligente di te (come dici a volte). Hai tanto da dare e il primo a non capirlo sei tu. La tua Nenè e qui al tuo fianco e lo sarà sempre per sostenerti. Dammi ancora qualche anno per il Nobel. Ti voglio bene.